

**SENSITIZATION OF PHILADELPHIA POSITIVE  
ACUTE LYMPHOBLASTIC LEUKEMIA CELLS  
RESISTANT TO IMATINIB BY TARGETING  
SPHINGOLIPID METABOLISM**

**A Thesis Submitted to  
the Graduate School of Engineering and Sciences of  
İzmir Institute of Technology  
in Partial Fulfillment of the Requirements for the Degree of**

**DOCTOR OF PHILOSOPHY**

**in Molecular Biology and Genetics**

**by  
Yağmur KİRAZ**

**November 2019  
İZMİR**

## ACKNOWLEDGMENTS

First and foremost, I would like to express my sincere appreciation to my supervisor Prof. Dr. Yusuf Baran for his support, guidance and encouragement throughout my PhD studies both in work environment and outside. It was truly a privilege for me to share of his academic successes but also of his extraordinary human qualities. I always will be grateful for the experiences that I have had while working with him.

A special thanks goes to Assoc. Prof. Dr. Chiara Luberto who has guided me with her scientific knowledge and always been encouraging and supportive whenever I feel needed during my studies. Her passion into science and excitement in regard to teaching has been a great motivation for me.

I would also like to thank Prof. Dr. Lina Obeid who gave me the chance to work in one of the pioneer laboratories in the field; The Lipid Cancer Lab in Health Science Center, Stony Brook University, NY, USA.

I want to thank to Prof. Dr. Yusuf A. Hannun for his valuable contributions and his comments throughout the project.

I want to thank the committee members; Prof. Dr. Bünyamin Akgül, Prof. Dr. Sevil Dinçer İşoğlu, Assoc. Prof. Dr. Özden Yalçın Özuysal and Prof. Dr. Ali Ünal for their contributions and constructive comments to my thesis.

I would like to thank to former and current graduate and undergraduate members of BARAN Lab; especially Nihan Aktaş, Gizem Tuğçe Ulu, Beyza Gürler and Erez Uzuner who were always been supportive. BARAN Lab is a great example of how to feel like a family in a professional environment.

I am also thankful to members of TLC Lab, who always have been helpful and answered all my questions with their experience and knowledge in the field. Also, I would like to thank Izolda Mileva, MS and Lipidomics Core Facility in Stony Brook University for their help in lipid experiments in this project.

Additionally, I thank to Jane Atallah, who worked with me and helped me with the experiments in TLC Lab, Dr. Sitapriya Moorthi for her constructive ideas and Gui-Qin for her helps when I needed.

I also thank Dr. Mona El Khatib who has been a great friend and an amazing example of a scientist for myself (also for her edits and contributions to my thesis). Also,

thanks to Pınar Karakaya, who has been the best friend anyone can ever ask for and supported me at every step of my life.

At last but not the least, I want to thank my mom Zekine Kiraz and my dad Abuzer Kiraz for their continuous support they have given me at every decision of mine throughout my life. Your love and encouragement are worth more than I can express on a paper.

This project was supported by TUBITAK BİDEB 2214-A International Research Fellowship Programme for PhD Students.

## ABSTRACT

### SENSITIZATION OF PHILADELPHIA POSITIVE ACUTE LYMPHOBLASTIC LEUKEMIA CELLS RESISTANT TO IMATINIB BY TARGETING SPHINGOLIPID METABOLISM

Philadelphia positive acute lymphoblastic leukemia (Ph+ALL) is a common subtype of ALL and characterized by having BCR/ABL translocation. Tyrosine kinase inhibitors (TKI) such as imatinib are used for the treatment in Ph+ALL, however, 60-75% of the patients can develop resistance against the TKIs. Bioactive sphingolipids are a group of lipids that play roles in various cellular mechanisms. Previous studies showed that sphingolipids and genes in the pathway were involved in response to TKI treatment in Ph+ALL.

Here, we investigated the roles of SPL on the growth inhibitory effects of imatinib and exploit sphingolipid metabolism by majorly inhibiting glucosylceramide synthase (GCS) to accumulate ceramide or sphingosine to further sensitize cells to imatinib and/or overcome resistance to imatinib in Ph+ALL.

Firstly, we detected that, sphingosine kinase-1 (SK-1) a well-studied SPL enzyme inhibition did not contribute to cytotoxic effects of imatinib in SD-1 Ph+ALL cells. Moreover, we determined that imatinib is inducing *de novo* synthesis pathway of SPL and increasing the levels of ceramide, sphingosine, hexosylceramides and sphingomyelin in SD-1 cells. Interestingly, newly generated imatinib-resistant cell line SD-1R was detected to have an aberration in this pathway resulting in development of resistance. Combination treatment with eliglustat (GCS inhibitor) resulted in a significant increase in ceramide and sphingosine levels and reflected on cell growth and sensitized cells to imatinib.

Taken together, it was shown for the first time in the literature that the cytotoxic effects of imatinib was due to induction of *de novo* synthesis pathway of sphingolipids and inhibition of GCS together with imatinib has synergistic cytotoxic effects on imatinib resistant Ph+ALL cells. As a conclusion, increasing the intracellular levels of ceramide (and/or sphingosine) can be a novel approach to sensitize drug resistant Ph+ALL cells.

## ÖZET

### SFİNGOLİPİD METABOLİZMASININ HEDEFLENMESİYLE İMATİNİBE DİRENÇLİ PHILADELPHIA POZİTİF AKUT LENFOBLASTİK LÖSEMİ HÜCRELERİNİN DUYARLI HALE GETİRİLMESİ

Philadelphia pozitif akut lenfoblastik lösemi (Ph+ALL), ALL'nin sıklıkla görülen bir alt tipi olmakla birlikte, BCR/ABL translokasyonunu taşımakla karakterizedir. Ph+ALL tedavisinde, imatinib gibi tirozin kiraz inhibitörleri (TKİ) kullanılmasına rağmen, hastaların %60-75'i TKİ'lere karşı direnç geliştirmektedir. Biyoaktif sfingolipidler, birçok hücrel mekanizmada rol oynayan bir lipid grubudur. Daha önce yapılan çalışmalar biyoaktif sfingolipidlerin ve bu yolaktaki genlerin Ph+ALL'de TKİ'ye verilen yanıtta rol aldığını göstermiştir.

Bu çalışmada, biyoaktif sfingolipidlerin imatinibin büyüme baskılayıcı rollerini ve sfingolipid metabolizmasından özellikle glukozilseramid sentaz (GSS) ve sfingozin kinaz-1'i (SK-1) inhibe ederek seramid veya sfingozinin birikimine yol açarak hücreleri imatinibe duyarlı hale getirmeyi ve/veya direnci geri çevirmeyi araştırdık.

Öncelikle, daha önce çalışılmış bir sfingolipid enzimi olan SK-1 inhibisyonunun imatinibin SD-1 Ph+ALL hücreleri üzerine sitotoksik etkilerine katkı yapmadığını tespit ettik. Daha da önemlisi, imatinibin sfingolipidlerin *de novo* sentez yolağını tetiklediğini ve seramid, sfingozin, heksozilseramid ve sfingomyelin düzeylerini artırdığını belirledik. İlginç bir şekilde, yeni geliştirilen imatinib-dirençli SD-1R hücrelerinde bu yolda tespit edilen bir anormallik direnç gelişimine neden olmuştur. Eliglustat (GSS inhibitörü) ile imatinibin kombinasyon tedavisi, seramid ve sfingozin seviyelerinde önemli artışa neden olarak, hücreleri imatinibe duyarlı hale getirdi.

Tüm bu veriler değerlendirildiğinde, imatinibin sitotoksik etkilerinin *de novo* sentez yolağının aktifleştirilmesi ile olduğu ve GSS inhibisyonu ile imatinib uygulamasının imatinib-dirençli Ph+ALL hücrelerinde sinerjik sitotoksik etkileri olduğu literatürde ilk defa bu çalışma ile gösterilmiştir. Sonuç olarak, hücre içi seramid (ve/veya sfingozin) düzeylerinin artırılması, ilaç dirençli Ph+ALL hücrelerinin duyarlı hale getirilmesi için yeni bir yaklaşım olabilir.

*To my beloved family,*

*and to the greatest journey started  
in 41°00'43.7"N 28°57'32.9"E ...*

# TABLE OF CONTENTS

LIST OF FIGURES .....	xi
LIST OF TABLES .....	xiv
CHAPTER 1. INTRODUCTION .....	1
1.1. Acute Lymphoblastic Leukemia .....	1
1.2. Philadelphia Positive Acute Lymphoblastic Leukemia .....	4
1.3. Treatment of Philadelphia Positive Acute Lymphoblastic Leukemia .....	5
1.3.1. Standard Chemotherapy .....	5
1.3.2. Targeted Therapy (Tyrosine Kinase Inhibitors) .....	6
1.3.2.1. Imatinib .....	6
1.3.2.2. Nilotinib and Dasatinib .....	8
1.3.2.3. Ponatinib .....	10
1.3.3. Monoclonal Antibodies & Immunotherapy .....	11
1.3.4. Stem Cell Transplant.....	12
1.4. Resistance to Tyrosine Kinase Inhibitors .....	13
1.4.1. BCR/ABL Mutations .....	14
1.4.2. Gene Amplifications .....	15
1.4.3. Genomic Deletions.....	16
1.4.4. Alterations in Protein Expression .....	17
1.4.5. Activation of Alternative Signaling Pathways.....	18
1.4.6. Alterations in Drug Influx/Efflux Mechanisms .....	20
1.5. BCR/ABL Signaling Mechanisms .....	21
1.6. Bioactive Sphingolipids .....	24
1.6.1. Ceramide Metabolism and Signaling .....	27
1.6.2. Antiproliferative Roles of Ceramide.....	29
1.6.3. Bioactive Sphingolipids in Drug Resistance in Cancer .....	31
1.6.4. Targeting Sphingolipid Signaling in Cancer Therapy .....	33
1.6.5. Targeting Sphingolipid Metabolism for the Treatment of Hematological Malignancies.....	35
1.7. Aim of the Project .....	37

CHAPTER 2. MATERIALS AND METHODS .....	39
2.1. Chemicals and Reagents .....	39
2.2. Cell Lines and Culture Conditions.....	39
2.3. Thawing Frozen Cells .....	40
2.4. Maintenance of CCRF-CEM, SUP-B15 and SD-1 Cell Lines .....	40
2.5. Freezing Cells .....	40
2.6. Generation of Imatinib Resistant SD-1R cells .....	41
2.7. Treatment with Imatinib and/or Other Inhibitors .....	41
2.8. Treatment with Exogenously Added Sphingolipids .....	42
2.9. Determining Cell Viability with Trypan Blue Exclusion Assay .....	42
2.10. Measuring Cell Proliferation by MTT Assay .....	42
2.11. Protein Isolation and Preparation .....	43
2.12. Protein Quantification by BCA Assay .....	43
2.13. Western Blotting .....	44
2.14. RNA Isolation .....	44
2.15. Quantification of RNA .....	45
2.16. cDNA Synthesis.....	45
2.17. Real Time Quantitative PCR .....	46
2.18. siRNA Transfection .....	46
2.19. Lipid Analysis by HPLC/MS/MS .....	47
2.20. Determination of Inorganic Phosphate (Pi) Concentrations .....	48
2.21. Measuring <i>In situ</i> GCS Activity by NBD-C6-Ceramide Labeling .....	49
2.22. Measuring <i>In situ</i> SK Activity by NBD-Sphingosine Labeling .....	50
2.23. Statistical Analyses .....	50
CHAPTER 3. RESULTS .....	51
3.1. SD-1 Ph+ ALL Cells Show Intrinsic Resistance to Imatinib .....	51
3.2. SK-1 Inhibition Does Not Contribute to Cytotoxic Effects of Imatinib...53	
3.3. Endogenous Sphingolipid Levels are Elevated in Response to Imatinib in SD-1 Cells .....	58
3.4. Endogenous Complex Sphingolipid Levels are Elevated in Response to Imatinib in SD-1 Cells .....	61



3.5. <i>De novo</i> Sphingolipid Synthesis Pathway is Induced by Imatinib in SD-1 Cells .....	65
3.6. Activation of <i>de novo</i> Sphingolipid Synthesis Participates in the Cytostatic Response to Imatinib Treatment of SD-1 Cells .....	69
3.7. Pharmacological Inhibition of GCS Exacerbates the Accumulation of Cytostatic/Cytotoxic Sphingolipids Induced by Imatinib and Sensitizes SD-1 Cells to the Drug .....	72
3.8. The Effect of siRNA Mediated Knock-Down of GCS on Imatinib Induced Changes in Endogenous Sphingolipid Levels and Cell Number of SD-1 Cells .....	77
3.9. Generation of Imatinib Resistant SD-1 Cells (SD-1R).....	82
3.10. Blunted Imatinib Induced changes in endogenous sphingolipid levels of SD-1R cells .....	85
3.11. Inhibition of GCS in Combination with Imatinib Treatment Promotes Accumulation of Growth Inhibitory Sphingolipids and Re-Sensitizes SD-1R Cells to the Drug .....	87
 CHAPTER 4. DISCUSSION.....	 92
 REFERENCES .....	 98

# LIST OF FIGURES

<b><u>Figure</u></b>	<b><u>Page</u></b>
Figure 1.1. Formation of Philadelphia chromosome .....	5
Figure 1.2. Sphingolipid synthesis and metabolism .....	25
Figure 1.3. Major sphingolipids and their involvement into cellular mechanisms.....	28
Figure 2.1. Generation of resistant cell line (SD-1R) by clonal selection .....	41
Figure 3.1. Determining the effect of imatinib on the viability of Ph+ ALL cell lines ..	52
Figure 3.2. Determining the effect of imatinib on the proliferation of SD-1 cell line....	52
Figure 3.3. Analysis of SK activity in response to increased concentrations of PF543 by HPLC .....	55
Figure 3.4. Quantification of SK activity in response to increased concentrations of PF543 .....	56
Figure 3.5. The protein levels of SK-1 and SK-2 treated with imatinib, PF543 and SKI-II by western blotting .....	56
Figure 3.6. SK activity in response to imatinib treatment, PF543 and their combination .....	57
Figure 3.7. Determining the effect of imatinib, PF543 and their combination on cell viability on SD-1 cell line .....	57
Figure 3.8. Analysis of endogenous ceramide levels of SD-1 cells in response to imatinib (most abundant species) .....	59
Figure 3.9. Analysis of endogenous ceramide levels of SD-1 cells in response to imatinib (less abundant species) .....	59
Figure 3.10. Analysis of endogenous ceramide levels of SD-1 cells in response to imatinib (the least abundant species).....	60
Figure 3.11. Analysis of endogenous sphingolipid levels of SD-1 cells in response to imatinib .....	60
Figure 3.12. Analysis of endogenous hexosylceramide levels of SD-1 cells in response to imatinib (most abundant species) .....	62
Figure 3.13. Analysis of endogenous hexosylceramide levels of SD-1 cells in response to imatinib (less abundant species) .....	63
Figure 3.14. Analysis of endogenous sphingomyelin levels of SD-1 cells in response to imatinib (most abundant species) .....	63

<b><u>Figure</u></b>	<b><u>Page</u></b>
Figure 3.15. Analysis of endogenous sphingomyelin levels of SD-1 cells in response to imatinib (less abundant species) .....	64
Figure 3.16. Analysis of endogenous sphingomyelin levels of SD-1 cells in response to imatinib (the least abundant species).....	64
Figure 3.17. Analysis of <i>de novo</i> sphingolipids in response to myriocin; A. dihydroC16-ceramide levels, B. dihydroceramide levels .....	65
Figure 3.18. The changes in total ceramide levels with imatinib treatment in presence of myriocin.....	66
Figure 3.19. The changes in sphingosine levels with imatinib in presence of myriocin .....	67
Figure 3.20. The changes in total hexosylceramide levels with imatinib in presence of myriocin.....	68
Figure 3.21. The changes in total sphingomyelin levels with imatinib in presence of myriocin .....	68
Figure 3.22. Contribution of <i>de novo</i> sphingolipid pathway to cytotoxic effects of imatinib in SD-1 cells.....	70
Figure 3.23. The effect of exogenous treatment with C6-ceramide on cell viability .....	70
Figure 3.24. The effect of exogenous treatment with sphingosine on cell viability .....	71
Figure 3.25. The effects of eliglustat treatment on GCS activity measured by production of A. NBD-C6-hexosylceramide and B. hexosylceramides ....	72
Figure 3.26. The changes in the total ceramide levels of SD-1 cells treated with imatinib and eliglustat and their combination.....	73
Figure 3.27. The changes in the total hexosylceramide levels of SD-1 cells treated with imatinib and eliglustat and their combination .....	74
Figure 3.28. The changes in the total sphingomyelin levels of SD-1 cells treated with imatinib and eliglustat and their combination .....	75
Figure 3.29. The changes in the sphingosine levels of SD-1 cells treated with imatinib and eliglustat and their combination .....	76
Figure 3.30. The effect of treatment with imatinib, eliglustat and their combination on cell viability of SD-1 cells .....	77
Figure 3.31. The effects of GCS siRNA transfection on GCS activity measured by A. GCS mRNA levels and B. NBD-C6-hexosylceramide levels .....	78

<b><u>Figure</u></b>	<b><u>Page</u></b>
Figure 3.32. Effect of GCS knockdown and imatinib treatment on the levels of hexosylceramides in SD-1 cells.....	79
Figure 3.33. Effect of GCS knockdown and imatinib treatment on the levels of ceramide in SD-1 cells.....	79
Figure 3.34. Effect of GCS knockdown and imatinib treatment on the levels of sphingomyelin in SD-1 cells .....	80
Figure 3.35. Effect of GCS knockdown and imatinib treatment on the levels of sphingosine in SD-1 cells .....	81
Figure 3.36. Effect of GCS knockdown together with imatinib treatment on cell viability in SD-1 cells .....	81
Figure 3.37. Comparative response to imatinib treatment by SD-1 and SD-1R cells measured by A. trypan blue assay B. MTT assay .....	83
Figure 3.38. Mechanism of resistance to apoptosis induced by imatinib in SD-1R cells A.Cleaved caspase-3 B.BCL2 and BCL-XL C.BCR/ABL levels ....	84
Figure 3.39. Changes in endogenous ceramide levels of SD-1 and SD-1R cells in response to imatinib.....	85
Figure 3.40. Changes in endogenous hexosylceramide levels of SD-1 and SD-1R cells in response to imatinib .....	86
Figure 3.41. Changes in endogenous sphingosine levels of SD-1 and SD-1R cells in response to imatinib.....	86
Figure 3.42. Changes in endogenous sphingomyelin levels of SD-1 and SD-1R cells in response to imatinib .....	87
Figure 3.43. The changes in the hexosylceramide levels of SD-1R cells treated with imatinib and eliglustat and their combination .....	88
Figure 3.44. The changes in the ceramide levels of SD-1R cells treated with imatinib and eliglustat and their combination.....	89
Figure 3.45. The changes in the sphingosine levels of SD-1R cells treated with imatinib and eliglustat and their combination .....	89
Figure 3.46. The effect of treatment with imatinib, eliglustat and their combination on cell viability of SD-1R cells .....	90
Figure 3.47. Effect of GCS knockdown together with imatinib treatment on cell viability in SD-1R cells .....	91

## LIST OF TABLES

<b><u>Table</u></b>	<b><u>Page</u></b>
Table 1.1. WHO classification of ALL.....	2
Table 2.1. Preparation of diluted bovine serum albumin (BSA) standards .....	43
Table 2.2 Annealing mixture of the cDNA preparation protocol .....	45
Table 2.3. The enzyme mix used in cDNA synthesis .....	46
Table 2.4. Standards used in inorganic phosphate determination.....	49

# CHAPTER 1

## INTRODUCTION

### 1.1. Acute Lymphoblastic Leukemia

Acute lymphoblastic leukemia (ALL) is a type of hematological cancer that arises from the lymphoid lineage of blood cells and is characterized by the accumulation of large numbers of immature lymphocytes. Different genetic and environmental factors have been identified to have predisposing roles in the disease progression. Down syndrome, Bloom syndrome and ataxia telangiectasia are the commonly known genetic abnormalities that have been identified in ALL cases together with certain virus infections such as Human Immunodeficiency Virus (HIV) and Epstein-Barr Virus (EBV). However, majority of ALL cases occur *de novo* as acute malignancies <sup>1-3</sup>.

Acute lymphoblastic leukemia is the most common childhood cancer. It is detected in 80% of childhood leukemias, on the other hand, it represents 20% of adult leukemias. Statistically, it is seen in 1.6-1.7 adults while 4-5 children per 100.000 population. In 2019, an estimated 5,930 number of new cases are reported together with 1,500 deaths from ALL only in the United States <sup>4</sup>. Although the advancements and intensification of the therapy led to improvements in the responses of pediatric patients, however, the prognosis of adults remains very poor. Most of the patients show response to induction therapy but only 30-40% of them are able to sustain long-term remission <sup>1</sup>.

The main characteristics of ALL is the accumulation of immature lymphoid cells in the bone marrow and peripheral blood. As a result of this abnormality, each patient can have their own specific or combination of different symptoms such as anemia, leukopenia and/or thrombocytopenia, easy bleeding or bruising and fatigue <sup>5-7</sup>.

ALL diagnosis requires the presence of at least 20% of lymphoblasts in the bone marrow and peripheral blood. Diagnosis is confirmed and the disease is sub-specified by additional tests on cell morphology, genetic markers, cytogenetic tests and immunophenotyping <sup>5,8</sup>.

Initially, the classification of ALL was performed by following the French American British (FAB) criteria that grouped ALL into 3 subtypes (L1, L2 and L3) based on morphological features <sup>9</sup>. Later on, the World Health Organization (WHO) International panel recommended to revoke this classification since it does not reflect clinical prognosis, immunophenotype or genetic abnormalities. WHO proposed an alternative classification that comprises morphological and cytogenetic features of lymphoblasts that divided ALL into 3 subtypes: B lymphoblastic, T lymphoblastic and Burkitt-cell leukemia <sup>10,11</sup>. Although Burkitt-cell leukemia was excluded in the revision in 2008, B-lymphoblastic type of ALL was divided into another two subtypes as follows: B-lymphoblastic leukemia with recurrent genetic abnormalities and B-lymphoblastic leukemia not otherwise specified. Current subclassification of ALL according to 2016 WHO baseline is shown in Table 1 <sup>12</sup>. Majority of the ALL cases is comprised by B-cell ALL whereas T-cell ALL only accounts for 25% of cases.

Table 1. WHO classification of ALL

B-cell lymphoblastic leukemia/lymphoma – not otherwise specified
B-cell lymphoblastic leukemia/lymphoma, with recurrent genetic abnormalities
<i>B-cell lymphoblastic leukemia/lymphoma with hypodiploidy</i>
<i>B-cell lymphoblastic leukemia/lymphoma with hyperdiploidy</i>
<b><i>B-cell lymphoblastic leukemia/lymphoma with t(9;22)(q34;q11.2)[BCR-ABL1]</i></b>
<i>B-cell lymphoblastic leukemia/lymphoma with t(v;11q23)[MLL rearranged]</i>
<i>B-cell lymphoblastic leukemia/lymphoma with t(12;21)(p13;q22)[ETV6-RUNX1]</i>
<i>B-cell lymphoblastic leukemia/lymphoma with t(1;19)(q23;p13.3)[TCF3-PBX1]</i>
<i>B-cell lymphoblastic leukemia/lymphoma with t(5;14)(q31;q32)[IL3-IGH]</i>
<i>B-cell lymphoblastic leukemia/lymphoma with intrachromosomal amplification of chromosome 21 (iAMP21)</i>
<i>B-cell lymphoblastic leukemia/lymphoma with translocations involving tyrosine kinases or cytokine receptors (BCR-ABL1-like ALL)</i>
T-cell lymphoblastic leukemia/lymphomas
<i>Early T-cell precursor lymphoblastic leukemia</i>

Risk stratification and prognosis assessment are the key factors to administer the most suitable treatment for the patients. Clinicians usually rely on the patients' age and white blood cell (WBC) count to decide the treatment regimen and its duration if the patient is suitable for stem cell transplantation (SCT). Poor prognosis is usually seen in patients >60 years old with 10-15% survival rate. This is mainly due to the increase in the

frequency of chromosomal abnormalities, hypodiploidy, complex karyotype and medical comorbidities with age <sup>13</sup>. The largest prospective study to determine the optimal induction therapy for adult ALL patients was MRC UKALL XII/ECOG E2993 and it was completed in 2005 with the participation of more than 1500 patients. In this study, they reported that the overall survival (OS) rate of the patients who were able to go through complete remission (CR) was 45%. However, for the other patients who did not achieve CR, the survival rate was 5%. On the other hand, they determined that the prognosis is directly proportional with the age factor, such that the younger the patients are, the more efficient the treatment is. Additionally, they reported that having less than  $30 \times 10^9$  WBC/L count for B-ALL and  $100 \times 10^9$  WBC/L count for T-ALL is another factor that contributes to OS and disease-free survival (DFS) rates in the patients <sup>14</sup>. These results, have led to the categorization of the Philadelphia negative ALL as follows: i) low risk (age <35 and low WBC count) with having 55% OS rate ii) intermediate risk (age >35 or high WBC count) with 34% OS rate and iii) high risk with 5% OS rate (both age >35 and high WBC count) <sup>14</sup>.

As much as the clinical factors and risk stratification is of primary importance to therapy, genetic changes can be a major determinant for the prognosis of ALL. Many different cytogenetic abnormalities and chromosomal translocations have been identified in ALL. The most frequently detected genetic abnormalities are: t(12;21) [ETV6-RUNX1], t(1;19) [TCF3-PBX1], t(9;22) [BCR-ABL1] (Philadelphia positive). More recently, a new group of patients have been identified, who carry a similar profile to BCR-ABL positive ALL but without having the BCR-ABL1 translocation. This group of patients is defined as Ph-like ALL and have poor prognosis somewhat similar to Ph-positive ALL patients. Ph-like ALL represents 10% of the childhood ALL, while it is about 25-30% of the cases in young adults <sup>15-17</sup>. More than 80% of the Ph-like ALL cases contains deletions in major transcription factors that are involved in B-cell maturation/development such as IKAROS family zinc finger 1 (IKZF1), early B-cell factor 1 (EBF1), transcription factor 3 (E2A) and paired box 5 (PAX5) <sup>17</sup>. Additionally, kinase-activating alterations including rearrangements of ABL1, ABL2, Janus kinase 2 (JAK2), erythropoietin receptor (EPOR), cytokine-receptor-like factor 2 (CRLF2), fms-related tyrosine kinase 3 (FLT3), interleukin 7 receptor (IL7R), SH2B3 have been identified in a great majority of the cases in Ph-like ALL <sup>17,18</sup>.



## 1.2. Philadelphia Positive Acute Lymphoblastic Leukemia

Philadelphia positive, also known as BCR/ABL positive acute lymphoblastic leukemia (Ph+ ALL), is the most common subtype of B-ALL detected in adults. It represents 25-30% of the adult ALL cases whereas only seen in about 5% of childhood ALL. The incidence of Ph+ ALL reaches up to 50% in patients over 60 years old <sup>19</sup>. Patients are presented with high but variable white blood cell (WBC) count and splenomegaly together with other symptoms such as fatigue, dizziness, etc. <sup>20</sup>.

The characteristics of the disease is having a reciprocal translocation that occurs between ABL1 gene that is located on the long arm of chromosome 9 and breakpoint cluster region (BCR) gene that is located on the long arm of chromosome 22. As a result, a fusion transcript, which eventually encodes BCR/ABL, is produced by the newly formed Philadelphia chromosome. It can be detected by molecular methods such as polymerase chain reaction (PCR) or fluorescence in situ hybridization (FISH) analysis <sup>21</sup>. Newly formed BCR/ABL protein has a constitutive kinase activity, which leads to the activation of multiple signaling pathways in the cells that are involved in the regulation of several cellular processes such as, cell proliferation, growth and survival. BCR/ABL protein can be found in various sizes depending on the breakpoint in BCR gene that results indifferent BCR isoform proteins with the following sizes 190, 210 and/or 230 kDa. The p210 BCR/ABL transcript is usually observed in chronic myeloid leukemia (CML) and in a minor portion of Ph+ ALL cases, whereas p190 BCR/ABL transcript is detected in majority of Ph+ ALL patients. Co-presence of both p190 and p210 BCR/ABL might be detected in some rare cases <sup>21,22</sup>. The presence of BCR/ABL is known to enhance some of the hallmarks of cancer such as resistance to cell death, being independent from growth factors and alterations in cell-cell interactions, thus resulting in a more aggressive clinical course.

Ph+ ALL is almost always found among B-lymphoblastic ALL except for a few reported cases with T-lymphoblastic ALL. Leukemic lymphoblasts can be distinguished based on the detection of a higher expression of CD34 cell surface marker and some (10-20%) myeloid markers <sup>23</sup>. Almost in 70% of the cases, additional chromosomal abnormalities including monosomy 7 or hyperdiploid karyotypes have been detected together with BCR/ABL translocation in Ph+ ALL <sup>20</sup>.

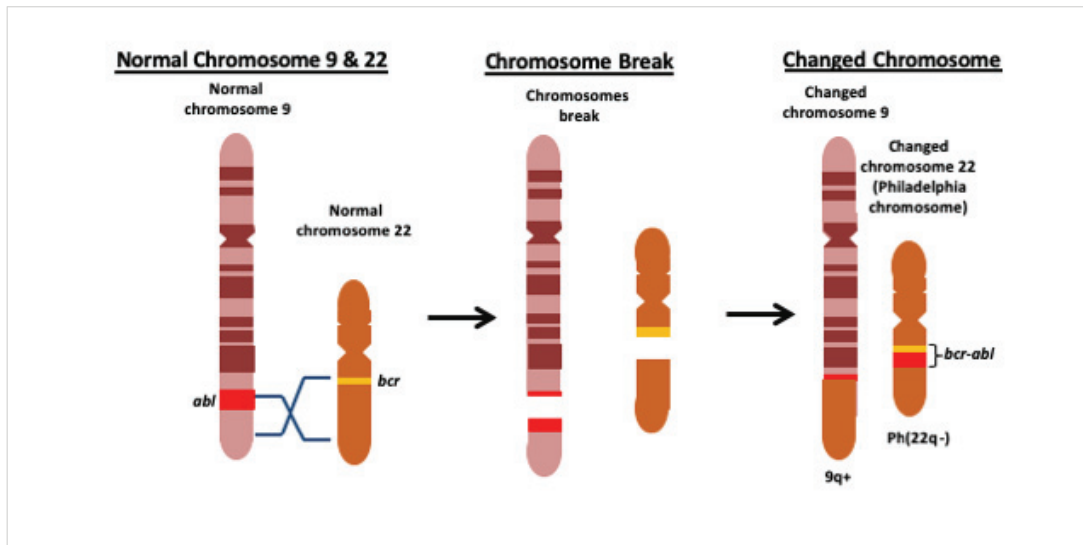


Figure 1.1. Formation of Philadelphia chromosome

### 1.3. Treatment of Philadelphia Positive Acute Lymphoblastic Leukemia

The treatment of Ph<sup>+</sup> ALL can be categorized into two as follows: pre-tyrosine kinase inhibitors (TKI) era and post-tyrosine kinase inhibitors era. The latter has started with the introduction of the first tyrosine kinase inhibitor imatinib in 2001 and followed by development of newer technologies <sup>24</sup>.

#### 1.3.1. Standard Chemotherapy

Ph<sup>+</sup> ALL patients that were given standard chemotherapy regimen without addition of TKIs to the therapy had shown very poor prognosis. Although chemotherapy is able to achieve complete remissions (CR) in more than 70% of the patients, relapse is seen in most of the patients within 6 months followed by death due to the disease <sup>20</sup>. The 5-year overall survival (OS) rates were no more than 10%. Notably, hyper-CVAD chemotherapy, which is a cocktail of cyclophosphamide, vincristine, doxorubicin and

dexamethasone alternating with methotrexate and cytarabine, was able to achieve 91% of CR rate together with an estimated 39% of 5-year OS<sup>25</sup>. However, in the long run, survival rates were similar, thus highlighting the need to develop and come up with new treatment options for Ph+ ALL.

### **1.3.2. Targeted Therapy (Tyrosine Kinase Inhibitors)**

Understanding the role and the mechanism of action of BCR/ABL led to the development of new tyrosine kinase inhibitors (TKIs), such as imatinib mesylate, which is the first-generation TKI. Identification of imatinib later on was followed by development of dasatinib and nilotinib as second-generation TKIs and finally by ponatinib as third-generation TKI. The common mechanism of action of these TKIs is to block the binding of adenosine triphosphate (ATP) to the ATP binding site of BCR/ABL which will eventually prevent the signal transduction toward downstream pathways of BCR/ABL<sup>24</sup>. BCR/ABL is known to activate multiple signaling pathways in the downstream including Ras, MAPK, Src, PI3K, Jak/STAT pathways. Targeting BCR/ABL activity by TKIs results in blockage in the signals through these major signaling pathways which eventually prevents cell proliferation and cancer progression. Introduction of TKIs into the therapy regimen has led to a revolution in the treatment of Ph+ ALL. The usage of each TKI alone or in addition to chemotherapy regimen is explained in the next sections with their expected and/or reported outcomes<sup>26</sup>.

#### **1.3.2.1. Imatinib**

The approval of imatinib (Gleevec® or Glivec®) in 2001 was a breakthrough that started a new era in cancer treatment. It was first discovered in the late 90s by Nicholas Lyndon, a biochemist and was suggested by Brian Druker, an oncologist to be used in CML treatment. In 1998, the first clinical trial of imatinib was completed and followed by the Food and Drug Administration's (FDA) approval in 2001. After overt effect of

imatinib for the treatment of CML patients, the research was driven toward the usage of imatinib in other cancers, which then showed success in cancers that harbored an overexpression in tyrosine kinases <sup>24</sup>.

Imatinib is a 2-phenyl amino pyrimidine derivative and works as a tyrosine kinase inhibitor targeting BCR/ABL, ABL, PDGFR and c-Kit kinase activities. The mode of action of tyrosine kinases is through a process referred to as protein tyrosine phosphorylation: the transfer of one phosphate (Pi) from ATP to the tyrosine residues on the substrate. Imatinib acts by binding to the ATP binding site, therefore keeping the conformation inhibited, which results in the inhibition of enzymatic activity <sup>24,27</sup>. Since BCR/ABL and other kinases activates multiple downstream signaling pathways, which will eventually induce leukemogenesis, this signal transformation to downstream signaling is blocked by imatinib treatment. Additionally, imatinib inhibits the entry of BCR/ABL into the nucleus, where it exhibits its anti-apoptotic functions <sup>28</sup>.

Imatinib is rather used as a combination with standard chemotherapy in Ph+ ALL treatment, where it has increased CR rates above 90% and 5-year OS rates up to 50 <sup>29-31</sup>.

In a more recent phase II trial completed with 54 older patients (median age of 51), the patients were treated with the combination of imatinib with hyperfractionated cyclophosphamide, vincristine, Adriamycin and dexamethasone (hyper-CVAD), showing a 93% of CR rate with 45% of complete molecular remission (CMR) at 3-months. Although a small portion of the patients (30%) went through allogenic hematopoietic stem cell transplantation (alloHSCT) in first CR, still the 5-year OS reached up to 43%, which was significantly higher than the previously reported rates <sup>6</sup>.

In another important clinical study: UKALLXII/ECOG2993, 441 newly diagnosed adult Ph+ ALL patients were enrolled into 3 groups as follows: 266 patients in pre-imatinib group in which the patients were not given imatinib at all during chemotherapy; 86 patients in late imatinib group where the patients were given imatinib alone right after 2 induction courses and 89 patients in early imatinib group in which imatinib was added into the second phase of induction course. It was reported that imatinib cohort has remarkably higher rates of CR, being 92% together with higher 4-year OS, compared to pre-imatinib cohort, which is showing 82% CR rates. Importantly, early introduction of imatinib showed further increase in the 4-year OS as 43%. They also reported that alloHSCT is still favored at the post-induction stage in Ph+ ALL no matter if the patients are given imatinib <sup>30</sup>.

Imatinib has also been used in combination with reduced-intensity chemotherapy to see its feasibility for these conditions. For this purpose, the GRAAPH-2005 trial was designed to include the following cohorts: imatinib combined with reduced chemotherapy (including only vincristine and dexamethasone) and imatinib with hyper-CVAD chemotherapy. The reduced intensity group showed higher CR rate (98%) compared to hyper-CVAD cohort (91%), which is thought to be due to the higher rate of induction deaths in hyper-CVAD group (being 6% vs. 1%). Moreover, 63% of the responsive patients were taken under alloHSCT and 14% of them went to autologous HSCT (autoHSCT), which then showed 37% and 46% OS, respectively without any correlation to the type of transplantation <sup>31</sup>.

The introduction of imatinib into the treatment regimen of Ph+ ALL have led to great advancements in the treatment of this deadly disease. However, despite this great improvement in therapy patients have developed resistance to imatinib, which necessitated the development of new treatments options for Ph+ ALL and hence the discovery of the next generation TKIs. Despite the fact that newer technologies have been developed and currently used in the clinics, imatinib resistance stands as the most challenging phenomenon in the treatment of Ph+ ALL together with causing the most share of mortalities. Since imatinib, in most of the countries, is still used in the first-line treatment, patients' prognosis mostly relies on their response to imatinib treatment. The mechanism of imatinib resistance will be detailed in the following sections together with possible actions against resistance and strategies to overcome imatinib resistance as well as sensitizing cells/patients to treatment.

### **1.3.2.2. Nilotinib and Dasatinib**

A second generation TKI Nilotinib (Tasigna<sup>®</sup>) is structurally derived from imatinib. It has the inhibitory effect against BCR/ABL, c-Kit and PDGFR as imatinib does and shows 20-50-fold more potency than imatinib. Although it has not received the FDA approval for its use in Ph+ ALL, clinical trials have continuously been going on for the patients that are showing imatinib resistance. In a phase II clinical study, nilotinib was used as monotherapy in Ph+ ALL patients who were relapsed or refractory resulted in

24% of CR rates <sup>32</sup>. On the other hand, combination of nilotinib with chemotherapy including vincristine, daunorubicin and prednisolone was investigated by a multicentric study and the results showed remarkably high CMR (94%) and 2-year relapse-free survivals (72%) <sup>33</sup>.

In another cohort study, EWALL, nilotinib was used in combination with reduced-intensity chemotherapy for the newly diagnosed Ph+ ALL patients. The results showed higher efficacy in patients older than 55 years in addition to 87% CR rates in these patients. Additionally, the OS was 73% at the follow-up of 8.5 months <sup>34</sup>.

The results of the most recent trial, GRAAPH-2014, in which the patients (median age of 47 years old) were given nilotinib with reduced-intensity chemotherapy, showed 98% of CR rates together with 93% cumulative molecular response rate. The percentage of the patients who underwent to alloHSCT was 73% in CR1 stage. This study carries importance in terms of shaping the treatment strategy for younger patients to see if combining nilotinib with low-intensity chemotherapy followed by alloHSCT shows better outcome for those patients <sup>35</sup>.

Another second-generation TKI, dasatinib (Sprycel<sup>®</sup>), is considered to be rather more a pan-TKI rather than only targeting ABL kinase. It also inhibits src, c-Kit, PDGFR and ephrin receptor kinases. Dasatinib differs from the other TKIs by having the ability of binding to both the active and inactive conformations of ABL and by targeting most of the TKI resistance-causing mutations in the kinase domains of ABL except for T315I mutation. Using dasatinib for Ph+ ALL patients has been approved by FDA for the patients who are intolerant to prior imatinib treatment in 2006. It has also been approved by FDA for the newly diagnosed pediatric patients in 2018 <sup>26,36,37</sup>. In a phase II clinical study, dasatinib was given as a monotherapy for the patients who are resistant or intolerant to imatinib and the results showed 58% of the patients in complete cytogenetic remission (CCyR) <sup>38</sup>. In another multicentric phase II trial, imatinib resistant or intolerant CML patients achieved 35% and 52% CR rates, respectively, by dasatinib treatment <sup>26</sup>. The results from clinical trials were mostly short-lived with maximum 3-months of progression free survival (PFS) rates. Hereupon, another study was designed to combine dasatinib with standard chemotherapy in the frontline treatment. In this phase II trial, newly diagnosed Ph+ ALL patients (median age 55 years old), were given dasatinib with hyper-CVAD chemotherapy. It was reported that the CR rate reached up to 96% in addition to 83% CCyR rates and 65% CMR rates. The patients also showed 44% of relapse free survival (RFS) and 46% of OS rates <sup>39</sup>.

Notably, intensive chemotherapy is not well tolerated in all patients. In some studies, it has been shown that moderate toxicity can be tolerated in elderly patients in which neither intense chemotherapy nor alloHSCT was used <sup>40,41</sup>. In a clinical study, GIEMMA group, dasatinib was combined with only prednisone for the newly diagnosed Ph+ ALL patients and the results showed CR for all the patients. Additionally, MMR was increasing gradually day by day and eventually achieving 52% at the end of induction course <sup>40</sup>.

In another study, similar results were observed for the patients who received dasatinib in combination with steroids. They reported 97% of CHR rate together with a successfully achieved CMR in 19% of the patients. On the other hand, the patients who did not achieve CMR underwent chemotherapy or alloHSCT. Together, there was 58% of 3-year OS was observed for the patients <sup>41</sup>.

In another international study, EWALL-PH-01, dasatinib was used again in combination with reduced-intensity chemotherapy (only vincristine and dexamethasone in induction; L-asparaginase, methotrexate and cytarabine in consolidation courses) for elderly patients who are over 55 years old. Although 96% of the patients achieved CR with 65% of MMR; OS was reported as 36%. After the CR, only 10% of the patients received alloHSCT, which proves that remission (with moderate long-term survival) is achievable for the elderly patients without intensive chemotherapy or alloHSCT <sup>42</sup>. Although better responses were reported with dasatinib treatment, the fact that it could not target BCR/ABL with T315I mutation brought out the need for new generation tyrosine kinase inhibitors.

### **1.3.2.3. Ponatinib**

Ponatinib (Iclusig®) is a third generation TKI after imatinib and dasatinib that was approved by FDA for its use in Ph+ ALL. In addition to its inhibitory effect on BCR/ABL by 520-times more potency; it also inhibits VEGFR, FGFR, ephrin, src, c-Kit, RET and FLT3. The novelty of ponatinib among other TKIs is due to its ability to target different mutations in the BCR/ABL kinase domain including the T315I, a point mutation which represents one of the major causes of TKI resistance. Notably, these mutations are

identified in 37% of the patients at the time of diagnosis before the initiation of treatment<sup>43,44</sup>.

In the study by Rousselot et al. they showed T315I mutation that was identified during diagnosis was correlated with early relapses in patients <sup>42</sup>.

In the clinical trials, ponatinib treatment for the patients who are resistant to earlier generation TKIs or carrying T315I mutation, resulted in 38% of CCyR rate and led to a 40% of 1-year OS rate. Ponatinib was also tried in combination with hyper-CVAD chemotherapy by a single-institution phase II study which showed the highest success rates reported so far in the field in terms of CR and OS rates. Their results showed 97% CR rate and no detection of minimal residual disease (MRD). Initial results also showed an estimated 2-year OS by 80% which then was updated by 97% of CR rates in the following study, together with 77% of CMR at the median follow-up of 33 months <sup>45,46</sup>.

In the GIEMMA LAL 1811 trial, ponatinib was used in combination with corticosteroids for the elderly/unfit patients. A remarkable portion of the patients (95%) achieved CHR right after the first cycle. This study also reported 45.8% of CMR rates in patients after ponatinib treatment, which was more than what had been reported in the dasatinib and corticosteroids study <sup>26</sup>.

On the other hand, despite the documented high response by the patients; the concern about the adverse side effects of ponatinib such as heart failures, vascular and arterial problems is still newsworthy and a limitation for the long-term / high concentration usage of ponatinib for patients <sup>47</sup>. Therefore, ponatinib is avoided as much as possible in the clinics except for the patients who already failed previous therapies.

### **1.3.3. Monoclonal Antibodies & Immunotherapy**

Monoclonal antibodies have been recently used as a novel therapy for the treatment of B-ALL. Antibodies targeting the specific markers that are overexpressed in Ph+ ALL lymphoblasts such as, CD19, CD20, CD22 are designed and used as treatment. They can be used in combination with hyper-CVAD chemotherapy and TKI; in such anti-CD20 monoclonal antibody rituximab was tested in a study. The results showed the



patients showed better outcome compared to the ones that received the standard treatment in previous studies <sup>48</sup>.

Another monoclonal antibody, inotuzumab ozogamicin, which is against CD22, was tested in relapsed Ph+ ALL patients and resulted in no significant changes between standard therapy and inotuzumab cohort <sup>49</sup>.

On the other hand, blinatumomab, which is designed to bind CD19 and CD3 bispecifically, has become the most promising monoclonal antibody with significant results in high-risk ALL patients and in Ph+ ALL patients who carry T315I mutation. The results showed 40% of CR rate in the patients with T315I mutation. Additionally, this study showed that blinatumomab was able to reverse MRD status into negative <sup>50,51</sup>.

An important breakthrough has been achieved in immunotherapy for cancer treatment, which is the development of chimeric antigen receptor T cell (CAR T-cell). CAR T-cell treatment is basically a strategy in which T-cells are taken from the patients and modified in the laboratory to express a receptor specific for a tumor antigen, after which it is re-infused back to the patient. These CARs are made up of fusion proteins of one specific monoclonal antibody against the cancer cells and one/more T-cell receptor intracellular domain.

Recently, CAR T-cell clinical trials have been going on for different hematological cancers and showing remarkably promising results <sup>52</sup>. Although the technology is too recent to report long-term outcomes, some studies are suggesting promising results also for Ph+ ALL patients. In a recent study, CD19 targeting CAR T-cells for concurrent chronic lymphocytic leukemia (CLL) and Ph+ ALL, The patient in this study showed reduced levels of detectable BCR/ABL along with no detectable MRD signatures <sup>53</sup>.

#### **1.3.4. Stem Cell Transplant**

Stem cell transplant is a clinical procedure for patients in which healthy stem cells are transplanted into the patients to regenerate healthy blood cells instead of the ones that are damaged by leukemogenesis or by intensive chemotherapy/radiotherapy. The main two types of transplants are allogenic and autogenic transplantation. In allogenic

transplantation (alloHSCT) the patient is given another individual's stem cells. In this case, the donor's bone marrow should match the patient's bone marrow, This can be tested by checking human leukocyte antigens (HLA) on white blood cells. The importance of finding a matching donor is to prevent graft-versus-host-disease (GVHD) in which the healthy transplanted cells attack the patient's cells. The higher the matching HLA score is the lower the GVHD can develop. On the other hand, in autologous transplantation (autoHSCT), the patients are given their own stem cells in which the healthy ones had been collected and selected from the bone marrow before the chemotherapy or radiotherapy starts <sup>54</sup>.

Before imatinib was introduced into Ph+ ALL treatment, patients were only receiving multiagent chemotherapy, which did not exhibit promising outcomes. Patients were undergoing alloHSCT, in case there was an available donor, right after they reach first remission. Patients who have taken alloHSCT showed 36% of 3-year OS compared to 17% of 3-year OS for the patients who received autoHSCT <sup>55</sup>. In a cohort study including 267 Ph+ ALL patients, 28% of the patients underwent alloHSCT in first complete remission resulted in 44% 5-year OS after matched transplant and 19% after chemotherapy. These results confirmed that alloHSCT is more favored over chemotherapy alone <sup>30</sup>. The need for alloHSCT has been questioned after TKIs became the prior treatment agent with much higher effectiveness against Ph+ ALL.

In the GRAAPH-2005 study, after patients were given imatinib with hyper-CVAD or steroids; the ones who had an available donor received alloHSCT after CR1. There were no detectable differences in RFS and OS rates between patients who received alloHSCT or autoHSCT <sup>31</sup>. Recently by using ponatinib and hyper-CVAD in the frontline for Ph+ ALL patients, more patients achieved molecular remission independently from whether they have undergone alloHSCT or not. These results showed the alloHSCT can be expendable in CR1 since it did not serve as a predictive factor for OS <sup>56</sup>.

#### **1.4. Resistance to Tyrosine Kinase Inhibitors**

There has been a consensus about how imatinib and other generation TKIs have moved Ph+ ALL treatment to a new era. Although the prognosis for CML patients have

improved, it is estimated that one third of these patients that are on the first-line therapy will develop resistance to imatinib and, thus, eventually require other therapies <sup>57</sup>. TKI resistance mechanisms can be grouped into two, BCR/ABL dependent and independent mechanisms. BCR/ABL dependent mechanisms includes BCR/ABL amplification or mutations in the TKI binding site, which is most commonly researched in clinical studies <sup>58,59</sup>. TKI resistance can also be classified based on how the resistance occurs as such primary or intrinsic and secondary or acquired resistance. In intrinsic resistance, the resistance mechanism already exists in the patients and therefore these patients do not respond to TKI treatment at all. On the other hand, acquired resistance is developed by time as the patient is exposed to long-term TKI treatment. Therefore, despite there is an initial response detected in patients, the established response is getting lost afterwards <sup>43</sup>. Different TKI resistance mechanisms seen in cancer cells are discussed detailed in the following section.

#### **1.4.1. BCR/ABL Mutations**

Most of the resistance (both types) is thought to be caused by mutations in the kinase domain of BCR/ABL protein. In the intrinsic resistance, BCR/ABL is initially mutated in the leukemic blasts, which makes TKIs dysfunctional from the beginning of the treatment. But in the acquired type of resistance, the model suggests that, non-resistant cells are eliminated during the first round of TKI treatment, which presents a survival advantage for the resistant clones. In many studies, it has been shown that consecutive TKI treatment results in more commonly observed TKI resistance <sup>36</sup>. Interestingly, in a group of patients who received imatinib and dasatinib treatment with no detected remission, newly formed BCR/ABL mutations, which were not detected after imatinib treatment, were observed. These group of patients are able to gain mutations against multiple drugs not just TKIs <sup>36</sup>.

The nature of this type of mutations is to occur at the critical locations where only TKI binding is prevented, however ATP binding and kinase activity is still allowed. Since each TKI bind the BCR/ABL in a specific conformation, resistance profiles differ between different TKIs. Some mutations occur at the active kinase site, which blocks TKI

binding locally, on the other hand, other mutations occur at residues that result in changing the whole 3D structure of the protein <sup>36,58</sup>. For example, since imatinib and nilotinib can only bind to inactive form of BCR/ABL, imatinib or nilotinib resistant patients usually show destabilization of the inactive conformation of BCR/ABL, which prevents the binding of these TKIs. So far, at least 55 residues that cause imatinib resistance at different levels have been identified <sup>58</sup>.

In a cohort study including 1700 patients that harbor BCR/ABL mutations were investigated. They reported that 11% of the patients were carrying at least 2 mutations in the kinase domain which can be seen as compound or polyclonally. Having multiple mutations in the same BCR/ABL molecule is referred to as compound mutations and makes up the majority of the group by 70%. Polyclonal mutations, on the other hand, refers to the ones having different mutations in different BCR/ABL isoforms. This study also confirmed that, specific and repetitive mutations are observed in different TKI resistance profiles. In total, 30 different mutations were observed including T315I, which is the most commonly detected mutation <sup>60</sup>.

In different studies that investigate BCR/ABL mutations in Ph+ ALL, many point mutations were identified and associated with different TKI resistance. O'Hare et al. showed that M244V and H396 mutations are associated to imatinib resistance but responsive to second generation TKIs <sup>61</sup>. In another study, they showed that dasatinib was able to overcome resistance caused by H396R mutation <sup>62</sup>. Although some newer generation TKIs target BCR/ABL protein that is carrying most of the mutations, there is still need for better coverage in terms of TKI targets.

### **1.4.2. Gene Amplifications**

BCR/ABL gene amplifications are known as the driver mechanism of oncogenic activation. Importantly, studies in the field suggest that gene amplification is the second major TKI resistance mechanisms, following BCR/ABL mutations, seen in the clinics. The long-term exposure to the drug can induce the amplification of the target gene, which might result in an increase in the protein levels of the target gene <sup>63,64</sup>. As a result, the tolerable amount of the drug becomes insufficient to successfully inhibit the targeted

protein and drug-target interaction is disrupted. This idea was suggested for the first time in a study that showed that the overexpressed oncogenes are located in the extrachromosomal site, thus, causing oncogenic stress, perturbed chromatin organization and unsymmetrical nuclear division <sup>65</sup>. This situation was observed as BCR/ABL amplification in the CML patients who were relapsed after imatinib treatment in which intensification of imatinib was not enough to achieve sufficient response from the patients <sup>66</sup>. Additionally, the same mechanism is confirmed by an in vitro study where continuous exposure to imatinib resulted in BCR/ABL amplification <sup>67</sup>. In a study where Mahon et al. generated imatinib resistant cells; Abl gene amplification was detected in the resistant clones <sup>68</sup>. Similarly, this type of mechanism of resistance was observed in other cases where EGFR or FLT3 was amplified as a result of their inhibitors <sup>69,70</sup>.

A second type of resistance caused by the amplification of certain genes is through amplification of genes that are in alternative signaling pathways which can compensate the lack of main signaling pathways <sup>71</sup>. An important example for such a mechanism is the amplification of MET gene, which encodes the receptor tyrosine kinase for hepatocyte growth factor in non-small cell lung cancer (NSCLC) patients. In different studies, increased levels of MET gene expression were detected in response to continuous treatment of EGFR inhibitors including gefitinib <sup>72-74</sup>. As a result, MET amplification caused constitutive receptor activation independently from a ligand that led to activation of downstream pathways <sup>74</sup>. Lately, targeting genes directly by using new gene-editing tools such as CRISPR are studied to prevent effects of gene amplifications in cancer.

### **1.4.3. Genomic Deletions**

Genomic deletions are a type of mutations, which can also be described as the loss of a certain part of a DNA sequence or a part of a chromosome. The size of the deleted part in the genome can vary from a single base to a whole chromosome. This mechanism come across as a resistance mechanism against TKIs. In a study, bone marrow samples from CML patients were collected first before the treatment starts and again after relapses were observed; and genome wide comparative genomic hybridization (CGH) was performed. They detected genomic deletions were responsible from 28% of the copy

number alterations in which the genes involved in mitogen-activated protein kinase (MAPK) signaling pathway were found to be the most frequently altered ones <sup>75</sup>.

On the other hand, miRNAs, which have a regulatory effect on many genes that are involved in cancer development and progression are among the genes that are most frequently deleted. MiRNAs have the ability of binding complementary sequences of transcribed mRNAs in the genome, which cause those mRNAs to degrade, thus resulting in a lack of the translation of the encoded protein. The proteins that are downregulated by miRNAs can be overexpressed again due to a deletion in the genomic region of certain miRNAs that are involved in those proteins' regulation <sup>76,77</sup>. In the same context, in a recent study, it was shown that miR-21 overexpression was associated with high EGFR activation in NSCLC cell lines and patient samples. They confirmed these results by inhibiting EGFR with AG1478 which resulted in downregulation of miR-21 <sup>78</sup>. Different groups have shown the regulation of resistance by miRNA expressions which is thought to be related to TKI resistance as well <sup>79,80</sup>. Indeed, in a study conducted by Nishioka et al. it was reported that downregulation of miR-217, which cause upregulation of DNA methyltransferases (DNMT) expression, was correlated to TKI resistance. To confirm, overexpression of miR-217 inhibited (DNMT) expression by binding of miR-217 to 3'-untranslated region (UTR) of DNMT3A, thus, resulting in the sensitization of TKI-resistant K562 cells to treatment <sup>81</sup>. Also in another study, a common genetic deletion polymorphism in B-cell chronic lymphocytic leukemia-lymphoma like 11 gene (BIM) was identified as a cause of resistance to TKI therapy, which was especially correlated to intrinsic resistance <sup>82</sup>. Recently, in another study, it was reported that exon 7 deletion in BCR/ABL gene and p.E282Q and p.L298R point mutations were correlated to TKI resistance in CML cases <sup>83</sup>. Genomic deletions were identified as a TKI resistance mechanism in Ph+ ALL too. In a cohort study with 97 Ph+ ALL patients, it was reported that deletions in CDKN2A/2B genes caused negative response to TKI <sup>84</sup>.

#### **1.4.4. Alterations in Protein Expression**

Among various mechanisms of developing resistance against chemotherapeutic drugs, the most common one is for a cell to increase the expression level of the direct

target or secondary target proteins. Although in some cases, alterations in protein expression is placed under the same mechanism as gene amplification; this type of mechanism differs from gene amplification by only accounting for the protein expression levels and not including gene alterations. Same adaptive mechanism is observed in TKI resistance as upregulation of BCR/ABL protein expression levels. A study have shown that nilotinib resistant CML cells have an upregulation in the expression levels of BCR/ABL protein <sup>85</sup>.

On the other hand, epigenetic modifications or environmental stress could also trigger this type of adaptive mechanism. It has been proven that long-term TKI exposure cause a decrease in the blood flow, which results in an increase in the incidence of hypoxic areas. This situation brings the upregulation of HIF-1a protein, which can induce multiple gene expressions such as MET, RTK that will eventually lead to an activation of the key survival pathways including MAPK and PI3K <sup>86</sup>. In another study, hypermethylation in PTEN gene promoter was detected in gefitinib resistant lung cancer cell, this study have shown that when PTEN was induced by exogenous activation, the cells were sensitized back to gefitinib <sup>87</sup>. Another survival-promoting protein Yes-associate protein (YAP) was also shown to be involved in TKI resistance in a study conducted by Lee et al. They showed that an increase in YAP protein levels leads to TKI resistance in lung cancer cells and suggested the usage of YAP inhibitors together with TKI as a treatment strategy <sup>88</sup>.

#### **1.4.5. Activation of Alternative Signaling Pathways**

BCR/ABL, a driver protein in leukemogenesis of CML and Ph+ ALL, activates multiple secondary signaling pathways that regulate proliferation, cell cycle regulation, survival etc. Cancer cells can activate those secondary signaling pathways through bypassing BCR/ABL activation or can activate alternative BCR/ABL independent signaling pathways to promote proliferation. The same mechanism is observed in resistance to various TKIs.

Gefitinib targets epidermal growth factor receptor (EGFR) and interrupts the signaling through EGFR. In the case of gefitinib resistance, instead of the signaling through EGFR; the cells activate HGF, MET, MAPK/extracellular signal regulated kinase

(ERK)1/2 and PI3K/Akt signaling cascade as an adaptive resistance mechanism <sup>89</sup>. On the other hand, insulin-like growth factor-1 (IGFR-1) overexpression is detected as a compensatory mechanism for the lack of EGFR signaling. It was shown that heterodimerization of EGFR and IGFR-1 results in activation of PI3K/Akt and MAPK pathways which eventually leads to resistance to gefitinib <sup>90</sup>. Some other mechanisms including loss of PTEN or Gab1/Shp2 overexpression by a PI3K-dependent induction were also reported as resistance mechanisms by different studies. Constitutive activation of Akt due to PTEN instability results in cetuximab and/or gefitinib resistance <sup>91</sup>. In another study, dephosphorylation of Akt, ERK and STAT5 was not achieved by imatinib in imatinib resistant cells while PTEN deactivation was detected <sup>92</sup>. Also, silencing of PTEN gene was shown to increase EGFR activity by disrupting the ubiquitylation and degradation of the receptor through degradation of newly formed ubiquitin ligase complex <sup>93</sup>.

In an important study by Quentmeier et al., it was shown that the insensitivity of BCR/ABL positive cell lines to imatinib is due to the activation of BCR/ABL independent PI3K/Akt/mTOR signaling. In a study, some signaling cascades other than PI3K such as ERK, JAK/STAT were inactivated due to imatinib. The inhibition of those pathways individually did not have any effect on cell proliferation. On the other hand, in contrast to imatinib, inhibition of PI3K, PDK1 and mTOR was able to inhibit PI3K/AKT1/mTOR signaling. This suggests that PI3K pathway is constitutively activated through an imatinib-independent mechanism, which may include RAS, CBL or p85 genes, in imatinib resistant cells <sup>94</sup>.

Another important mechanism for resistance to TKI is the overexpression of genes, which belong to the family of inhibitor of apoptosis. One of the most commonly observed mechanism is overexpression of survivin protein, which is encoded by BIRC5 gene. Survivin works by inhibiting caspase activation that leads to dysregulation of apoptosis. Overexpression of survivin has been associated with chemoresistance by different studies. In a study by Xia et al., survivin overexpression was detected in lapatinib resistant breast cancer cells and confirmed by clinically collected data <sup>95</sup>. Additionally, survivin was detected at higher levels in the blast crisis and accelerated phases in CML patients, which suggests the involvement of survivin in the progression of CML patients from chronic phase to further aggressive phases <sup>96,97</sup>. Another study have shown that the level of survivin was correlated to the level of BCR/ABL expression, thus, suggesting that survivin may be regulated by BCR/ABL kinase. This mechanism, then, was



confirmed by Carter et al., where survivin expression was targeted by BCR/ABL and MAPK at mRNA and protein levels in a patient during the blast crisis phase. Additionally, inhibition of survivin was shown to increase imatinib sensitivity and overcome resistance in CML cells <sup>98</sup>.

#### **1.4.6. Alterations in Drug Influx/Efflux Mechanisms**

Multiple mechanisms have been identified that decrease the intracellular concentration of a chemotherapeutic drug, which results in treatment failure. One of these culprits is the alterations in drug influx/efflux mechanism. The mechanism is represented by either an increase in the expression of efflux pumps or a decrease in the levels of influx pumps. The major efflux pumps are listed as ATP-binding cassette (ABCB1)/P-glycoprotein (P-gp) and ABCG2/breast-cancer-related protein (BCRP) whereas the most commonly studied influx pump is organic cation transporter-1 (Oct-1) <sup>99</sup>. Although some TKIs have been detected to inhibit ABC transporter activities by binding to their ATP-binding sites, this type of mechanism is still observed in the cases of TKI resistance. TKIs such as cediranib, lapatinib and sunitinib have been reported to reverse resistance through transporter proteins by inhibiting the action of ABC proteins. Herewith, using those inhibitors have been suggested for combinational therapies in cancer treatment <sup>100,101</sup>.

Different studies have reported the involvement of efflux pumps in chemotherapy resistance. ABCB1 was shown to play different roles in chemoresistance in various leukemias. In a study by Mahon et al., it was shown that imatinib resistant cells overexpressed P-gp, which was later confirmed by different studies where they sensitized cells to imatinib through the inhibition of P-gp pump activities by using different inhibitors or RNAi <sup>102-104</sup>. Although second generation TKIs were able to overcome imatinib resistance in some cases, P-gp was found to contribute to nilotinib resistance as well <sup>85</sup>. Importantly, dasatinib and sunitinib have been shown to be substrates of ABCB1 and -2 <sup>105,106</sup>. Gefitinib on the other hand, has been shown to inhibit ABCG2 activity <sup>107</sup>.

Clinical studies have confirmed the association between efflux proteins and chemotherapy resistance. In a cohort study, it was reported that the response to daunorubicin and cytarabine was correlated with ABCB1 expression and activity levels

in CML patients who are mainly in the blast crisis phase. This data showed that the BCR/ABL level is not the only determining factor for prognosis of the patients in blast crisis and multiple factors should be considered for the risk of resistance development <sup>108</sup>. In another study, they observed high levels of ABCB1 expression in each phases of the disease in CML patients but detected that ABCB1 was more involved than multidrug-resistant protein 1 (MRP1) in CML patients who are in the blast crisis phase <sup>109</sup>.

BCRP2 on the other hand, is another efflux pump, which was shown to be involved in drug resistance in cancer. It is encoded by the gene ABCG2 and has been studied in different leukemias. In a study by Nakanishi et al. a cell line, which was resistant to substrates of ABCG2 and imatinib, was able to be sensitized to imatinib by inhibiting ABCG2. Interestingly, ABCG2 related imatinib resistance was reduced by inhibition of BCR/ABL, thus, suggesting the regulation of ABCG2 by BCR/ABL <sup>110</sup>. A single nucleotide polymorphism seen in ABCG2 gene is responsible for the expression level, ATPase activity and drug transport functions of ABCG2. Daily concentration of imatinib could be determined by looking at the polymorphism that the patients harbor, such as having 421 C/C genotype requires higher concentrations whereas 421 C/A or 421 A/A genotype could receive lower concentrations of imatinib. So a genetic screening for ABCG2 gene could be a useful approach to make dosage decisions for the patients <sup>111,112</sup>.

## **1.5. BCR/ABL Signaling Mechanisms**

As of 1990, BCR/ABL has been identified as the driver oncogene in the progression of CML and Ph+ ALL <sup>113</sup>. Since then, the mechanism and the working principle of BCR/ABL has been extensively studied and well-understood. Two key motifs within BCR site has been determined to be certainly required for leukemia formation. One of the motifs is located at the N-terminus of the protein and responsible for heterodimerization, phosphorylation and activation, which leads to the activation of downstream signaling pathways. The second motif is the binding site for GRB2 adapter protein and found to be stoichiometrically phosphorylated in leukemic cells. GRB2 together with GAB2 activates PI3K pathway, which contributes to survival and proliferation of leukemic cells <sup>114</sup>. In a study, GAB2 was suggested as the strongest

contributor to BCR/ABL independent TKI resistance since it was amplifying the signal coming from BCR/ABL towards targets such as PI3K and RAS pathways <sup>115</sup>.

One of the major pathways that is activated through BCR/ABL signaling is PI3K/AKT/mTOR pathway, which was activated through GAB2. The PI3K signaling has been shown to have important roles in BCR/ABL driven leukemogenesis <sup>116</sup>. In recent studies, it was reported that TGF- $\beta$  in addition to AKT signaling play important roles in leukemia progression. Naka et al. showed that AKT, nuclear FOXO3a and SMAD2/3 are inactivated in the progenitor CML cells in mice while it was known that BCR/ABL activates PI3K, which causes phosphorylation and enables the transport of FOXO3a to the nucleus <sup>117</sup>. On the other hand, mTOR, which is located downstream to PI3K/AKT pathway, is a serine/threonine kinase and functions together with two complexes mTORC1 and -2. It was also demonstrated that both of the TORC proteins are important in the survival and proliferation mechanisms in BCR/ABL positive cells <sup>118</sup>. In a study by Mohi et al., using the mTOR inhibitor rapamycin in combination with imatinib has been found to prolong survival in CML models as well as being effective in resistance caused by BCR/ABL mutations <sup>119</sup>. In other studies including patient samples and BCR/ABL positive cell lines, mTORC1/2 inhibitors showed inhibitory effects on proliferation <sup>120,121</sup>.

AMP-activated protein kinase (AMPK) pathway is another pathway that regulates mTOR signaling in a direct and an independent manner. After activation, AMPK activates TSC complex by phosphorylation, thus, resulting in the suppression of Rheb activity, which is a regulator of mTOR activation <sup>122</sup>. In an important study by Puissant et al., using resveratrol, which is a natural flavonoid found in red grapes, showed inhibitory effects on cell proliferation of imatinib sensitive and resistant CML cells even the ones carrying T315I mutation, through the modulation of AMPK <sup>123</sup>. The fact that AMPK induction causes mTOR inhibition independent of the resistance status, therefore, suggesting the idea of using AMPK activators in BCR/ABL positive leukemias <sup>124</sup>.

Phosphorylation of Tyr177 in BCR site regulates the SH2 dependent binding of GRB2 to BCR/ABL protein. Similar to GRB2, son of sevenless (SOS), which is an effector of GRB2, regulates RAS activation.

Additionally, it has been reported that BCR/ABL can activate ERK by the signaling through RAS/RAF/MEK/ERK pathway <sup>125,126</sup>. ERK has been found to be constitutively active in BCR/ABL transformed stem cells. Importantly, ERK has been shown to be involved in imatinib resistance as well <sup>120</sup>.

The role of JNK pathway, which is another major signaling pathway in the cells, has not been fully elucidated in leukemia. Whereas some studies suggested the proapoptotic roles of JNK in response to different agents in BCR/ABL positive cells, some others have shown that BCR/ABL induced leukemia promoting features of JNK. Mancini et al. reported that BCR/ABL activity inhibits JNK activation whereas imatinib causes rephosphorylation of JNK, thus, resulting in activation of apoptosis<sup>127</sup>. Moreover, resveratrol treatment has been shown to induce autophagy in CML cells through JNK dependent accumulation of p62<sup>123</sup>. All these studies exhibited the controversial roles of JNK pathway in BCR/ABL induced leukemogenesis and more needs to be done to clarify its exact role.

Phosphorylation and constitutive activation of STAT5 has been identified in different hematological cancers including BCR/ABL positive leukemias. Additionally, STAT5 activation has been shown to contribute to growth and viability in BCR/ABL transformed cells. In other studies, silencing STAT5 by siRNA inhibited colony formation in CML progenitor cells<sup>128,129</sup>. Together with the roles of STAT5 in a BCR/ABL dependent manner, JAK kinases have been found to be activated in BCR/ABL positive cells<sup>130</sup>. JAK2 can form a complex with BCR/ABL through C-terminus of BCR/ABL and is involved in the activation of SRC kinase LYN. However, JAK2 or the binding site on BCR/ABL are not found to be required for the induction of leukemia<sup>131,132</sup>. On the other hand, the involvement of JAK2 signaling in the TKI resistance has been suggested however there is a need for it to be further investigated together with the need of further investigation<sup>133</sup>.

Hedgehog (Hh) pathway has been identified as one of the key signaling pathways that are essential for stem cells throughout differentiation. The signaling through this pathway finalizes with translocation of GLI transcription factors into the nucleus, which results in cell proliferation, survival through mediation of the expression of Cyclin D, c-myc and BCL2 genes<sup>134</sup>. The involvement of Hh pathway in the CML progression has been identified by Dierks et al. where they showed an overexpression of SMO, GLI1 and PTCH1 in BCR/ABL transformed cells in mice. Additionally, this data was confirmed with data from patient samples who are either in chronic or blast crisis phase<sup>135</sup>. It was also reported that *Smo* deficient mice showed downregulation of BCR/ABL levels and the incidence of CML-like leukemia. SMO antagonist cyclopamine treatment has been shown to prolong survival in addition to a decrease in the CML stem cells. In a promising

clinical study, another SMO antagonist P-04449913 (Pfizer) showed a dramatic elimination of stem cells in different leukemias including CML <sup>136</sup>

Last but not least, Wnt/ $\beta$ -catenin pathway works as another downstream pathway of BCR/ABL signaling. Its association with BCR/ABL has been identified for the first time in a study where they detected an accumulation of nuclear  $\beta$ -catenin in granulocyte progenitor cells in CML patients who are in blast crisis <sup>137</sup>. The elevated levels of  $\beta$ -catenin have been linked to self-renewal features of malign progenitor cells. Additionally, the role of Wnt pathway in CML progression has been reported in other studies in which various target genes of Wnt including c-myc, cadherin, MDI1, FZD2, prickle 1 and ROK13A has been found to be overexpressed during accelerated phase and blast crisis in CML patients <sup>138</sup>. In a recent study, it was suggested that  $\beta$ -catenin signaling was required in CML stem cells but not in normal hematopoietic stem cells suggesting  $\beta$ -catenin to be a potential target in earlier phases of the disease <sup>139</sup>.

## 1.6. Bioactive Sphingolipids

Bioactive sphingolipids are a major class of lipids that have structural roles in membrane formation in addition to their involvement in various cellular mechanisms including growth, proliferation, cell cycle regulation, signal transduction, cell-cell interactions, recognition, etc. Sphingolipids were isolated for the first time from the brain tissue by J. L. W. Thudichum who named them as “sphingosin”, inspired from the Greek mythical creature, the Sphinx <sup>140</sup>. Further studies have clarified the chemical structures and biological roles of sphingolipids. Sphingosine structurally is the major sphingoid base and found in all sphingolipids, which is the distinguishing characteristics of sphingolipids among all lipids. Sphingolipid metabolism is mainly found in eukaryotes but exceptionally it is found in the *Sphingomonas* bacteria. The sphingolipid pathway has a metabolic entry point which starts with the enzyme serine palmitoyl transferase and has an exit point where sphingosine-1-phosphate (S1P) lyase is produced. Multiple pathways together with complex crosstalks are involved in the sphingolipid metabolism <sup>140</sup>.

Ceramide, being the central hub of the sphingolipid metabolism, is located at the central position in the sphingolipid metabolism. As a first step in the sphingolipid *de novo*

synthesis pathway serine palmitoyl transferase (SPT) catalyzes the reaction for the condensation of serine and palmitate to form 3-keto-dihydrosphingosine. A series of reactions eventually ends up with the production of ceramide followed by production of other sphingolipids <sup>141,142</sup>. In the first downstream pathway, ceramide is phosphorylated and ceramide-1-phosphate (C1P) is produced by the action of the enzyme ceramide kinase (CK); or sphingomyelin (SM) can be produced by addition of a phosphocholine headgroup taken from phosphatidylcholine (PC) to ceramide which is catalyzed by sphingomyelin synthases (SMS) <sup>143–145</sup>.

On the other hand, ceramide can be converted into glucosylceramide and galactosylceramide by receiving a glucose molecule through the action of glucosylceramide synthase (GCS) and therefore complex sphingolipids are produced. All those reactions that are converting ceramide to other sphingolipids are reversible. For example; the breakdown of glucosylceramide and galactosylceramide back to ceramide is catalyzed by a hydrolyzing reaction through  $\beta$ -glucosidases and galactosidases. Also, SM is converted back to ceramide through the action of several sphingomyelinases (SMase) including acid SMase, neutral SMase and alkaline SMase <sup>146–148</sup>.

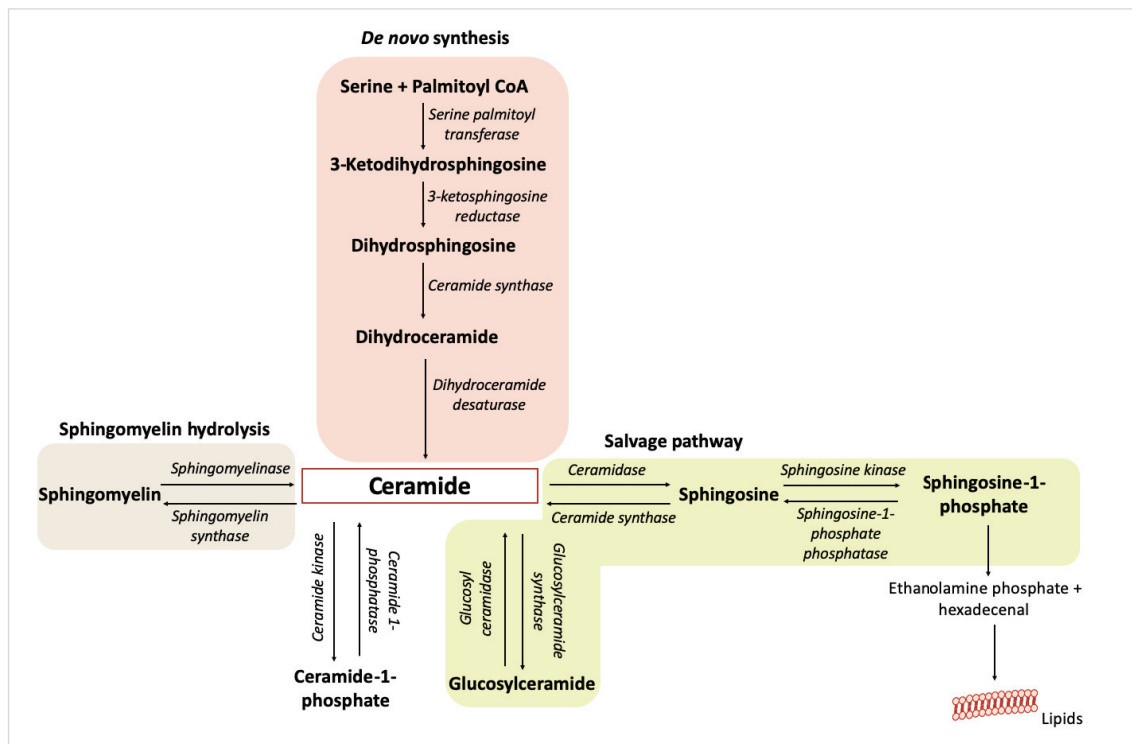


Figure 1.2. Sphingolipid synthesis and metabolism.

Ceramide, itself can be broken down and form sphingosine by multiple ceramidases. Here, sphingosine may go into “salvage pathway” and recycled back into sphingolipid pathway or can be phosphorylated by the enzyme sphingosine kinases (SK-1 and SK-2) and produce sphingosine-1-phosphate (S1P). Again, the reaction can be reversed by S1P phosphatases. Moreover, S1P is cleaved by S1P lyase and forms ethanolamine phosphate and hexadecenal. As the final recycling step, ethanolamine phosphate and hexadecenal can be reduced to palmitate and as mentioned, can be used in the first step of sphingolipid *de novo* pathway<sup>149-152</sup>. Sphingolipids exhibit a complex and interconnected pathway, which orchestrate cellular reactions through biochemical interactions. In a cell, when SMases are activated, ceramide is produced as a response however, this ceramide might be converted to C1P, S1P or glucosylceramide through subsequent action of the responsible enzymes such as ceramidase, CK, SK, GCS or SMS. On the other hand, relative levels of these sphingolipids might create a response at higher levels than expected. As an example; SM usually abounds in the cells, which makes small changes in SM to reflect severe changes on ceramide levels. Additionally, the concentration of ceramide in the cells is an order of magnitude higher than those of sphingosine, which results in the same situation where small changes in ceramide levels can reflect as double amount of changes in sphingosine levels. Similarly, a small amount of phosphorylation in the sphingosine (2-3%) might result in 2-3-fold changes in the S1P levels. Therefore, when an enzyme in the sphingolipid metabolism responds to a change in the cells, there might be other signaling effectors other than the direct product of this enzyme. Consequently, determining the actual sphingolipid that is mediating the signal carry importance in these type of processes in the cells.

The signaling and regulatory effects of sphingolipids are in part due to subcellular localization of sphingolipids. For example, neutral SMase 2 is usually found in the inner leaflet of the plasma membrane while acid SMase is located to the endolysosomal pathway but can be relocated to the outer leaflet of the plasma membrane. In addition, SK-1 and SK-2 usually take action on the sphingosine substrates that resides in the membranes, which results in the translocation of these enzymes to the membranes from their cytosolic compartment. Therefore, SK enzymes are known as having various subcellular localizations, which could determine their final functions<sup>153,154</sup>.

Bioactive sphingolipids can be divided into three subgroups based on their biophysical properties as follows: the ones carrying ionic charges and neutral pH; the ones carrying neutral hydrophobic molecules and the ones possessing single-chain lipids.

C1P and phosphatidylinositol-3-phosphate belong to the first group and they usually are unable to move from their own compartments and unable to flip across bilayer membranes. Ceramide and diacylglycerol (DAG) on the other hand, are under the second group and are stable at their compartment, but able to flip across membranes<sup>155</sup>. S1P and derivatives of sphingosine falls under third group and are composed of a single chain, in addition to that, they have the ability to dissolve in aqueous environment and flip between membranes<sup>156</sup>.

### **1.6.1. Ceramide Metabolism and Signaling**

The structure of ceramide is formed of sphingosine composed of an amine linked fatty acid chain that varies in length from C14 to C26. It has been indicated that ceramides having different fatty-acid chain length are responsible for different functions in the cells. Therefore, ceramide synthase (CerS) genes carry importance in the cell fate. CerS genes were first identified as longevity assurance gene (LAG1) due to their roles in longevity/life-span in *Saccharomyces cerevisiae*<sup>157</sup>. Afterwards, the mouse homologue LASS1 was discovered and identified to be responsible for the synthesis of C18-ceramide<sup>158</sup>. Other classes of CerS genes were identified later on and named as LASS proteins (LASS1-6), which were then renamed as ceramide synthases 1-6 (CerS1-6). CerS proteins reside in the endoplasmic reticulum (ER) membrane and they contain a TLC (TRAM-Lag1p-CLN8) domain. This domain is crucial for the catalytic activity of CerS and required for the synthesis of ceramides<sup>159</sup>. In addition, all CerS except for CerS1 contain another domain, which is the homeobox transcription factor (HOX) that is known to be responsible for the enzymatic activity, however, the physiological roles of this domain remain unclear<sup>160,161</sup>.

As mentioned before, each CerS is responsible for the synthesis of ceramides with different fatty-acid chain lengths. It has been identified that CerS1 catalyzes the synthesis of C18-ceramide whereas CerS5-6 is responsible for the generation of mainly C16-ceramide in addition to C12- and C14-ceramides. CerS2 on the other hand generates long chain ceramides such as C22-, C24- and C26-ceramide. CerS3 was shown to contribute



to the synthesis of C18- and C24-ceramides whereas CerS4 is responsible for the generation of C18- and C20-ceramides <sup>162</sup>.

*De novo* synthesis of ceramide occurs in the ER and the reaction starts with a key enzyme SPT, which catalyzes the condensation of serine and palmitate to form 3-keto-dihydrosphingosine. Then, 3-keto-dihydrosphingosine is reduced to dihydrosphingosine by the enzyme 3-ketosphingosine reductase. The formed dihydrosphingosine is converted to dihydroceramide by the family of CerS; followed by the final step to produce ceramide catalyzed by dihydroceramide desaturase (DEGS) <sup>163</sup>. Newly generated ceramides are transported to Golgi apparatus by two different mechanism; either by vesicular trafficking or with the help of ceramide transfer protein (CERT). Further metabolization of ceramide to generate other complex sphingolipids occurs in Golgi apparatus.

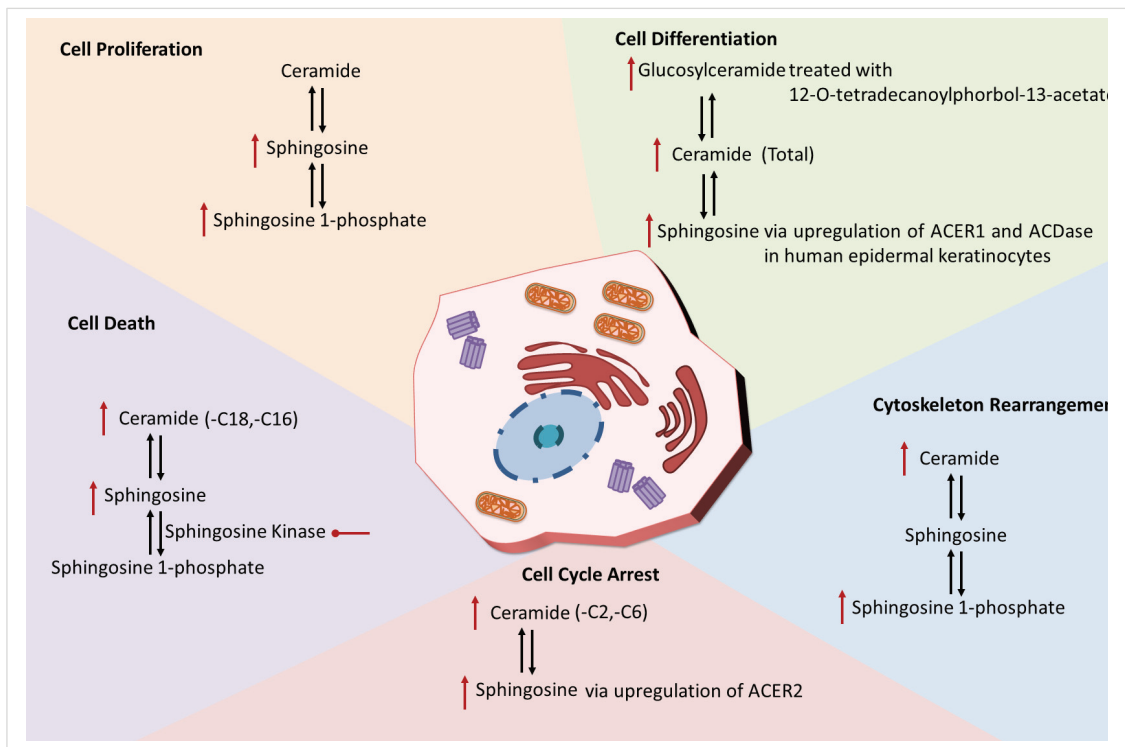


Figure 1.3. Major sphingolipids and their involvement into cellular mechanisms.

Different studies have revealed the involvement of CerS genes and ceramides in cancer progression. In a study by Karahatay et al. although C18-ceramide levels were detected as low; C16-ceramide levels were detected as dramatically high in head and neck squamous cell carcinoma (HNSCC) patients compared to their own health tissues. The levels of C16- and C18-ceramides were associated with the expression levels of CerS1

and -6 genes <sup>164</sup>. In a recent study conducted with the participation of 44 patients, they reported that ceramide levels were elevated in breast cancer patients. Moreover, they showed that the levels of ceramides are inversely correlated with the aggressiveness of the cancer; <sup>165</sup>.

Ceramide is involved in different cellular functions in cancer such as growth inhibition, apoptosis or senescence. The regulation of these biological mechanisms occurs through lipid-protein interactions <sup>166,167</sup>. In most of the cases, direct targets of ceramide are either protein phosphatases or kinases, which control the activation of important signaling pathways that promote and maintain cancer progression. Akt, protein kinase C (PKC) and MAPK pathways are identified as downstream targets of ceramide. The first identified ceramide-associated regulatory proteins are phosphatase-1 and -2 (PP1 and PP2A), which are also known as Ceramide Activated Protein Phosphatases (CAPP) <sup>166,168</sup>. The activation of CAPPs induces the activation of apoptotic Bcl-2 proteins, cell cycle regulatory proteins cyclin dependent kinases (CDK) and the tumor suppressor protein Rb <sup>166</sup>. Additionally, ceramide activates cathepsin D, which is a ceramide binding protein that results in activation of apoptosis. Similar to cathepsin D activation, ceramide also activates protein kinase zeta (PKC-zeta) that induces the formation of a pro-apoptotic complex composed of PKC-zeta and PAR-4 (prostate apoptotic response-4) in stem cells that undergo differentiation process <sup>169,170</sup>. Moreover, the activation of PKC-zeta has been shown to inactivate Akt, which results in growth arrest in vascular muscle cells. One of the best characterized ceramide-binding protein, CERT, has been shown to be involved in the sensitivity of cancer cells against chemotherapeutic agents. Therefore, it was suggested that the changes in sphingolipid metabolism regulated by CERT might be an important factor in the survival fate of cancer cells <sup>171,172</sup>.

### **1.6.2. Antiproliferative Roles of Ceramide**

The predominant function of ceramide is to induce apoptosis in cancerous cells. Apoptosis is a process, which can be triggered by different factors and orchestrated by multiple signaling pathways. The role of ceramide in apoptosis has been suggested by different studies where ceramide production was shown to be regulated by the apoptosis-

inducing factors such as stress, different signals, chemotherapeutic drugs etc. Moreover, many different studies in the literature showed that increasing the endogenous level of ceramides by using different inhibitors of sphingolipid pathway's enzymes results in apoptosis in cancer cells <sup>162,173-178</sup>. It was also reported that exogenous treatment with ceramide induces apoptosis in different cancers including leukemia.

Obeid et al. for the first time, identified the pro-apoptotic function of ceramide by exposing cells to C2-ceramide, which is a synthetic ceramide analog N-acetylsphingosine, This resulted in DNA fragmentation, which is characteristic response for apoptotic cells <sup>176</sup>. Similarly, it was shown that C6-ceramide induced apoptosis through inhibition of Bcl-2 <sup>179</sup>. Since then, the role of ceramide as a secondary lipid messenger in apoptotic signaling pathway has been investigated by many studies.

The apoptotic roles of ceramide have been studied in leukemia. In different studies, exogenous treatment with C2- and C6-ceramide has been shown to induce apoptosis in K562, a CML cell line <sup>180,181</sup>. The apoptotic function of C6-ceramide has been shown to be associated with caspase-8 and JNK signaling in K562 cells <sup>180</sup>. Moreover, different delivery methods of ceramide such as through nanocarriers have been identified to inhibit large granular lymphocytic leukemia (LGL) in mice models. Liu et al. reported the apoptotic action of ceramide was through downregulation of surviving, which is an anti-apoptotic protein <sup>182</sup>.

The effect of exogenous ceramide treatment is thought to be through its resembling action of intracellularly induced ceramide generation. Exogenous ceramide was shown to induce the expression of CerS genes, thus, leading to the generation of endogenous ceramide <sup>183</sup>. Notably, the cellular functions of ceramide vary by the length of fatty-acid chain. In a study where C16-ceramide was detected as low and C18-ceramide as high, suggesting the pro-apoptotic role of C18-ceramide but not C16-ceramide in HNSCC patients <sup>164,184</sup>. In another study, overexpression of CerS6 was shown to induce the growth of HNSCC cells whereas the production of C18-ceramide through CerS1 overexpression inhibited the proliferation of these cells <sup>185</sup>.

Another well characterized function of ceramide is to induce cell cycle arrest especially at G0/G1 phase. This action of ceramide is associated to the activation of the tumor suppressor protein retinoblastoma (Rb). Ceramide has been reported to inhibit CDK2 through activation of phosphatase whereas showing no detectable effect on CDK4 <sup>186,187</sup>. The growth inhibitory effect of ceramide has been shown by an in vivo study where using ceramide coated catheters caused growth arrest in vascular muscle cells. Later on,

the mechanism has been shown to be through inhibition of Akt by ceramide, which was regulated by PKC-zeta activation <sup>188,189</sup>.

In addition to ceramide's role in activation of apoptosis and its growth inhibitory effects, it is also capable of inducing senescence. This latter role of ceramides was suggested for the first time by Veneable et al. where they showed an increased level of ceramides in human fibroblasts that were undergoing senescence <sup>190</sup>. In the same study, senescence related morphological and biochemical changes including activation of Rb and alterations in CDKs were detected in response to ceramide treatment. Senescence is known to be regulated by alterations in telomere length through the activation of telomerase. Telomerase is identified as a down-stream targets of ceramide, therefore, suggesting a relation between aging/senescence and ceramide. Ceramide is known to regulate telomerase activation either by dysregulation of c-myc, which results in the inactivation of hTERT promoter or the recruitment of Sp3/HDAC1 complex into hTERT to promote its repression <sup>191,192</sup>. Additionally, shortening of telomeres through an independent mechanism from telomerase was shown to be regulated by ceramide with an action through the telomere binding function of glyceraldehydes-3-phosphate dehydrogenase (GAPDH) <sup>193</sup>.

### **1.6.3. Bioactive Sphingolipids in Drug Resistance in Cancer**

As mentioned and detailed previously, drug resistance against chemotherapeutic drugs is the main obstacle in cancer therapy. The relationship between cancer drug resistance and sphingolipid metabolism has been reported in various studies. Therefore, targeting sphingolipids as an approach against drug resistance has been suggested and applied in various studies involving different type of cancers <sup>194–196</sup>.

The most common mechanism of resistance through sphingolipids is the alteration of ceramide accumulation in the cells. Most of the generated ceramide is metabolized into glucosylceramides by overactivation of GCS in some cancers. This action was identified to contribute to development of drug resistance including many different cancers, especially breast cancer <sup>195,197</sup>. The action of GCS is known to occur through multiple mechanisms including an action through P-gp (drug transporter protein); decreasing the

concentration of C18-ceramide and causing accumulation of different glycosylceramide species. The link between GCS and MDR has been implicated by different studies. It was shown that silencing GCS by siRNA transfection resulted in the inhibition of MDR1 expression, which leads to the reversal of drug resistance<sup>198,199</sup>.

Moreover, a P-gp inhibitor has been shown to inhibit GCS and cause a decrease in glucosylceramide levels<sup>198</sup>. The effect of GCS on drug resistance has been addressed in other cancers including colon cancer, head and neck carcinoma, melanoma and leukemia. Increased activity of GCS and SMS together with lower ceramide levels were detected in chemotherapy sensitive AML patients compared to others. In an *in vitro* study, overexpression of GCS caused doxorubicin resistance in HL-60, an AML cell line. Additionally, increased level of GCS was detected in resistant K562 cells in which GCS inhibition sensitized K562 cells to Adriamycin<sup>200,201</sup>.

Another sphingolipid family enzyme ceramidase is classified into acid, neutral and alkaline ceramidase based on their enzymatic activity in different environments. Since it is able to breakdown ceramide to generate sphingosine and followed by production of S1P, cells use this mechanism to alter ceramide levels as a strategy for drug resistance<sup>202</sup>. In a prostate cancer cell line, DU145, elevated expression levels of acid ceramidase showed increased resistance to various agents including doxorubicin, cisplatin, etoposide and gemcitabine, whereas inhibition of ceramidase sensitized the cells to those agents<sup>203</sup>. Acid ceramidase overexpression was identified in resistance to TNF- $\alpha$  induced apoptosis in fibrosarcoma cell line, L929, in addition to the reversal of resistance by exogenous ceramide or an acid ceramidase inhibitor N-oleoylethanolamine treatment<sup>204</sup>. Although more studies need to be done in order to get an insight into the roles of ceramidases in chemoresistance, these pioneering studies revealed ceramidases as a potential target to overcome drug resistance in cancer.

Sphingosine kinase-1 and -2 has been widely studied in the literature and the roles of SK-1 and -2 enzymes in different cellular mechanisms including drug resistance have been addressed almost completely in various cancers. The action mechanism of SK could be through two different but interrelating mechanism, one of which is preventing the accumulation of ceramide and the other one is the induction of S1P generation<sup>205,206</sup>. Overexpression of SK-1 has been detected in different cancers resistant to different chemotherapeutic drugs.

In CML, SK-1 activity was increased by BCR/ABL through an antiapoptotic protein Mcl-1 while imatinib has been detected to inhibit SK-1 activity<sup>207</sup>.

Overexpression of SK-1 was detected in doxorubicin resistant myelodysplastic syndromes and acute leukemia cells where the resistance could be reversed by silencing SK-1 by siRNA <sup>208,209</sup>.

In some solid tumors such as ovarian cancer, resistance to 4-HPR (N-(4-hydroxyphenyl)retinamide) is mediated by SK-1 <sup>210</sup>. Moreover, resistance to camptothecin has been linked to high SK-1 activity in a prostate cancer cell line PC3 <sup>211</sup>. In addition, SK-1 and -2 was found to contribute to oxaliplatin resistance in a colon cancer cell line, RKO, in which silencing them were reported to reverse oxaliplatin resistance<sup>212</sup>.

In general, from the discussed studies, the literature linking drug resistance and sphingolipids have been mostly focused on the actions of SK-1,-2 and GCS and their products.

#### **1.6.4. Targeting Sphingolipid Signaling in Cancer Therapy**

Recent studies have suggested that the targeting of sphingolipid mechanism is a new promising approach in cancer treatment. The strategy with sphingolipids is mainly to accumulate intracellular levels of ceramide to promote cell death in cancer cells. In addition to the aim of accumulating intracellular ceramide, decreasing the levels of pro-survival sphingolipids such as SIP serves as another important approach to battle cancer.

Some chemotherapeutic agents have been shown to increase intracellular ceramide levels through induction of *de novo* synthesis pathway. Different studies showed either SMase or *de novo* pathway activation by daunorubicin, fludarabine, etoposine and gemcitabine <sup>166</sup>. On the other hand, targeting ceramide catabolizing/converting enzymes, which results in the accumulation of ceramide has been suggested as a mechanism to induce cell death in different cancers <sup>213,214</sup>.

Combining the standard chemotherapeutic agents with sphingolipid enzymes has been suggested to be used in cancer treatment. In an *in vivo* study by Modrak et al. combination of gemcitabine with sphingomyelin resulted in the inhibition of tumor growth synergistically, in pancreatic cancer cells. In another study, SM treatment was detected to cause an increase in cell membrane permeability, which resulted in increased

levels of cellular uptake of doxorubicin, thus leading to an enhanced therapeutic effects of doxorubicin in various cancer cell lines<sup>215,216</sup>.

Another major strategy in cancer treatment involving sphingolipids is to downregulate S1P levels by blocking the action of SK enzymes. Various *in vitro* and *in vivo* studies reported the anti-proliferative effects of SK1 inhibitors in different cancers. Since S1P can work through two different mechanism: by staying intracellular and directly activating downstream targets, or by moving outside of the cells and binding its own membrane receptors (sphingosine-1-phosphate receptor-1-5 -S1PRs-) and activating G-protein coupled receptor signaling. To this end, the studies showed inhibition of sphingosine-1-phosphate receptors (S1PRs) have been shown to inhibit cell growth<sup>206</sup>.

Different inhibitors of sphingolipid pathway have been shown to induce accumulation of ceramide by blocking the reactions that convert ceramide to complex sphingolipids. For instance, an acid CDase inhibitor B13, caused the inhibition of tumor growth through the accumulation of ceramide in colon cancer and prostate cancer mouse models<sup>217,218</sup>. Similarly, inhibition of SMS, which has been shown to increase ceramide accumulation, caused inhibition of tumor growth in multiple types of cancers<sup>219,220</sup>.

In addition to increasing ceramide levels, increase in dihydroceramide levels has come along as a treatment strategy, which was shown by various studies. Treatment with  $\gamma$ -tocopherol (a dietary form of vitamin E), induced apoptosis by causing an accumulation in dihydroceramides<sup>221</sup>. Interestingly, fenretinide had been thought to induce ceramide generation for a long time until different groups have reported the increase dihydroceramide levels due to dysregulation of DES by fenretinide treatment<sup>222,223</sup>.

Targeting sphingolipids as a strategy to overcome chemoresistance has been widely studied in different cancers. To this end, GCS inhibitors have been widely used in cancer treatment thanks to their action through MDR proteins as previously described in section 1.6.3. Combination of GCS inhibitor with MDR inhibitors induced cell death in different solid tumor cell lines including melanoma, prostate, breast, colon and pancreatic cancers<sup>224</sup>.

Additionally, SK-1 inhibitor is used to overcome MDR-associated gemcitabine resistance in acute myeloid leukemia (AML) in addition to CML cell lines and patient samples<sup>207,225</sup>. Sphingosine, which is one of the sphingolipid breakdown products, induced apoptosis in Adriamycin resistant cells<sup>226</sup>. Also, pharmacological and genetic inhibition of acid ceramidase restored sensitivity to daunorubicin in hepatoma cells<sup>203</sup>.

All in all, these studies show that targeting the sphingolipid pathway to be a promising strategy in cancer treatment in terms of both inhibiting tumor growth and overcoming resistance to chemotherapeutics in different cancers including leukemia. The studies aimed to increase the levels of an apoptotic sphingolipid ceramide which serves as an important regulator in cancer progression. Additionally, altering ceramide metabolism by inhibiting the enzymes involved in the sphingolipid pathway in order to inhibit the production of complex sphingolipids showed promising results.

### **1.6.5. Targeting Sphingolipid Metabolism for the Treatment of Hematological Malignancies**

So far, the importance and potential benefits of targeting sphingolipids have been evaluated for the treatment of different cancers including leukemia and solid tumors. Here, the potential effect of targeting sphingolipid metabolism will be discussed from the perspective of BCR/ABL positive hematological cancers including CML and Ph+ ALL.

Several studies suggested that the usage of ceramide modulating agents in combination with BCR/ABL inhibitors provides an effective approach to increase the efficacy of TKI treatment in BCR/ABL positive hematological malignancies. Similar to previously described strategy, inducing the accumulation of ceramide by the application of a GCS inhibitor, PDMP, showed apoptotic effects and restored sensitivity to imatinib and nilotinib in T315I mutated CML cells <sup>227</sup>. In a previous study by our group, imatinib treatment induced ceramide generation, especially C18-ceramide, in imatinib sensitive but not in resistant K562 cells, thus, suggesting a potential involvement of CerS1. After examining the role of CerS1 by using siRNA, it was reported that CerS1 (through C18-ceramide generation), not fully but partially, is involved to imatinib induced cell death. In the same study, imatinib resistant K562 cells was found to have elevated SK-1 levels together with increased S1P levels, compared to their parental imatinib sensitive cells, therefore suggesting a potential role of SK-1 in imatinib resistance in CML for the first time in the literature. It was reported that, overexpression of SK-1 in sensitive CML cells was shown to gain resistance against imatinib whereas suppressing SK-1 re-sensitized cells to imatinib <sup>228</sup>.



Later on, the mechanism was investigated by Li et al. and reported that the BCR/ABL regulated SK-1 activity was through MAPK, PI3K and JAK2 signaling through a positive feedback loop<sup>229</sup>. The mechanism between SK-1 and BCR/ABL was shown to be via suppression PP2A-mediated dephosphorylation and degradation of BCR/ABL through S1P receptor 2 (S1PR2). In the same study, imatinib resistant K562 cells and patient samples carrying T315 mutation were sensitized to imatinib by targeting S1P/S1PR2 signaling. Notably, higher expression levels of SK-1 and S1PR2 was detected in the patients with T315I mutation suggesting a potential link between BCR/ABL mutational status and SK-1 levels in CML patients<sup>230</sup>.

More studies from our group and other groups reported that BCR/ABL inhibitors such as nilotinib, dasatinib and GFN-2 induced ceramide generation via increasing the expression of CerS genes. Different TKIs has been shown to act through different CerS genes such that; dasatinib was associated with CerS2, -5 and -6 whereas nilotinib was shown to increase CerS5 expression<sup>229,231,232</sup>. GCS inhibitor PDMP in combination with nilotinib or dasatinib was shown to have cytotoxic effects on CML cells through accumulation of intracellular ceramide levels<sup>231</sup>. These studies highlighted the interplay between BCR/ABL, ceramides, SK-1, GCS and CerS to feed into pro-survival effects of BCR/ABL in CML. Moreover, these crosslinks put forward the use of sphingolipid inhibitors together with TKIs for the treatment of BCR/ABL positive hematological malignancies.

Ph+ ALL treatment has resided as challenging for a long time as detailed previously in sections 1.2 and 1.3. Previous studies in CML has served as a base to initiate the studies in sphingolipid metabolism and Ph+ ALL. The first study revealed the role of SK in ALL by using an SK-1 and -2 inhibitor, SKI-II in combination with vincristine. SK inhibition caused an accumulation in ceramide levels and even more when applied together with vincristine, which results in a synergistic effect on cell death in primary lymphoblasts<sup>233</sup>. Moreover, in another study they combined only SK-2 inhibitor together with doxorubicin or vincristine, which led to an additive effect suggesting the previously seen synergy that was due to SK-1 inhibition<sup>234</sup>.

After the promising results seen in ALL, the role of SK-1 has been investigated in Ph+ ALL. In the first cohort study by Li et al. they detected an elevated level of SK-1 expression in BCR/ABL positive ALL patients, compared to BCR/ABL negative ones. This study was the first to reveal the potential relationship between BCR/ABL and SK-1, similar to the one addressed in CML<sup>207,229</sup>. Moreover, in another study it was reported

that combination of SK inhibitors with imatinib showed synergistic cell death in BCR/ABL positive ALL cell lines <sup>235</sup>.

After addressing the importance of SK-1 in ALL, the increase in the levels of SK-2 and its activation has been identified in ALL patient samples. Furthermore, SK-2 inhibition resulted in dysregulation of histone acetylation of c-Myc promoter, which was identified as a new mechanism of action of SK-2. Decreased levels of c-Myc expression through SK-2 suppression was detected in BCR/ABL transformed ALL cells, thus, resulting in prolonged survival in mice models <sup>234</sup>.

## **1.7. Aim of the Study**

The emerging need of novel strategies for the treatment of Ph+ ALL resulted in seeking new treatment options. Previously described mechanisms implicated rewiring sphingolipid metabolism by using different inhibitors of sphingolipid enzymes especially SK and GCS, therefore revealing novel therapeutic approaches by mainly inducing ceramide accumulation. Previous studies reported the potential role of SK-1 and -2 in Ph+ ALL <sup>207,234,236</sup> but the mechanism of SK inhibition from sphingolipid perspective that results in additive effects on cell death has not been clarified.

Additionally, the roles of other sphingolipids especially ceramide in imatinib induced cell death has not been addressed at all by any of these studies. Given the knowledge in the literature and knowing that TKI, especially imatinib resistance has been identified as the most challenging phenomenon in Ph+ ALL treatment, we wanted to investigate the roles of sphingolipids in imatinib induced cell death in the context of Ph+ ALL and reveal the potential link between imatinib resistance and sphingolipids in Ph+ ALL. There is only a limited number of studies in the literature that is discussing and addressing imatinib resistance mechanisms in Ph+ ALL and none of them is from sphingolipid perspective. Therefore, by investigating the involvement of sphingolipids in imatinib resistance, we are also aiming to exploit sphingolipid metabolism to increase sensitivity to imatinib by mimicking the clinical resistance models.

The starting point was to choose an intrinsically more resistant cell line to begin with to mimic intrinsic resistance seen in the patients; then continued with generating a

resistant cell line, which mimicked the acquired resistance condition in patients. We tackled the roles of sphingolipids in imatinib induced cell death in Ph+ ALL in a similar to the manner to what was previously described in CML. Then, we investigated the involvement of each sphingolipids and addressed their contribution to cell death induced by imatinib. Afterward, the roles of sphingolipids in imatinib resistance in Ph+ ALL was evaluated together with determining the sphingolipids that are contributing in imatinib resistance and how they could be rewired to overcome imatinib resistance in Ph+ ALL. Additionally, we investigated the roles of SK, GCS and CerS in imatinib induced changes in Ph+ ALL as referred to in previous studies in both Ph+ ALL and CML.

## CHAPTER 2

### MATERIALS AND METHODS

#### 2.1. Chemicals and Reagents

Cell culture medium RPMI 1640 was obtained from Thermo Fisher Scientific, Waltham, MA, USA (Gibco) and penicillin streptomycin is from Life Technologies (Gibco). Fetal bovine serum was obtained from Thermo Fisher Scientific, Waltham, MA, USA (Gibco). Imatinib was purchased from Santa Cruz Biotechnology, Dallas, TX, USA; eliglustat tartrate, PF543 and SKI-II were obtained from Sigma Aldrich, St. Louis, MO, USA; myriocin was purchased from Cayman Chemical, Michigan, USA. All the chemicals were dissolved with certain solvents (DMSO or water) and stock solutions were kept at indicated temperature as indicated by the manufacturer.

#### 2.2. Cell Lines and Culture Conditions

Philadelphia chromosome positive human acute lymphoblastic leukemia cell line SUP-B15 was purchased from the American Type Culture Collection (Manassas, VA, USA) and SD-1 was purchased from the German Collection of Microorganisms and Cell Cultures (Leibniz Institute DSMZ, Germany). Philadelphia chromosome negative acute lymphoblastic leukemia cell line CCRF-CEM was purchased from the American Type Culture Collection (Manassas, VA, USA). The cells were maintained in RPMI 1640 media containing 10% fetal bovine serum and 1% penicillin-streptomycin at 37°C and 5% CO<sub>2</sub> in a humidified incubator.

Mycoplasma detection was done every month to detect any possible contamination by using MycoAlert™ Mycoplasma Detection Kit (Lonza).

### **2.3. Thawing Frozen Cells**

After receiving the cell lines CCRF-CEM SUP-B15 and SD-1; the cells were thawed in a water bath at 37°C and immediately transferred into 5 ml pre-warmed media for centrifugation. Then, the cells were centrifuged at 800 rpm for 5 min to get rid of the supernatant that contains DMSO. The pellet is resuspended with fresh pre-warmed media and transferred into T25 tissue culture flasks for initial maintenance and later on transferred to T75 flasks for regular maintenance. This process is repeated every 3 months to keep the passage number low to keep the cells in a healthy state.

### **2.4. Maintenance of CCRF-CEM, SUP-B15 and SD-1 Cell Lines**

All the cells in suspension was taken from the tissue culture flasks and transferred into falcon tubes. The clusters were disrupted by gently pipetting the cells. Then, the cells were centrifuged at 600 rpm for 5 min and the pellet was resuspended with fresh media. After counting the cells by using trypan blue dye; SUPB-15 cells were seeded at the density of  $0.5 \times 10^6$  cells/ml and CCRF-CEM and SD-1 cells were seeded at  $0.3 \times 10^6$  cells/ml in T75 tissue culture flasks with the final volume of 20-30 ml media.

### **2.5. Freezing Cells**

Cells were frozen at earlier stage of the experiments to store them for using in further studies. Around  $20 \times 10^6$  cells were collected by centrifugation and the pellet was resuspended with 10 ml of the freezing media containing 20% of FBS and 10% DMSO with RPMI 1640 media. The cells and freezing media were mixed well and 1 ml from cell suspension transferred into each cryogenic vial. The vials are placed into a MRFrosty freezing container (Thermo Scientific) and incubated at -80°C overnight and then stored in liquid nitrogen (-196°C) for longer period.

## 2.6. Generation of Imatinib Resistant SD-1 Cells

Cells were cultured in the presence of step wise increasing concentrations of imatinib, starting with a concentration of  $0.05 \mu\text{M}$ <sup>228</sup>. Cells were routinely seeded at  $0.3 \times 10^6$  cells/ml in growth medium containing imatinib; every 48 h, media and drug were refreshed; once the cells reached the maximum confluency ( $1 \times 10^6$  cells/ml), the cells were diluted back to  $0.3 \times 10^6$  cells/ml and the concentration of imatinib was doubled. Once cells were able to grow in the presence of  $10 \mu\text{M}$  of imatinib, the drug concentration was kept constant and these cells were named SD-1R and maintained in the same  $10 \mu\text{M}$  concentration of imatinib throughout the study.

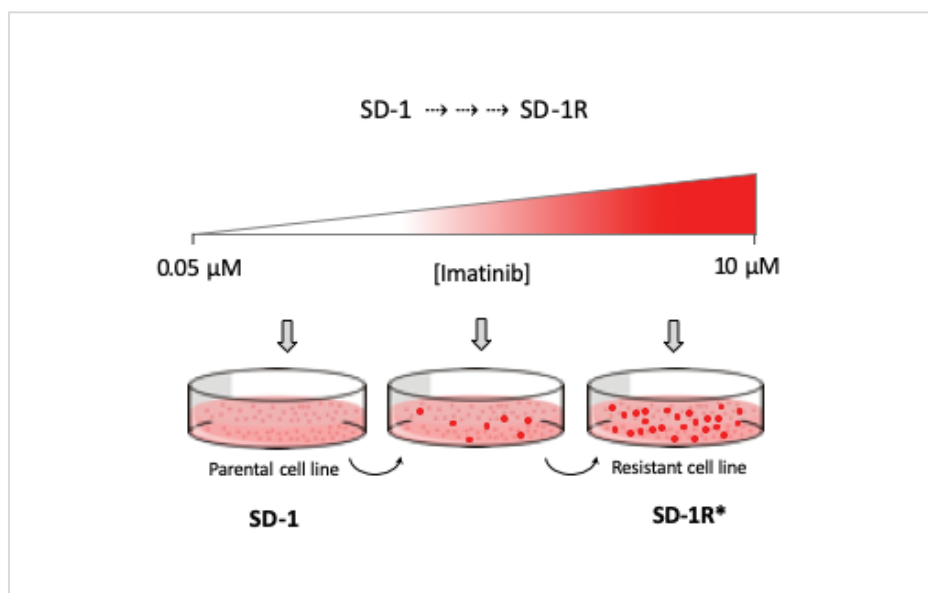


Figure 2.1. Generation of resistant cell line (SD-1R) by clonal selection

## 2.7. Treatment with Imatinib and/or Other Inhibitors

The inhibitors were kept at the certain temperature as suggested by their manufacturer until the day they are used. SD-1R cells were washed in PBS and maintained in drug-free growth medium for 2 passages; at the time of experiments, they

were seeded at  $0.3 \times 10^6$  cells/ml and treated side by side with parental SD-1 sensitive cells at the indicated concentrations of imatinib and/or other inhibitors.

## **2.8. Treatment with Exogenously Added Sphingolipids**

Cells were prepared for the treatment as described previously. C6-Ceramide and sphingosine are not directly applied onto the cells with their stock solutions but first diluted in growth media as indicated concentrations and then applied to the cells.

## **2.9. Determining Cell Viability with Trypan Blue Exclusion Assay**

SD-1 and SD-1R cells were seeded at  $0.3 \times 10^6$  cells/ml in 3 ml media in a 6-well plate and treated as described in the experiments. At the indicated time point, cells were diluted 1:1 (v/v) with 0.4% Trypan Blue staining solution (Life Technologies) and live (white) and dead (blue) cells were counted using a hemocytometer (Bright-Line Hemocytometer, Hausser Scientific )<sup>237</sup>.

## **2.10. Measuring Cell Proliferation by MTT Assay**

Cells were plated at  $2 \times 10^4$  cells/well in 200  $\mu$ l media in a 96-well-plate and exposed to drug/inhibitor for the indicated time. Then 20  $\mu$ l of MTT solution (5  $\mu$ g/ml) (Sigma Aldrich, St.Louis, MO, USA) was added into the wells and incubated for 3h. The cells were pelleted by centrifugation at 250 g for 10min and the produced formazans were dissolved by adding 150  $\mu$ l of DMSO into each well. Each sample was mixed thoroughly, and the absorbance was measured at 540nm in a plate reader (Molecular Devices, SpectraMax M5)<sup>238</sup>.

## 2.11. Protein Isolation and Preparation

Approximately  $1 \times 10^6$  cells were collected by centrifugation and resuspended in 1% SDS to lyse the cells. The samples were boiled in a dry block heater for 10 min and stored at  $-80^\circ\text{C}$  until they are used.

## 2.12. Protein Quantification by BCA Assay

Protein concentration was quantified by Pierce BCA Protein Assay Kit (Thermo Fisher Scientific, Waltham, MA, USA) as described by the manufacturer.

Shortly, 25  $\mu\text{l}$  of each sample and standards of bovine serum albumin (BSA) (Table 2.1) were added into a 96-well plate. 200  $\mu\text{l}$  of working reagent (50:1, Reagent A:B) was added onto each sample and incubated at  $37^\circ\text{C}$  for 30 min in dark. The absorbance is measured at 563 nm with using a plate reader. The protein concentrations are calculated based on the standard curve.

Table 2.1. Preparation of diluted bovine serum albumin (BSA) standards.

Vial	Volume of Diluent ( $\mu\text{l}$ )	Volume and Source of BSA ( $\mu\text{l}$ )	Final BSA concentration ( $\mu\text{g/ml}$ )
1	0	300 of stock	2000
2	125	375 of stock	1500
3	325	325 of stock	1000
4	175	174 of vial 2 dilution	750
5	325	325 of vial 3 dilution	500
6	325	325 of vial 5 dilution	250
7	325	325 of vial 6 dilution	125
8	400	100 of vial 7 dilution	25
9	400	0	0: blank



### **2.13. Western Blotting**

After collecting and quantifying proteins, 20 µg of total proteins were prepared in Laemmli buffer and were separated by Precast Midi 4-20% SDS-Page Gel (Novex, Tris-Glycine, Invitrogen) and blotted onto nitrocellulose membrane (BioRad Laboratories, Hercules, CA, USA). The membrane was blocked with 5% non-fat milk in PBS with 0.1% Tween for 1h at room temperature. The protein levels were detected by using 1:1000 dilution of anti-cleaved caspase-3 (Cell Signaling Technology, Danvers, MA, USA#9661), anti-β-Actin (Cell Signaling Technology, Danvers, MA, USA#4970), anti-GAPDH (Cell Signaling Technology, Danvers, MA, USA#2118), anti-c-ABL (Santa Cruz Biotechnology, Inc. CA, USA #sc-23), anti-BCL2 (Santa Cruz Biotechnology, Inc. CA, USA #sc-7382), anti-BCL-XL (Santa Cruz Biotechnology, Inc. CA, USA #sc-8392) primary antibodies overnight at 4°C in 5% bovine serum albumin (BSA) solution. Then, anti-rabbit or mouse secondary antibodies (1:5000) were used and proteins were visualized by using Pierce ECL Western Blotting Substrate (Thermo Fisher Scientific, Waltham, MA, USA) on an autoradiography film (Lab Scientific, inc) by an image processor (Konica Minolta SRX-101A) <sup>239</sup>.

### **2.14. RNA Isolation**

Total RNA was isolated using the RNeasy Mini Kit (Qiagen, Hilden, Germany) according to the manufacturer's instructions. As a summary; approximately 1x10<sup>6</sup> cells were collected by centrifugation and 350 µl RLT buffer was added onto the samples to disrupt the cells. The same amount of 70% ethanol (350 µl) was added to the lysate and mixed gently. The sample is transferred to an RNeasy spin column with a 2 ml collection tube and centrifuged for 30 s at 10,000 rpm. After the flow through is discarded, 700 µl of Buffer RW1 was added to the column and centrifuged again for 30 s at 10,000 rpm. 80 µl from DNase I incubation mix (10 µl DNase I stock solution + 70 µl Buffer RDD) was directly added to the RNeasy column and incubated at room temperature for 15 min. 500 µl of Buffer RPE was added to the column and centrifuged for 30 s at 10,000 rpm, the

same step was repeated with another centrifuge for 2 min at 10,000 rpm. The spin column was placed in a new 1,5 ml collection tube and 35  $\mu$ l RNase-free water was added directly to the column. The tubes were centrifuged for 1 min at 10,000 rpm to elute the RNA.

## 2.15. Quantification of RNA

The amounts of isolated RNAs were quantified by using NanoDrop UV-Vis spectrophotometer (Thermo Scientific™). After blanking the instrument with elution water, 2  $\mu$ l from each sample was loaded and measured at 260 nm. The amount of RNA in the samples were reported in ng/ $\mu$ l. The purity of RNA was determined by the ratio of 260:280 which is accepted as “pure” if the ratio is around  $\sim$ 2.0 for RNA samples. Also 260:230 ratio was considered as another purity indicator and if around  $\sim$ 2.0 the samples were accepted as “pure”.

## 2.16. cDNA Synthesis

Equal amounts of total RNA (1 $\mu$ g) were used to reverse transcribe into cDNA. The annealing mixture is prepared as shown in Table 2.2. The mixture is placed in a thermocycler and annealed by using the following parameters: 10 min at 70°C, 10 min at 25°C, store at 4°C. In the meantime, the enzyme mix is prepared as shown in Table 2.3 and cDNA is synthesized by using a thermocycler by using the following parameters: 10 min at 25°C, 45 min at 37°C, 45 min at 42°C 15 min at 70°C, store at 4°C.

Table 2.2. Annealing mixture of the cDNA preparation protocol.

<b>Ingredient</b>	<b>Final Concentration</b>	<b>Final amount</b>
RNA	50ng/ $\mu$ l	1 $\mu$ g
Random hexamers (100ng/ $\mu$ l)	25ng/ $\mu$ l	5 $\mu$ l
Water		Add to 20 $\mu$ l

Table 2.3. The enzyme mix used in cDNA synthesis.

5X first strand buffer	8 $\mu$ l
DDT	4 $\mu$ l
dNTP (10mM each)	2 $\mu$ l
SUPERase inhibitor	1 $\mu$ l
SuperScript II	1 $\mu$ l
Water	4 $\mu$ l

## 2.17. Real Time Quantitative PCR

After dilution of the cDNA (1:5 with RNase-free water) the following mixture was prepared for a total of 20 $\mu$ L of PCR reaction: 10 $\mu$ l of iTaq: 1 $\mu$ l of Taqman probe (20X): 5 $\mu$ l of cDNA: 4 $\mu$ l nuclease-free water. The following Taqman probes (Thermo Fisher Scientific, Waltham, MA, USA) were used for the detection of the mRNA expression levels: *UGCG* (Hs00916612\_m1) and *GAPDH* (Hs02786624\_g1). Real Time PCR was performed by using the Applied Biosystem 7500 Real Time PCR systems and cycle threshold ( $C_t$ ) values were obtained for the indicated genes. Expression of the target gene was normalized to the internal control gene (*GAPDH*) and amplification efficiency, and expressed as the mean of normalized expression (MNE) <sup>239,240</sup>.

## 2.18. siRNA Transfection

siRNA for *UGCG* gene and non-targeting (scrambled) sequence were purchased from Thermo Scientific (Ambion In Vivo #4457298 and #4390843, respectively) and were transfected into cells using the Neon<sup>TM</sup> Transfection System (Invitrogen) as described <sup>241</sup>. Briefly, 2x10<sup>6</sup> cells for each transfection were prepared as described by the manufacturer, and cells were transfected two times (100nM each siRNA) with a 24h interval in between by using the optimum parameters (pulse voltage: 1350V, pulse width:

10ms, pulse number: 3) in 2ml for the first two hours then diluted to 7ml for longer incubation. Preliminary experiments showed loss of the siRNA effectiveness after 24 hours.

## **2.19. Lipid Analysis by HPLC/MS/MS**

Lipid analyses were done in Lipidomics Core Facility in Cancer Center in Stony Brook University, USA. Approximately,  $2 \times 10^6$  cells were collected by centrifugation and washed once with 1X PBS. Cell pellets were resuspended in 2ml lipid extraction mixture containing ethyl isopropanol (70%):acetate (2:3, v/v) and the appropriate internal standards. After centrifugation and collection of the supernatant, the cell pellets were reextracted with an additional 2ml of lipid extraction mixture, centrifuged and the supernatants combined for a total of approximately 4ml. Lipid extracts were aliquoted for quantitation of ceramide/sphingoid bases/hexosylceramide and sphingomyelin by LC/MS and for normalization with phospholipids. The samples for MS analysis were first separated chromatographically by using Thermo Accela HPLC (Thermo Fisher Scientific, Waltham, MA, USA). Conditions for operation were optimized with a Peek Scientific C-8 column (3  $\mu$ m particle, 4.6 x 150 mm). To maximize intensity and integrity of analytes, the column temperature was set to 30°C by maintaining base line separation in the meantime. Mobile phase A (MPA) was prepared as follows: MS grade water containing 0.2% formic acid and 2 mM ammonium formate (pH 5.6), while mobile phase B (MPB) consisted of: MS grade methanol containing 0.2% formic acid and 1mM ammonium formate (pH 5.6). The conditions for chromatography consisted of: constant gradient for 0.5 min at 70% MPB upon sample injection, followed by an increase to 90% MPB by 5 min, then increased to 99% MPB by 17 min, and kept constant until 26 min; at 26 min, MPB was reduced to 70% within the next 0.5 min and then re-equilibrated for 7 min, for a total gradient of 35 min. For sphingomyelin quantitation, the lipids were first subjected to mild base hydrolysis: 1ml of MeOH and 20 $\mu$ l NaOH is added onto dried SM samples, following a vortex the samples were incubated at room temperature (RT) for 3h. After the incubation period, the samples were vortexed again and 1ml of MeOH, 2ml of chloroform and 1.8ml of H<sub>2</sub>O is added into the samples. The samples were vortexed well

after adding each solution to make sure all the solutions are mixed homogenously. Then the samples were centrifuged at 3000rpm for 5 min at RT. After aspirating the upper phase, lower phase is transferred into a clean glass tube without any contamination from upper phase. Transferred lower phase is dried by a SpeedVac vacuum concentrator and dried lipids are resuspended in 100 $\mu$ l of mobile phase. Finally, the following settings were used for LC/MS analysis for sphingomyelin quantitation: upon sample injection the gradient was increased from 60% MPB to 99% MPB over the first 16 min, then maintained at 99% MPB until 29 min into the gradient, at which point the gradient was returned to 60% MPB within 4 min and allowed to equilibrate for the remainder of the 35 min method. For the hexosylceramide quantification conditions for chromatography consisted of: constant gradient for 3 min at 80% MPB upon sample injection, followed by an increase to 99% MPB by 16 min, then stayed at 99% MPB by 29 min, decreased back to 80% MPB for 5 min for a total gradient of 35 min. Detection was accomplished utilizing a Thermo Scientific Quantum Access triple quadrupole mass spectrometer (Thermo Fisher Scientific, Waltham, MA, USA) equipped with an Electrospray Ion Source operating in positive ion Multiple Reaction Monitoring (MRM) mode. The HESI source was operated at 400°C vaporizer temperature and 300°C capillary temperature in positive ionization mode with a spray voltage of 4000 V. Gases were set at 60, 0, and 15 for sheath, ion sweep, and auxiliary gases, respectively. Mass spectrometry detection of labeled lipids was accomplished using transitions as described by Snider et al.<sup>242</sup>.

## **2.20. Determination of Inorganic Phosphate (Pi) Concentrations**

After taking the samples for lipid determination, 1 ml from the samples were aliquoted into glass tubes and dried by using a nitrogen evaporator. 2 ml of chloroform, 2 ml of methanol and 1.8 ml of dH<sub>2</sub>O was added and vortexed well. Tubes were centrifuged at 3000 rpm for 5 min to separate two phases. The upper phase which is the aqueous phase was aspirated and lower phase which has the organic phase is transferred into new glass tubes for Pi analysis. These lipids were dried using a heat block at ~70-80°C and NaH<sub>2</sub>PO<sub>4</sub> standards were prepared in separate glass tubes as shown in the Table 2.4.

Table 2.4. Standards used in inorganic phosphate determination.

Number of nmoles	1.0mM NaH <sub>2</sub> PO <sub>4</sub>
0	0 µl
5	5 µl
10	10 µl
20	20 µl
40	40 µl
60	60 µl
80	80 µl

After drying the samples and preparing standards, 600 µl of Ashing buffer is added into each tube and vortexed well. Then the samples were put in a heat block at ~160°C for overnight incubation. Next day, the samples were removed from the heat block and 0.9 ml of H<sub>2</sub>O, 500 µl of 0.9% ammonium molybdate and 200 µl of 9.0% Ascorbic acid were added into samples and vortexed well. The samples were incubated in a water bath for 30min at 45 °C. 200 µl from each tube was aliquoted in a multiwell plate and read at 600 nm by using a plate reader.

## 2.21. Measuring *In situ* GCS Activity by NBD-C6-Ceramide Labeling

Cells were seeded at 0.5x10<sup>6</sup>cells/ml in 2ml media in a 6-well-plate. At the appropriate time points, 1 µM of NBD-C6-Ceramide (Avanti Polar Lipids, inc.) was added into the media and the cells were collected after 45min of incubation. After the collection of the cells by centrifugation, lipids were extracted as described previously by using lipid extraction buffer. Then the samples were dried by a nitrogen evaporator and dried lipids were reconstituted by 150µl mobile phase. Incorporation of NBD-C6-Ceramide in complex sphingolipids was detected by HPLC conditions equipped with a Fluorescence detector (1260 Infinity, Agilent Technologies). NBD method was run on a

C8 reverse phase column. The fluorescence was read with excitation at 470nm and emission at 530 nm. Mobile Phase A was MS grade water with 1 mM ammonium formate and 0.2% formic acid. Mobile Phase B was MS grade methanol with 1mM ammonium formate and 0.2% formic acid. Mobile Phase C was acetonitrile with 1% formic acid. The method ran 40% A 40% B and 20% C for 3 min. Then ran at a gradient to reach 30% A 65% B and 5% C at the 5 min timepoint. Then continued to adjust the gradient to 10%A 85% B and 5% C at the 20min timepoint and further to 1% A 94% B and 5% C at the 24 min time point. From there the gradient was returned to 40% A 40% B and 20% C at the 26 min timepoint and held there til the end of the 30 min cycle. The method was run at a flow rate of 0.5mL/min. The fluorescent peaks for NBD labeled hexosylceramides were confirmed by the retention times of NBD-C6-Hex standards <sup>243</sup>.

## **2.22. Measuring *In situ* SK Activity by NBD-Sphingosine Labeling**

To measure SK activity, cells were plated at  $0.5 \times 10^6$  cells/ml in 2 ml media in a 6-well plate. At the indicated time points, 200 nM of NBD-Sphingosine (Avanti Polar Lipids, inc.) was added into the media and the cells were collected after 15min of incubation. NBD-Sphingosine and NBD-Sphingosine-1-phosphate were detected in HPLC with the same method used in NBD-C6-Ceramide method by using standards.

## **2.23. Statistical Analyses**

All the experiments were repeated as triplicates. The error bars on the graphs represent the standard deviation (SD) from 3 different experiments. Statistical analyses were performed by one-way ANOVA, two-way ANOVA with Bonferroni's post-test or a Student's *t*-test by using GraphPad Prism software (GraphPad Software, San Diego, CA, USA). Asterisks on the plotted graphs indicate statistical significance as \* $P < 0.05$ , \*\* $P < 0.01$  and \*\*\* $P < 0.001$  were significant and  $P > 0.05$  was not significant.

## CHAPTER 3

### RESULTS

#### 3.1. SD-1 Ph+ ALL Cells Show Intrinsic Resistance to Imatinib

Our study aims at testing the possibility of modulating the sphingolipid pathway to sensitize Ph+ ALL cells to imatinib and in particular to sensitize imatinib resistant Ph+ ALL cells. Thus, first off, we wanted to identify a Ph+ ALL cell line intrinsically resistant to the drug. SD-1 and SUP-B15 Ph+ ALL cells have been reported to respond differently to imatinib, with SUP-B15 being more sensitive than SD-1 cells<sup>94</sup>. To confirm this difference, SD-1 and SUP-B15 cells were exposed to increasing concentrations of imatinib (2, 5, 10 and 20  $\mu\text{M}$  for SD-1 and 0.5, 1, 2, 5 and 10  $\mu\text{M}$  for SUP-B15 cells) for 48h and cell viability was measured by trypan blue exclusion assay.

As shown in Figure 3.1, imatinib decreased the number of viable SUP-B15 cells by  $\sim 50\%$  at 1  $\mu\text{M}$  whereas SD-1 cells required 5  $\mu\text{M}$  and 10  $\mu\text{M}$  imatinib to reduce the viable cells by  $\sim 50\%$  and  $70\%$ , respectively. At this time point with 10  $\mu\text{M}$  imatinib about 20% of trypan blue positive SD-1 cells were present along with caspase activation. On the other hand, neither trypan blue positive SD-1 cells nor caspase-3 activity could be detected at 5  $\mu\text{M}$  imatinib at 24 h (data not shown) but approximately 20% of trypan blue cells were detected with 5  $\mu\text{M}$  imatinib at 48 h (data not shown). This data suggests that at lower concentrations imatinib shows cytostatic effects on SD-1 cells whereas as the concentration increases the effect is seen as a mixture with cytotoxicity.

The range of response of SD-1 cells to imatinib (from 0 to 20 $\mu\text{M}$ ) was confirmed by assessing cell proliferation using MTT assay after 48 h of treatment (Figure 3.2). Similar to the cell number data, taken by trypan blue exclusion assay, the  $\text{IC}_{50}$  value for SD-1 cells was calculated to be at  $5.5 \pm 1.42 \mu\text{M}$  (Figure 3.2) for 48 h according to MTT assay results. The further experiments were done by using 5  $\mu\text{M}$  of imatinib as an  $\text{IC}_{50}$  value for 48 h. Additionally, 10  $\mu\text{M}$  of imatinib is used to assess the changes of  $\text{IC}_{50}$  value for 24 h.



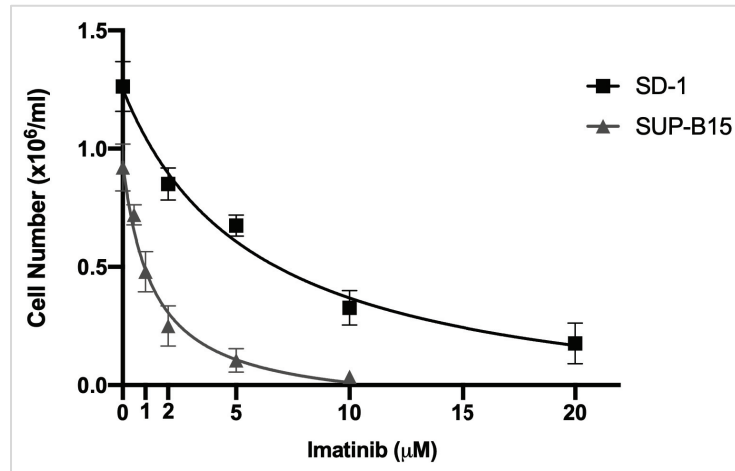


Figure 3.1. Determining the effect of imatinib on the viability of Ph+ ALL cell lines. Cell viability is assessed by trypan blue exclusion assay for SUP-B15 and SD-1 cells seeded at  $0.3 \times 10^6$  cells/ml in a 6-well plate and exposing to increased concentrations of imatinib from (0-20 $\mu$ M) for 48 h. The error bars represent the standard deviation (SD) from 3 different experiments.

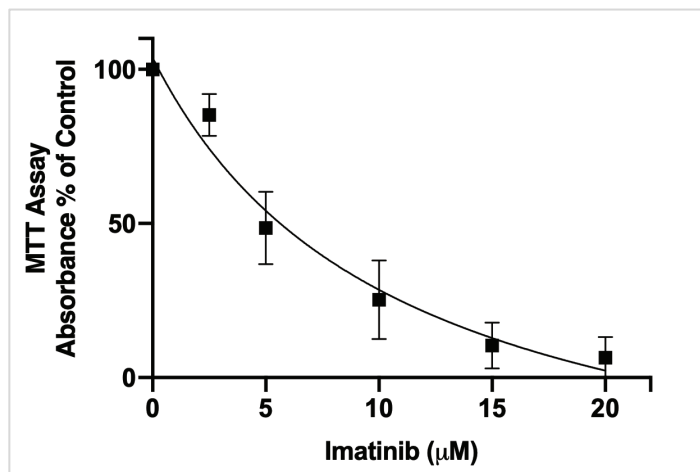


Figure 3.2. Determining the effect of imatinib on the proliferation of SD-1 cell line. The effect of imatinib on cell proliferation is evaluated by an MTT assay procedure on SD-1 cells incubated with increased concentrations of imatinib (2.5-, 5-, 10-, 15-, 20 $\mu$ M) for 48 h. Results are represented in the graph as the percentage of the absorbance and normalized by untreated control cells. The error bars represent the SD from 3 different experiments.

Overall these results suggest that SD-1 cells tend to be intrinsically more resistant to imatinib compared to SUP-B15 cells, as correlated with the literature and that imatinib showed a more cytostatic effect at lower concentrations (up to 5  $\mu$ M) and a mixed effect (cytostatic and cytotoxic) at higher concentrations. So, SD-1 cells were found to be

suitable for our studies to mimic the intrinsic resistance seen in Ph+ ALL patients in the clinics.

### **3.2. SK-1 Inhibition Does Not Contribute to Cytotoxic Effects of Imatinib**

Similar to the literature on CML, we wanted to inhibit sphingosine kinase-1 (SK-1) protein activity to be able to get a response in the cell viability with this inhibition. For this purpose, we used the most selective and potent inhibitor of SK-1, known in the literature, PF-543 to get the most specific and maximal inhibition on SK-1 activity<sup>244</sup>. As reported in the literature<sup>244</sup>, the effective concentration for the inhibition of SK-1 by PF543 was at nano molar. Therefore, we tried a range of concentrations starting from 200- up to 800 nM for SD-1 cells and measured SK activity by using HPLC.

As shown in the raw HPLC data in Figure 3.3 NBD labeled sphingosine was detected by the peak at 8.5 min whereas the product NBD-S1P was detected by the peak at 9.5 min based on the data from the standards (data not shown). In the control data set, NBD-Sphingosine and NBD-S1P peak were both giving high fluorescence measured by laser unit (LU) which showed that NBD-labeled S1P was detectable in these cells. Then, with 200 nM of PF543 the NBD-S1P peak is dropped dramatically while with 400 nM of PF543 the drop was even higher and stayed constant by 800 nM PF543 suggesting the maximal inhibition by PF543 is seen by 400 nM.

This data was quantified to see statistical meaning of the changes and as shown in Figure 3.4 it was plotted as S1P/Sph ratio of area under curve (AUC) which corresponds to SK activity. The level of SK activity was almost at 0.8 AUC in the control group, whereas it was decreased to 0.2 AUC by 200 nM of PF543, showing around 75% inhibition.

Moreover, by the application of 400 nM of PF543, SK activity level was detected as around 0.1 AUC which was significantly lower than the one seen by 200 nM of PF543 in which showed around 0.19 AUC. After confirming the inhibitory effect of PF543, 400 nM of PF543 was used in the following experiments as a concentration that showed maximum inhibition of SK activity (Figure 3.4).

Since the effect of imatinib on SK activity was previously described in CML cells<sup>228</sup>, we wanted to see if Ph+ ALL cells have the same regulatory mechanism for SK in presence of imatinib. So, we treated SD-1 cells with imatinib, PF543 and SKI-II at their IC<sub>50</sub> and IC<sub>50</sub>/2 concentrations for 24 hours and detected the SK-1 and SK-2 protein levels by using untreated SD-1 cells as a control group in western blotting. The data showed imatinib treatment decreased SK-1 protein levels similar to the action of SKI-II which is a SK-1 and -2 inhibitor known by its degradant effect on SK proteins suggesting that imatinib is causing either degradation of SK-1 protein or decreasing the expression levels of SK-1 (Figure 3.5). In addition, as seen in the data, PF543 does not change the protein level of SK (Figure 3.5) although the used concentrations of PF543, 200- and 400 nM was shown to inhibit SK activity by 75- and 90%, respectively (Figure 3.4).

On the other hand, SK-2 levels did not change by any of the inhibitors except SKI-II at 10µM (Figure 3.5) which again is known to degrade both SK-1 and SK-2, so the inhibitory effect of imatinib seems to be only through SK-1 but not SK-2 in Ph+ ALL cells. This data also suggests that imatinib does not have any inhibitory effects on SK-2 protein at least at the expression level.

Then, to determine the effect of imatinib on SK activity, we treated the cells with imatinib at IC<sub>50</sub> concentration (5 µM), PF543 at its known inhibitory concentration (400nM) and with their combinations and measured SK activity by using NBD-Sphingosine labeling via HPLC. Figure 3.6 shows the SK activity levels in response to different treatments. As seen in figure 3.6, imatinib brings down SK activity levels from 1.8 AUC to around 1.0 AUC at its IC<sub>50</sub> concentration. SD-1 cells, treated with PF543, as anticipated, had 0.4 AUC SK activity level (Figure 3.6).

Last but not least, imatinib treatment in combination with PF543 had SK activity levels around 0.25 AUC, showing a partial additive effect with imatinib and PF543 on SK activity (Figure 3.6). Here, we showed that imatinib as well as reducing the protein levels of SK, as previously shown in the western data, also inhibits SK enzyme activity. Additionally, the inhibitory effect on SK activity by imatinib was detected to increase additively in presence of PF543.

Finally, to assess the effects of these changes on cell viability and to see if there is any additive cytotoxic effects of imatinib and PF543; trypan blue exclusion assay was performed to see if the inhibition of SK activity reflects on cell viability in SD-1 Ph+ ALL cells.

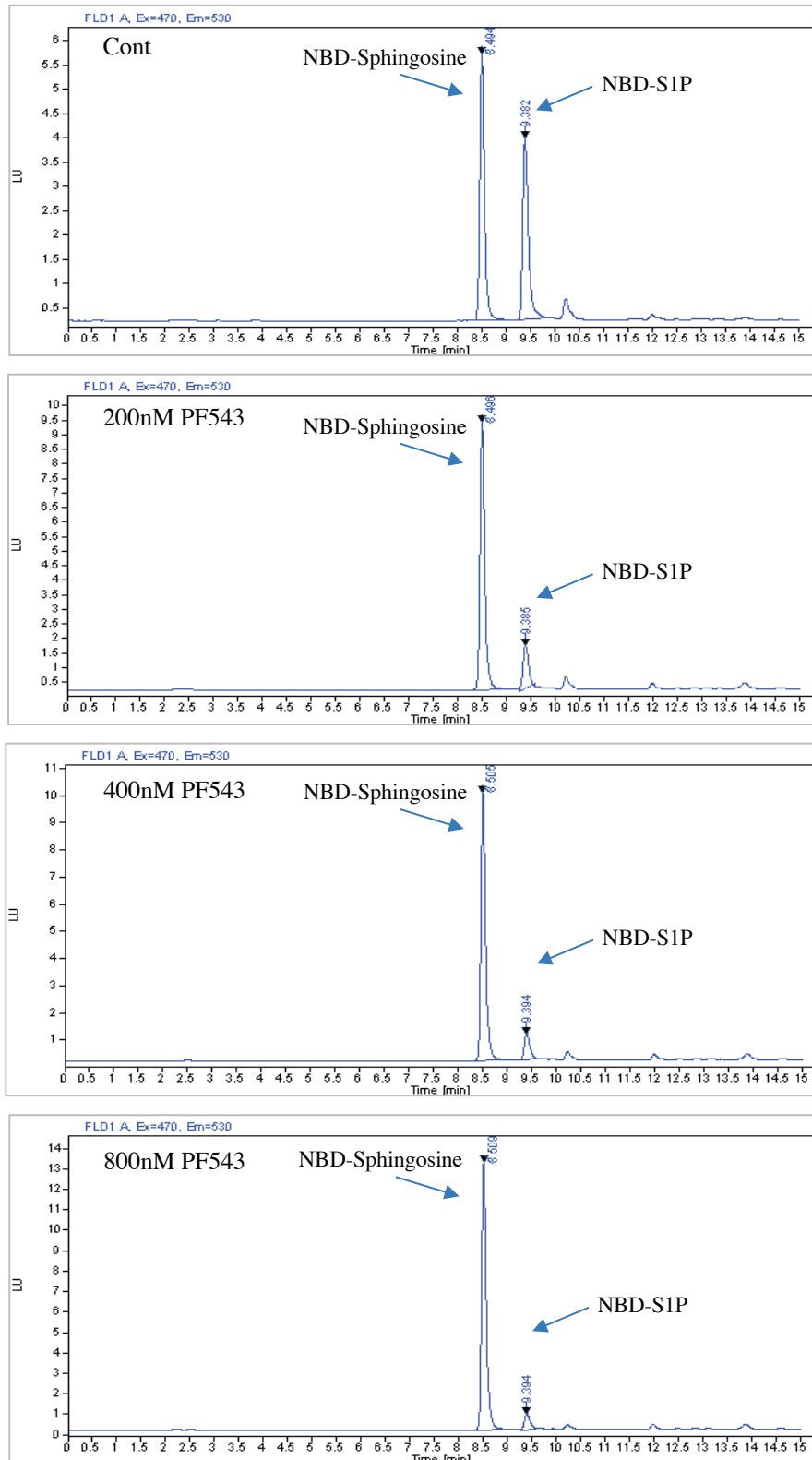


Figure 3.3. Analysis of SK activity in response to increased concentrations of PF543 by HPLC. SK activity was measured by production of NBD-Sphingosine-1-phosphate (NBD-S1P) in SD-1 cells treated with NBD-Sphingosine by HPLC on the cells seeded at  $0.3 \times 10^6$ /ml in 6-well plates with (0-, 200-, 400- and 800nM) and without PF543 for 24 h.

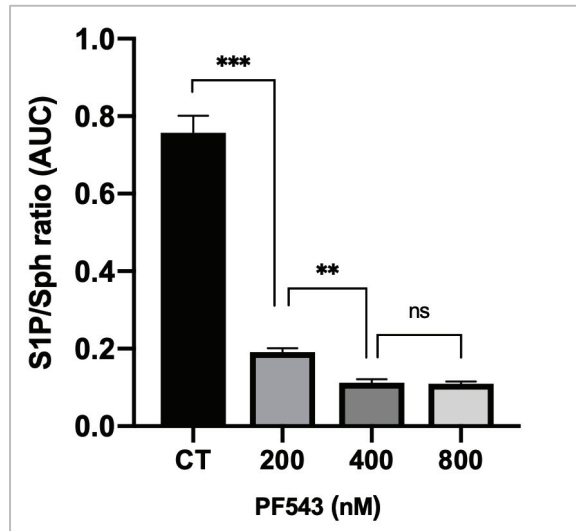


Figure 3.4. Quantification of SK activity in response to increased concentrations of PF543. SK activity was measured by production of NBD-S1P in SD-1 cells treated with NBD-Sphingosine by HPLC on the cells seeded at  $0.3 \times 10^6$ /ml in 6-well plates with (200-, 400- and 800nM) and without PF543 for 48 h. The data is plotted as the ratio of S1P/Sph AUC (Area Under Curve) on the y axis. The error bars represent the SD from 3 different experiments. Asterisks indicate statistical significance: ns  $P > 0.05$ , \* $P < 0.05$ , \*\* $P < 0.01$ , \*\*\* $P < 0.001$ .

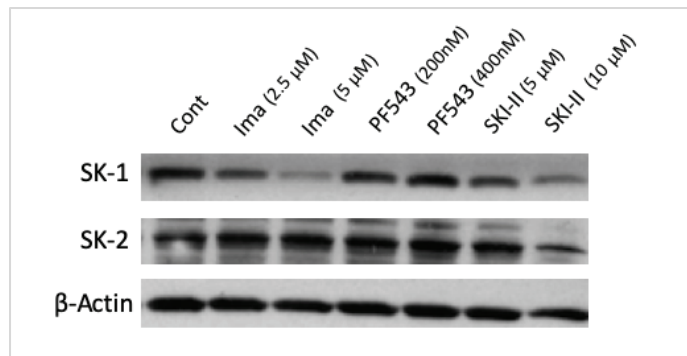


Figure 3.5. The protein levels of SK-1 and SK-2 treated with imatinib, PF543 and SKI-II by western blotting. Protein levels of SK-1 (50kDa) and SK-2 (75kDa) was determined by western blotting, on SD-1 cells seeded at  $0.3 \times 10^6$ /ml treated with imatinib, PF543 and SKI-II for 24 h.  $\beta$ -Actin (42 kDa) was used as internal control.

To this end, SD-1 cells treated with  $IC_{50}$  concentration of imatinib (5  $\mu$ M), 400 nM of PF543, together with their combination were grown for 48 hours and viable cells were counted by using trypan blue dye as described in methods.

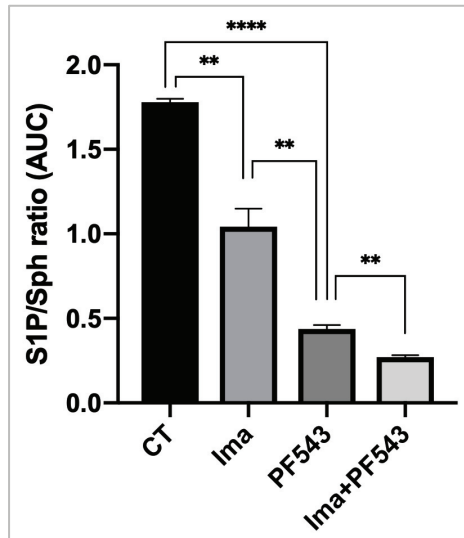


Figure 3.6. SK activity in response to imatinib treatment, PF543 and their combination. SK activity was measured by production of NBD-S1P in SD-1 cells treated with NBD-Sphingosine by HPLC on the cells seeded at  $0.3 \times 10^6/\text{ml}$  in 6-well plates with  $5 \mu\text{M}$  of imatinib,  $400 \text{ nM}$  of PF543, and their combination for 24 h. The data is plotted as the ratio of S1P/Sph AUC on the y axis. The error bars represent the SD from 3 different experiments. ns  $P > 0.05$ , \* $P < 0.05$ , \*\* $P < 0.01$ , \*\*\* $P < 0.001$ , \*\*\*\* $P < 0.0001$ .

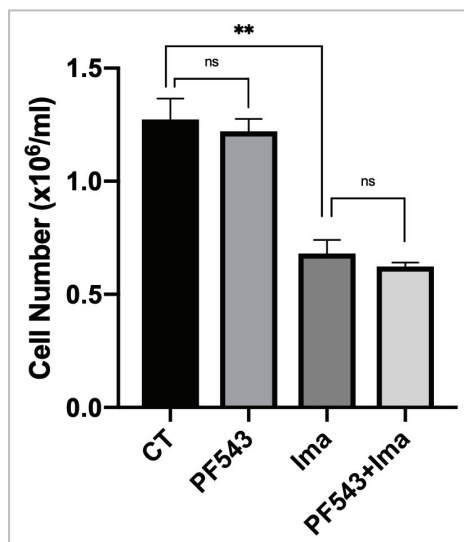


Figure 3.7. Determining the effect of imatinib, PF543 and their combination on cell viability on SD-1 cell line. Cell viability was assessed by trypan blue exclusion assay for SD-1 cells seeded at  $0.3 \times 10^6$  cells/ml in a 6-well plate and exposed to PF543 ( $400 \text{ nM}$ ), imatinib ( $5 \mu\text{M}$ ) and their combination for 48 h. The error bars represent the SD from 3 different experiments. ns  $P > 0.05$ , \* $P < 0.05$ , \*\* $P < 0.01$ .

Interestingly enough, contrary to the literature, SK-1 inhibition by PF543 did not show any effect on cell viability in SD-1 cells whereas imatinib was showing 50% inhibition on cell viability as anticipated. Moreover, there was no change on cell viability when PF543 was applied together with imatinib (Figure 3.7).

This data is the first in the literature, showing that the additive inhibition of SK-1 enzyme by imatinib and PF543 treatment does not reflect on cell viability in Ph+ ALL cells, which distinguishes this data from the literature. Until now, the only established link between SPLs and Ph+ ALL resided in the role of SK1 and SK2 in the development of this leukemia and as pharmacological targets to sensitize Ph+ ALL cells to imatinib. Interestingly, in SD-1 cells there was no link between SKs and the mechanism of imatinib-induced cytotoxicity or imatinib-resistance in SD-1R cells. These results indicate that the impact of SPL metabolism in the development of imatinib resistance can vary among different cell lines.

### **3.3. Endogenous Sphingolipid Levels are Elevated in Response to Imatinib in SD-1 Cells**

After seeing that there were no additive effects with imatinib and PF543, we wanted to see whether imatinib induces changes in sphingolipids in SD-1 cells. Cells were treated with 10  $\mu$ M imatinib for 24 h (conditions that elicit a 50% decrease in cell number) and endogenous ceramide and sphingosine levels as well as complex sphingolipids were measured by HPLC/MS/MS as described in the methods. The levels of almost all ceramide species were increased (Figure 3.8, 3.9 and 3.10). While C16-, C18-, C24:1-, C22:1-, and C26:1-ceramides showed a 2-fold increase, C14- and C18:1-ceramides showed 3-fold increase. Some long chain ceramide species (C20-, C20:1-, C24-, and C26-ceramide), although showing a tendency to increase upon treatment with imatinib, were not statistically different from controls (Figure 3.8, 3.9 and 3.10).

Figure 3.8 shows the most abundant ceramides by mass, among all ceramides with different chain length. Additionally, other ceramide species that are relatively less abundant by mass were plotted in Figure 3.9, whereas the least abundant species, in which two of them were not statistically different than controls are shown in Figure 3.10.

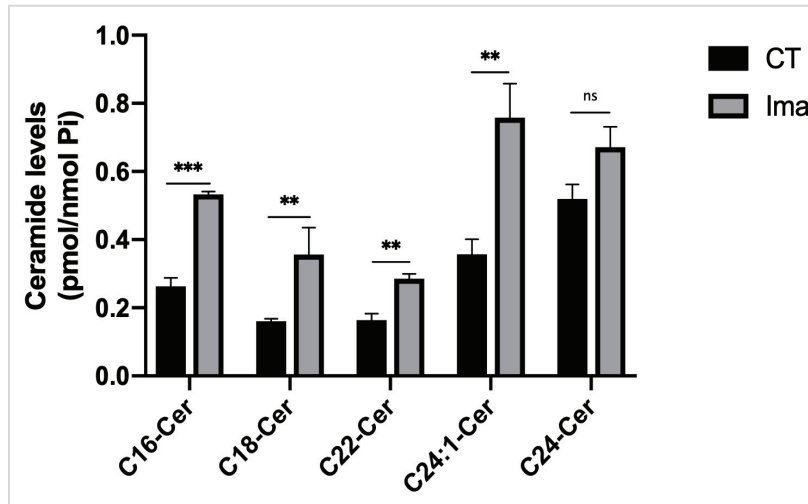


Figure 3.8. Analysis of endogenous ceramide levels of SD-1 cells in response to imatinib (most abundant species). SD-1 cells, grown in T25 flasks ( $0.3 \times 10^6$  cells/ml) were treated with vehicle (DMSO) or imatinib ( $10 \mu\text{M}$ ) for 24 h and ceramide (C16-, C18-, C22-, C24:1, C24-ceramide) levels were measured by HPLC/MS as described. The levels of measured sphingolipids were normalized to Pi concentrations and final levels are represented on the Y axis as pmol/nmol Pi. The error bars represent the SD from 3 different experiments. ns  $P > 0.05$ , \* $P < 0.05$ , \*\* $P < 0.01$ , \*\*\* $P < 0.001$ .

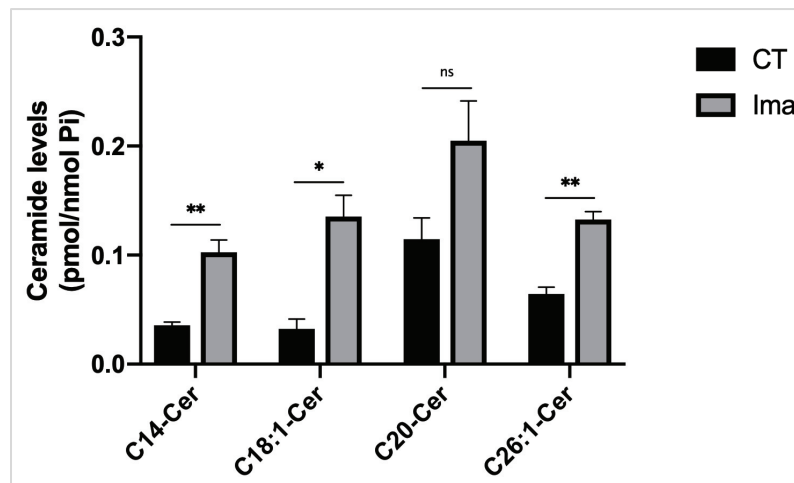


Figure 3.9. Analysis of endogenous ceramide levels of SD-1 cells in response to imatinib (less abundant species). SD-1 cells, grown in T25 flasks ( $0.3 \times 10^6$  cells/ml) were treated with vehicle (DMSO) or imatinib ( $10 \mu\text{M}$ ) for 24 h and ceramide (C14-, C18:1-, C20-, C26:1-ceramide) levels were measured by HPLC/MS as described. The levels of measured sphingolipids were normalized to Pi concentrations and final levels are represented on the Y axis as pmol/nmol Pi. The error bars represent the SD from 3 different experiments. ns  $P > 0.05$ , \* $P < 0.05$ , \*\* $P < 0.01$ .



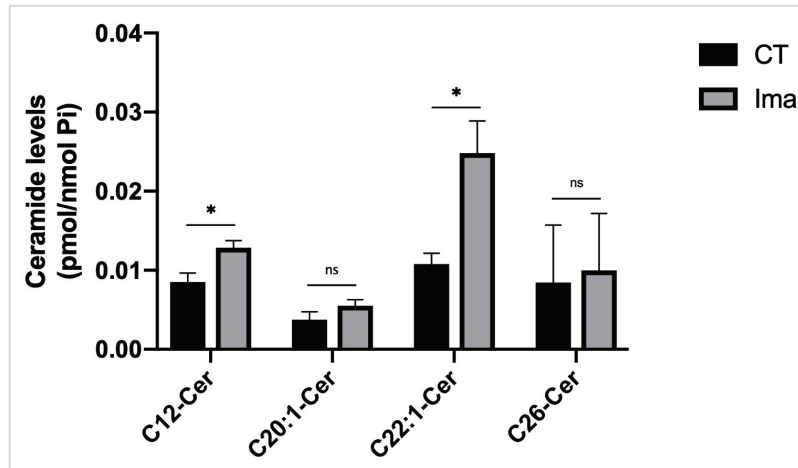


Figure 3.10. Analysis of endogenous ceramide levels of SD-1 cells in response to imatinib (the least abundant species). SD-1 cells, grown in T25 flasks ( $0.3 \times 10^6$  cells/ml) were treated with vehicle (DMSO) or imatinib ( $10 \mu\text{M}$ ) for 24 h and ceramide (C12-, C20:1-, C22:1-, and C26-ceramide) levels were measured by HPLC/MS as described. The levels of measured sphingolipids were normalized to Pi concentrations and final levels are represented on the Y axis as pmol/nmol Pi. The error bars represent the SD from 3 different experiments. ns  $P > 0.05$ , \* $P < 0.05$ .

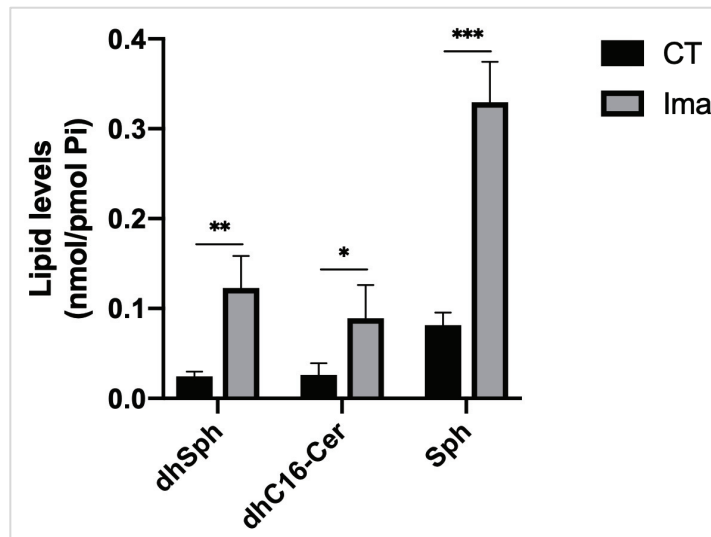


Figure 3.11. Analysis of endogenous sphingolipid levels of SD-1 cells in response to imatinib. SD-1 cells, grown in T25 flasks ( $0.3 \times 10^6$  cells/ml) were treated with vehicle (DMSO) or imatinib ( $10 \mu\text{M}$ ) for 24 h and sphingolipid (dihydrosphingosine, dihydroC16-ceramide and sphingosine) levels were measured by HPLC/MS as described. The levels of measured sphingolipids were normalized to Pi concentrations and final levels are represented on the Y axis as pmol/nmol Pi. The error bars represent the SD from 3 different experiments. ns  $P > 0.05$ , \* $P < 0.05$ , \*\* $P < 0.01$ , \*\*\* $P < 0.01$ .

In addition to ceramide, other sphingolipids of *de novo* pathway; dihydrosphingosine (dhSph) and dihydroceramide (dhCer) were also significantly increased upon imatinib treatment. Additionally, we detected 4-fold increase in sphingosine levels in response to imatinib treatment (Figure 3.11).

### **3.4. Endogenous Complex Sphingolipid Levels are Elevated in Response to Imatinib in SD-1 Cells**

To further examine the involvement of sphingolipid metabolism in imatinib treated SD-1 cells, the levels of hexosylceramide (HexCer), a further metabolized product of ceramide, were also detected by HPLC/MS. In addition to ceramide and other sphingolipids of *de novo* pathway, the levels of complex sphingolipids such as hexosylceramide (HexCer) and sphingomyelin (SM) were also changed by imatinib treatment. Here, the most abundant HexCer species were plotted in Figure 3.12 followed by representing other HexCer species in Figure 3.13.

Analysis of HexCer levels showed a significant 1.5 to 3-fold elevation in C16-, C18:1, C20:1-, C22:1-, and C22-HexCer levels. A 2-fold increase was detected in the levels of C18-, C20-, and C26:1-HexCer in response to imatinib treatment compared to untreated control cells (Figure 3.12 and 3.13). These results suggest that, followed by ceramide generation/accumulation, imatinib is also inducing the conversion of ceramide to HexCer in SD-1 cells. In other words, ceramides are being further metabolized to HexCer by imatinib treatment in Ph+ ALL cells.

In addition to changes in HexCer levels, we also examined the changes in another major sphingolipid, sphingomyelin (SM) levels in response to imatinib. As shown in (Figure 3.14 and 3.15); C14- and C16-SM exhibited the greatest changes by having more than 2-fold increase, whereas C18-, C18:1-, C20-, C22:1-, and C24:1-SM levels were elevated almost 2-fold after treatment with 10  $\mu$ M imatinib for 24 h (Figure 3.14, 3.15 and 3.16).

All these results show for the first time in the literature that imatinib induces an increase in the levels of sphingolipids starting from *de novo* pathway sphingolipids, continued by an increase in ceramide and sphingosine levels which both are cytotoxic

sphingolipids in these SD-1 Ph+ ALL cells. The increase in ceramide results in further metabolism of imatinib to HexCer and SM.

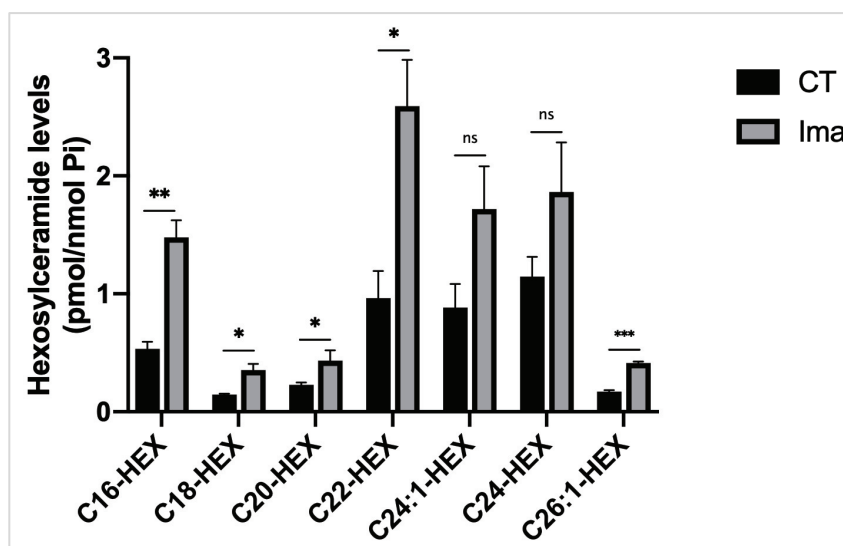


Figure 3.12. Analysis of endogenous hexosylceramide levels of SD-1 cells in response to imatinib (most abundant species).SD-1 cells, grown in T25 flasks ( $0.3 \times 10^6$  cells/ml) were treated with vehicle (DMSO) or imatinib ( $10 \mu\text{M}$ ) for 24 h and HexCer (C16-, C18-, C20-, C22-, C24:1-, C24-, and C26:1-hexosylceramide) levels were measured by HPLC/MS as described. The levels of measured sphingolipids were normalized to Pi concentrations and final levels are represented on the Y axis as pmol/nmol Pi. The error bars represent the SD from 3 different experiments. ns  $P > 0.05$ , \* $P < 0.05$ , \*\* $P < 0.01$ , \*\*\* $P < 0.001$ .

Overall, these data suggest that sphingolipid metabolism is involved in response to imatinib in SD-1 cells by;

- (i) increasing ceramide and sphingosine levels, either by inducing their generation in a greater rate or by preventing the further metabolism of these sphingolipids and causing their accumulation;
- (ii) inducing further metabolism of ceramide into two group of complex sphingolipids, SM and HexCer either by increasing the flux through ceramide or by blocking the further catabolism of these complex sphingolipids.

Importantly, the increase in the levels of dhSph and dhCer, both of which are upstream of ceramide in *de novo* synthesis pathway, suggests that ceramide and sphingosine accumulation in response to imatinib treatment is very likely to be due to an induction of *de novo* synthesis pathway of sphingolipids.

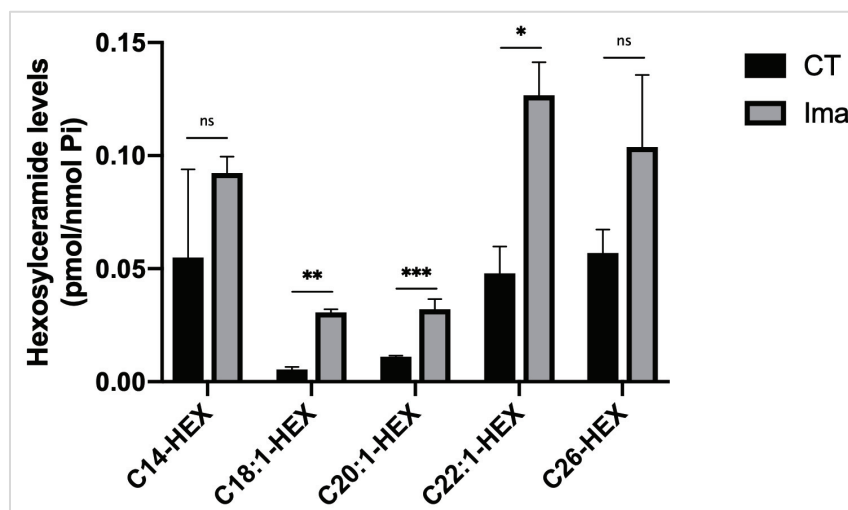


Figure 3.13. Analysis of endogenous hexosylceramide levels of SD-1 cells in response to imatinib (less abundant species). SD-1 cells, grown in T25 flasks ( $0.3 \times 10^6$  cells/ml) were treated with vehicle (DMSO) or imatinib ( $10 \mu\text{M}$ ) for 24 h and HexCer (C14-, C18:1-, C20:1-, C22:1-, and C26-hexosylceramide) levels were measured by HPLC/MS as described. The levels of measured sphingolipids were normalized to Pi concentrations and final levels are represented on the Y axis as pmol/nmol Pi. The error bars represent the SD from 3 different experiments. ns  $P > 0.05$ , \* $P < 0.05$ , \*\* $P < 0.01$ , \*\*\* $P < 0.001$ .

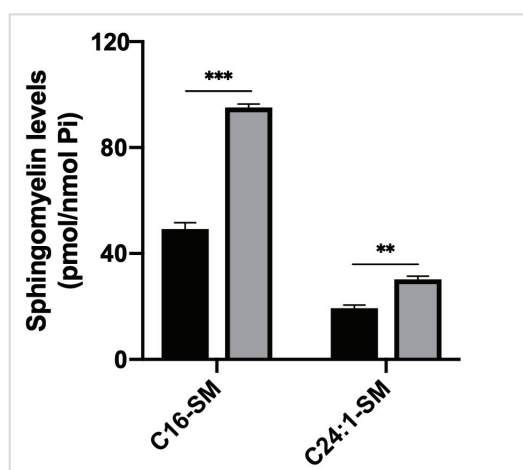


Figure 3.14. Analysis of endogenous sphingomyelin levels of SD-1 cells in response to imatinib (most abundant species). SD-1 cells, grown in T25 flasks ( $0.3 \times 10^6$  cells/ml) were treated with vehicle (DMSO) or imatinib ( $10 \mu\text{M}$ ) for 24 h and SM (C16-, and C24:1-sphingomyelin) levels were measured by HPLC/MS as described. The levels of measured sphingolipids were normalized to Pi concentrations and final levels are represented on the Y axis as pmol/nmol Pi. The error bars represent the SD from 3 different experiments. ns  $P > 0.05$ , \* $P < 0.05$ , \*\* $P < 0.01$ , \*\*\* $P < 0.001$ .

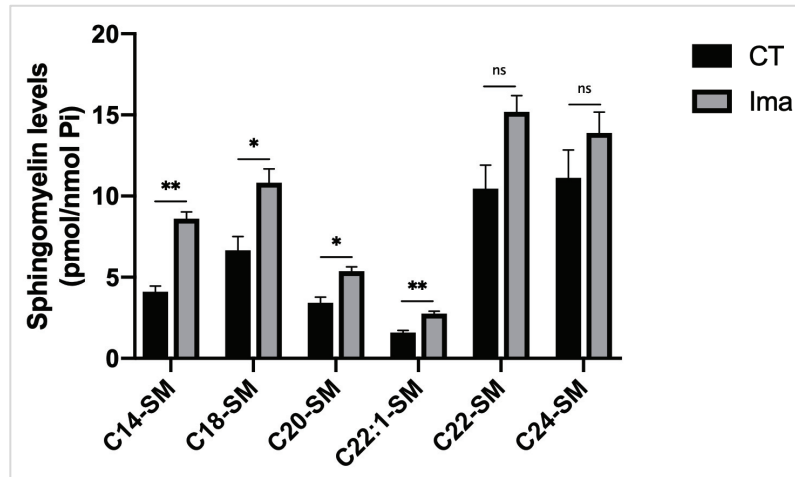


Figure 3.15. Analysis of endogenous spingomyelin levels of SD-1 cells in response to imatinib (less abundant species). SD-1 cells, grown in T25 flasks ( $0.3 \times 10^6$  cells/ml) were treated with vehicle (DMSO) or imatinib ( $10 \mu\text{M}$ ) for 24 h and SM (C14-, C18-, C20-, C22:1-, C22-, and C24-sphingomyelin) levels were measured by HPLC/MS as described. The levels of measured sphingolipids were normalized to Pi concentrations and final levels are represented on the Y axis as pmol/nmol Pi. The error bars represent the SD from 3 different experiments. ns  $P > 0.05$ , \* $P < 0.05$ , \*\* $P < 0.01$ .

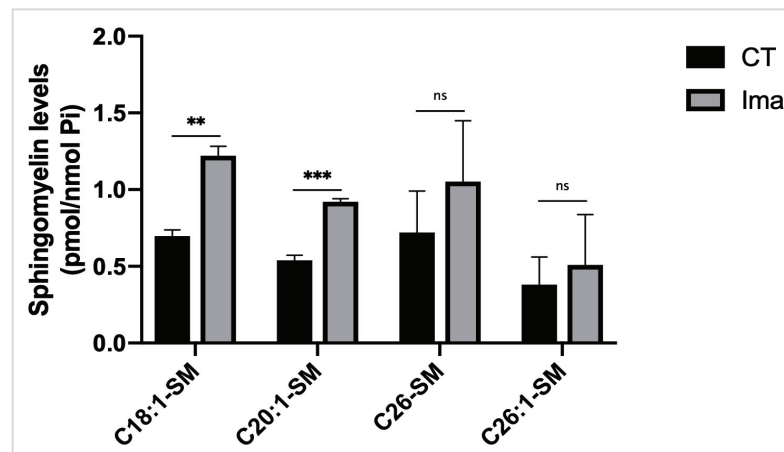


Figure 3.16. Analysis of endogenous spingomyelin levels of SD-1 cells in response to imatinib (the least abundant species). SD-1 cells, grown in T25 flasks ( $0.3 \times 10^6$  cells/ml) were treated with vehicle (DMSO) or imatinib ( $10 \mu\text{M}$ ) for 24 h and SM (C18:1-, C20:1-, C:26-, and C26:1-sphingomyelin) levels were measured by HPLC/MS as described. The levels of measured sphingolipids were normalized to Pi concentrations and final levels are represented on the Y axis as pmol/nmol Pi. The error bars represent the SD from 3 different experiments. ns  $P > 0.05$ , \* $P < 0.05$ , \*\* $P < 0.01$ , \*\*\* $P < 0.001$ .

On the other hand, S1P levels were barely detectable in every experimental condition (data not shown). Overall these results suggest that treatment with imatinib in SD-1 cells affects the levels of multiple endogenous sphingoid bases and ceramides possibly through induction of *de novo* sphingolipid synthesis.

### 3.5. *De novo* Sphingolipid Synthesis Pathway is Induced by Imatinib in SD-1 Cells

Since the observed changes in sphingolipid levels seemed to affect every step of the *de novo* biosynthetic pathway, we investigated whether these lipid changes were due to activation of this specific pathway. Thus SD-1 cells were pre-treated with 500 nM myriocin, an SPT inhibitor that blocks the very first step in *de novo* sphingolipid synthesis, for 1 h and exposed to 10  $\mu$ M imatinib for 24 h and sphingolipid levels were measured and compared to control cells. Effectiveness of myriocin treatment was confirmed by the reduction of dhSph and dhCer levels in control cells (Figure 3.17).

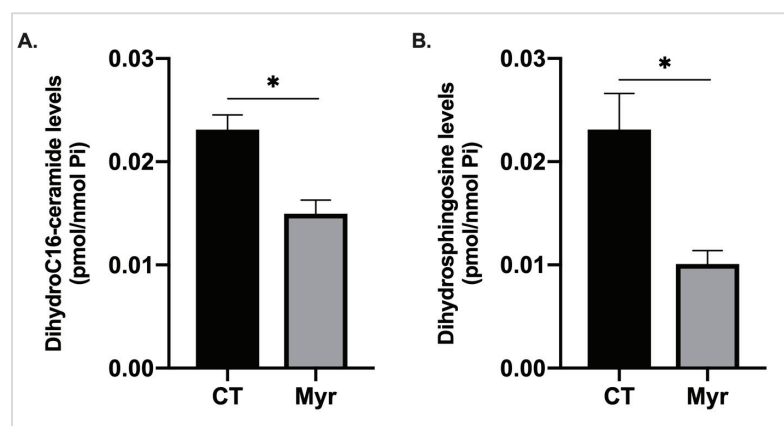


Figure 3.17. Analysis of *de novo* sphingolipids in response to myriocin; A. dihydroC16-ceramide levels, B. dihydroceramide levels. SD-1 cells, grown in T25 flasks ( $0.3 \times 10^6$  cells/ml) were treated with vehicle (DMSO), imatinib (10  $\mu$ M) and myriocin (500 nM) for 24 h and dhCer and dhSph levels were measured by HPLC/MS as described. The sphingolipid levels were normalized to Pi concentrations, and final levels are represented on the Y axis as pmol/nmol Pi. The error bars represent the SD from 3 different experiments. ns  $P > 0.05$ , \* $P < 0.05$ .

While treatment with imatinib (10  $\mu$ M for 24 h) increased total ceramide levels as expected, treatment with myriocin significantly reduced the accumulation of ceramide which reached levels similar to untreated cells (Figure 3.18). Similar results were observed in the case of sphingosine (Figure 3.19). The increase in sphingosine levels with imatinib treatment is almost completely prevented by presence of myriocin suggesting that similar to the ceramide levels, sphingosine levels that are increased by imatinib is also due to induction of *de novo* synthesis pathway but not through recycling pathway (Figure 3.19).

These data suggest that imatinib treatment in SD-1 cells activates *de novo* sphingolipid synthesis and that this pathway contributes significantly to imatinib-induced accumulation of cytotoxic sphingolipids such as ceramide and sphingosine.

Next, to determine the origin of increased HexCer levels in response to imatinib, HexCer levels were measured in the same experimental setting with myriocin treatment.

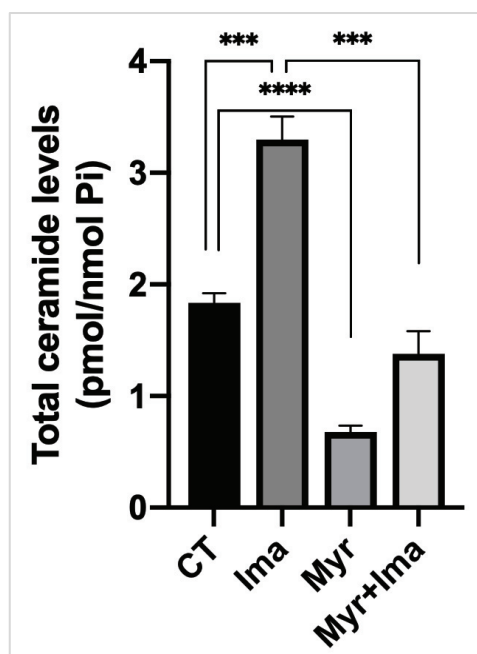


Figure 3.18. The changes in total ceramide levels with imatinib treatment in presence of myriocin. SD-1 cells, grown in T25 flasks ( $0.3 \times 10^6$  cells/ml) were treated with vehicle (DMSO), imatinib (10 $\mu$ M), myriocin (500nM) and myriocin (500nM)+imatinib(10 $\mu$ M) for 24 h and ceramide levels were measured by HPLC/MS as described. The sphingolipid levels were normalized to Pi concentrations, all the ceramide species were summed, and final levels are represented on the Y axis as pmol/nmol Pi. The error bars represent the SD standard deviation (SD) from 3 different experiments. ns  $P > 0.05$ , \* $P < 0.05$ , \*\* $P < 0.01$ , \*\*\* $P < 0.001$ , \*\*\*\* $P < 0.0001$ .

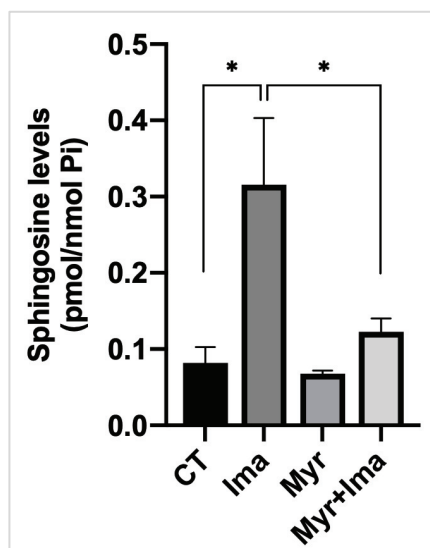


Figure 3.19. The changes in sphingosine levels with imatinib in presence of myriocin. SD-1 cells, grown in T25 flasks ( $0.3 \times 10^6$  cells/ml) were treated with vehicle (DMSO), imatinib ( $10 \mu\text{M}$ ), myriocin ( $500 \text{nM}$ ) and myriocin+imatinib for 24 h and sphingosine levels were measured by HPLC/MS as described. SPL levels were normalized to Pi concentrations and final levels are represented on the Y axis as pmol/nmol Pi. The error bars represent the SD from 3 different experiments. ns  $P > 0.05$ ,  $*P < 0.05$ .

Interestingly, HexCer levels were diminished from  $4.2 \text{ pmol/nmol Pi}$  in untreated control cells to  $1.2$ - and  $1.5 \text{ pmol/nmol Pi}$  in myriocin and myriocin and imatinib cotreated cells, respectively (Figure 3.20). As anticipated, imatinib alone treatment increased HexCer levels by almost 2-fold compared to control cells (Figure 3.20). These data suggested that inhibition of *de novo* ceramide synthesis is sufficient to prevent the accumulation of HexCer in response to imatinib and therefore HexCer generated by imatinib induction completely relies on *de novo* synthesized ceramide.

Additionally, we measured SM levels in the same experimental setting detailed above, to see whether the increase in this sphingolipid by imatinib treatment is also hailed from *de novo* synthesis pathway. The data showed that even though both myriocin alone and myriocin and imatinib cotreatment decreased SM levels by  $21.1$ - and  $17.6\%$  respectively, compared to control cells, the change was detected as not significant (Figure 3.21).

These results suggest that, blocking *de novo* synthesis of ceramide is not fully reflected on SM production induced by imatinib which might be due to either need of more time to observe an effect on SM levels or HexCer being the predominant complex sphingolipid utilizing *de novo* synthesized ceramide.



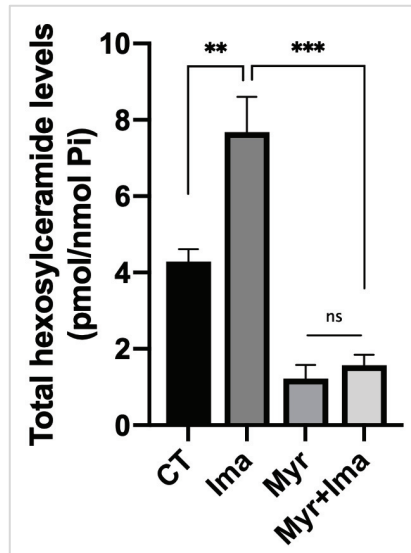


Figure 3.20. The changes in total hexosylceramide levels with imatinib in presence of myriocin. SD-1 cells, grown in T25 flasks ( $0.3 \times 10^6$  cells/ml) were treated with vehicle (DMSO), imatinib ( $10 \mu\text{M}$ ), myriocin ( $500 \text{ nM}$ ) and myriocin+imatinib for 24 h and HexCer levels were measured by HPLC/MS as described. HexCer levels were normalized to Pi concentrations and final levels are represented on the Y axis as pmol/nmol Pi. The error bars represent the SD from 3 different experiments. ns,  $**P < 0.01$ ,  $***P < 0.001$ .

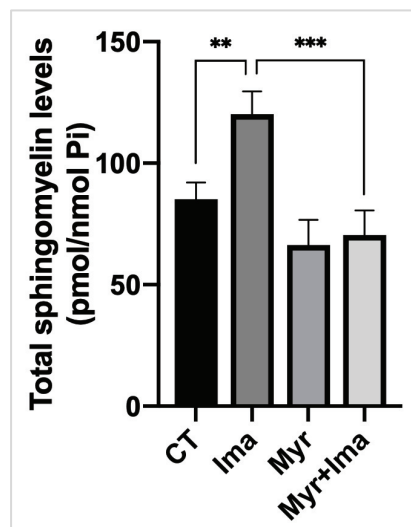


Figure 3.21. The changes in total sphingomyelin levels with imatinib in presence of myriocin. SD-1 cells, grown in T25 flasks ( $0.3 \times 10^6$  cells/ml) were treated with vehicle (DMSO), imatinib ( $10 \mu\text{M}$ ), myriocin ( $500 \text{ nM}$ ) and myriocin+imatinib for 24 h and SM levels were measured by HPLC/MS as described. The SM levels were normalized to Pi concentrations and final levels are represented on the Y axis as pmol/nmol Pi. The error bars represent the SD from 3 different experiments. ns  $P > 0.05$ ,  $*P < 0.05$ ,  $**P < 0.01$ ,  $***P < 0.001$ .

All together the lipid results support a scenario whereby imatinib induces *de novo* sphingolipid synthesis in SD-1 Ph<sup>+</sup> ALL cells. Then, dihydrosphingosine and dihydroceramide are produced and these reactions are followed by sphingosine and ceramide production through *de novo* induction, in which then fluxed further and converted in part into hexosylceramide and sphingomyelin by the action of GCS and SMS enzymes. Since the conversion to HexCer is seen clearly at the indicated time point, the data suggests that the activity of GCS enzyme is at a high rate.

### **3.6. Activation of *de novo* Sphingolipid Synthesis Participates in the Cytostatic Response to Imatinib Treatment of SD-1 Cells**

To assess whether the sphingolipids that are generated through the *de novo* pathway are involved in the cytotoxic effect of imatinib in SD-1 cells, the effect of inhibition of the *de novo* pathway on cell viability was tested upon imatinib treatment. SD-1 cells were pre-treated with 500 nM myriocin for 1 h followed by addition of 10  $\mu$ M imatinib for 24 h and viable cells were counted by trypan blue exclusion assay. As shown in Figure 3.22, there were no significant changes between the number of control cells ( $0.69 \times 10^6$  cells/ml) and myriocin treated cells ( $0.64 \times 10^6$  cells/ml) suggesting that myriocin, at the concentration employed, was not toxic to the cells.

As expected, imatinib treatment inhibited cell growth by ~50% resulting in  $0.34 \times 10^6$  cells/ml; importantly, pretreatment with myriocin brought back the number of imatinib treated cells at  $0.55 \times 10^6$  cells/ml (Figure 3.22), thus significantly reverting the cytotoxic / cytostatic effect of the drug. These results suggest that sphingolipids produced via *de novo* synthesis contribute to the inhibitory effect of imatinib on cell number in SD-1 cells.

Since treatment with imatinib caused accumulation of the cytotoxic/cytostatic sphingolipids; ceramide and sphingosine and the levels of both these lipids were significantly reduced by myriocin (Figure 3.18 and 3.19), while myriocin also protected from the cytotoxic / cytostatic effects of imatinib (Figure 3.22), we wondered whether one of these two lipids were responsible for the observed cytotoxic / cytostatic effects of imatinib.

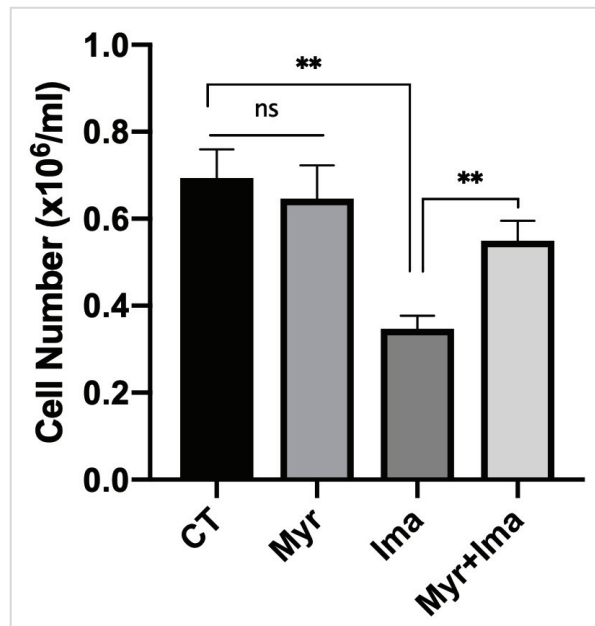


Figure 3.22. Contribution of *de novo* sphingolipid pathway to cytotoxic effects of imatinib in SD-1 cells. Cell viability is assessed by trypan blue exclusion assay for SD-1 cells seeded at  $0.3 \times 10^6$  cells/ml and treated with vehicle (DMSO), myriocin (500nM), imatinib (10 $\mu$ M) and myriocin+imatinib for 24 h. The error bars represent the SD from 3 different experiments. ns  $P > 0.05$ , \*\* $P < 0.01$ .

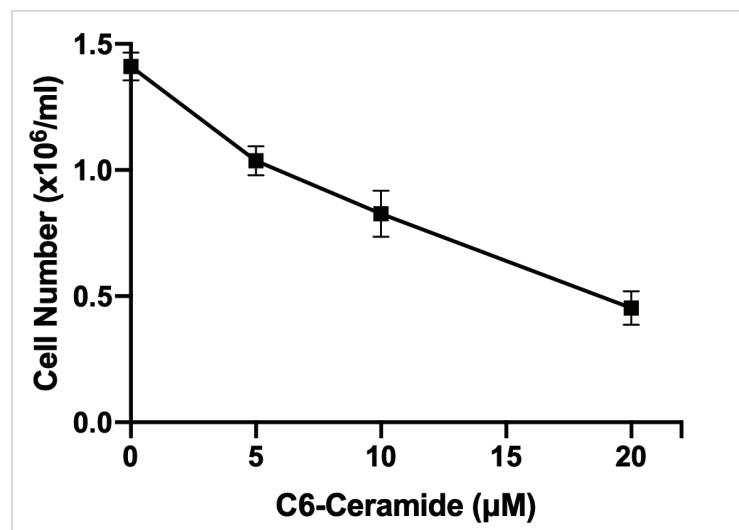


Figure 3.23. The effect of exogenous treatment with C6-ceramide on cell viability. The effect of exogenous treatment with C6-ceramide (0-, 5-, 10-, and 20  $\mu$ M) on cell viability is evaluated by trypan blue exclusion assay on SD-1 cells seeded at  $0.3 \times 10^6$  cells/ml for 48 hours. The error bars represent the SD from 3 different experiments.

Thus, the effect on cell number of exogenous treatments with either one of these lipids was determined. As shown in Figure 3.23, SD-1 cells were treated with increasing concentrations of the cell permeable ceramide analogue C6-ceramide (from 0 to 20  $\mu\text{M}$ ) for 48h and the cell number was determined by trypan blue exclusion assay as previously described. A dose dependent inhibitory effect of C6-ceramide was observed already at 5  $\mu\text{M}$  (30% decrease compared to control cells) which increased with increasing concentrations of the lipid, reaching a 70% growth inhibition at 20  $\mu\text{M}$  (Figure 3.23).

Interestingly, exogenous addition of sphingosine was also effective similar to C6-ceramide. Sphingosine treatment showed growth inhibitory effects starting slightly by 2.5  $\mu\text{M}$  and gradually continued as the concentration increases. The inhibitory effect of sphingosine was similar to what was seen with C6-ceramide treatment by showing 50% decrease in cell viability at 7.5  $\mu\text{M}$  together with further cytotoxicity with 10  $\mu\text{M}$  sphingosine (Figure 3.24). Finally, the growth of more than 80% of the cells were habiteded by 10  $\mu\text{M}$  sphingosine treatment.

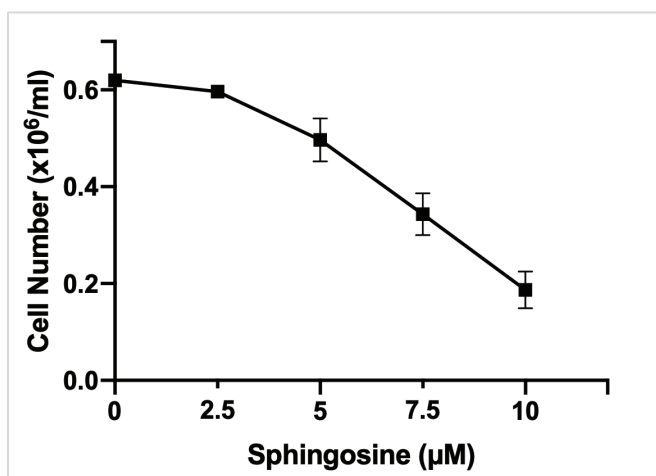


Figure 3.24. The effect of exogenous treatment with sphingosine on cell viability. The effect of exogenous treatment with sphingosine (0-, 2.5-, 5-, 7.5- and 10  $\mu\text{M}$ ) on cell viability is evaluated by trypan blue exclusion assay on SD-1 cells seeded at  $0.3 \times 10^6$  cells/ml for 24 h.

All together these results point to imatinib-induced stimulation of the *de novo* sphingolipid pathway which contributes to accumulation of cytotoxic/cytostatic sphingolipids (ceramide and sphingosine), and they show that a significant portion of the ceramide formed from the *de novo* pathway in response to imatinib is being also converted into more complex sphingolipids (HexCer and SM).

### 3.7. Pharmacological Inhibition of GCS Exacerbates the Accumulation of Cytostatic/Cytotoxic Sphingolipids Induced by Imatinib and Sensitizes SD-1 Cells to the Drug

Given that a portion of ceramide generated in response to imatinib treatment in SD-1 cells is shunted through HexCer and that accumulation of ceramide or of the metabolically connected sphingosine could be one of the mechanisms of imatinib induced cytotoxicity, we sought to test the effects of enhancing accumulation of ceramide (and possibly sphingosine) by blocking its conversion into HexCer. HexCer measurements represent the combination of glucosylceramide (GluCer) and galactosylceramide (GalCer) levels, thus first, we determined the contribution of GluCer to HexCers levels. To this aim, we employed eliglustat, a potent FDA approved specific inhibitor of GCS and currently utilized for the treatment of Gaucher's disease, a lysosomal storage disorder characterized by the toxic accumulation of GluCer<sup>245,246</sup>.

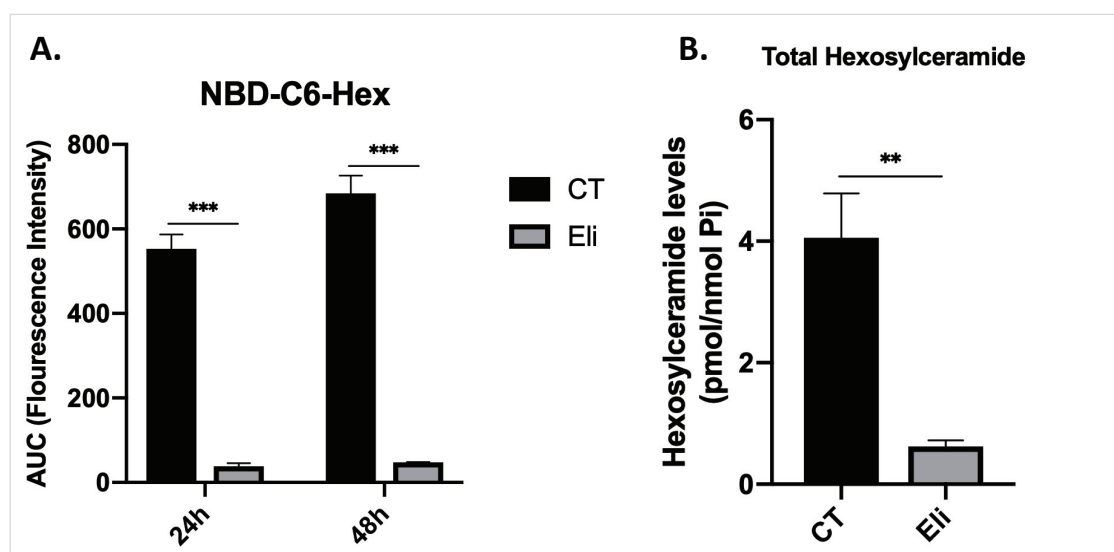


Figure 3.25. The effects of eliglustat treatment on GCS activity measured by production of A. NBD-C6-hexosylceramide and B. hexosylceramides. A. SD-1 cells treated with NBD-C6-ceramide by HPLC on the cells seeded at  $0.3 \times 10^6$ /ml in 6-well plates with and without eliglustat (100 nM) for 24 and 48 hours. The data is plotted as AUC on the y axis. B. The effect of eliglustat (100nM) treatment for 24 hours on the total levels of hexosylceramide measured by HPLC/MS. The error bars represent the SD from 3 different experiments. ns  $P > 0.05$ , \* $P < 0.05$ , \*\* $P < 0.01$ , \*\*\* $P < 0.001$ .

Cells were treated with 100 nM eliglustat for 24 and 48h and, for each time point, 1  $\mu$ M NBD-C6-ceramide was added 1h before collecting the cells. Lipids were extracted and NBD-C6-ceramide and NBD-C6-GluCer were measured by HPLC/MS/MS. As shown in Figure 3.25, 100 nM eliglustat exerted  $\sim$  90% inhibition of GCS activity at both 24h and 48h. Importantly, inhibition of GCS activity by 24h treatment with 100 nM eliglustat was also confirmed by measuring endogenous HexCer levels by HPLC/MS. Total HexCer levels decreased from 4.0 pmol/nmol Pi to 0.6 pmol/nmol Pi in eliglustat treated SD-1 cells (Figure 3.26). Importantly, these results show the efficacy of inhibition of GCS by eliglustat and they reveal that GluCer is far more abundant than GalCer as HexCers are mostly gone after inhibition of GCS.

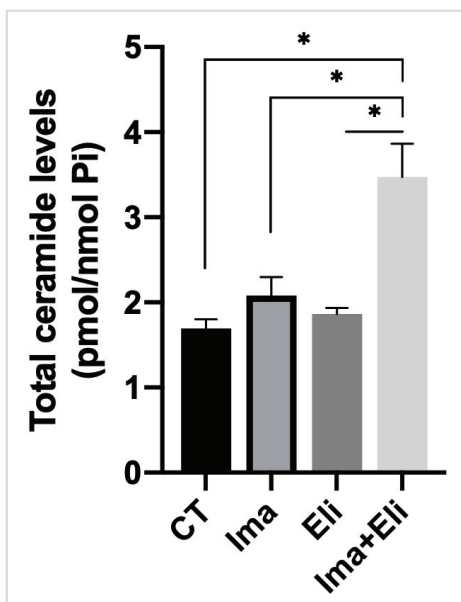


Figure 3.26. The changes in the total ceramide levels of SD-1 cells treated with imatinib and eliglustat and their combination. SD-1 cells, grown in T25 flasks (seeded at  $0.3 \times 10^6$  cells/ml) were treated with vehicle (DMSO), imatinib (5 $\mu$ M), eliglustat (100nM) and eliglustat (100nM)+imatinib(5 $\mu$ M) for 24 h and ceramide levels were measured by HPLC/MS as described. The ceramide levels were normalized to Pi concentrations, all the ceramide species were summed and final levels are represented on the Y axis as pmol/nmol Pi. The error bars represent the SD from 3 different experiments. ns  $P > 0.05$ , \* $P < 0.05$ , \*\* $P < 0.01$ .

Next, to see the effect of pharmacological inhibition of GCS on imatinib induced changes in endogenous sphingolipid levels, sphingolipid levels were detected as described before. The data showed that total ceramide levels are increased from 1.69

pmol/nmol Pi in control cells to 2.07 pmol/nmol Pi in 5  $\mu$ M imatinib treated cells (Figure 3.26). Although total ceramide levels are not significantly changed with eliglustat treatment, they further increased with eliglustat and imatinib cotreatment to an absolute level of 3.47 pmol/nmol Pi.

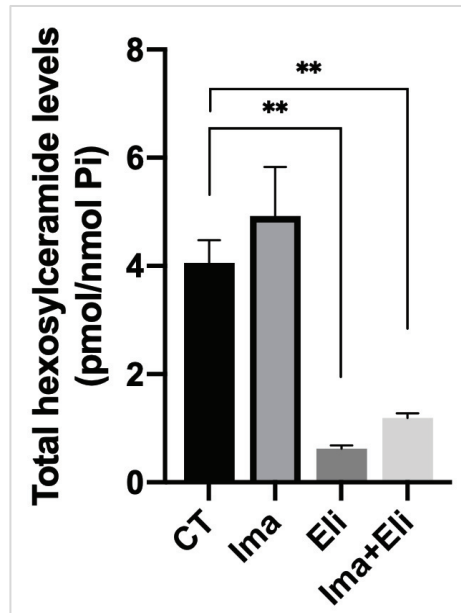


Figure 3.27. The changes in the total hexosylceramide levels of SD-1 cells treated with imatinib and eliglustat and their combination. SD-1 cells, grown in T25 flasks (seeded at  $0.3 \times 10^6$  cells/ml) were treated with vehicle (DMSO), imatinib (5  $\mu$ M), eliglustat (100nM) and eliglustat (100nM)+imatinib(5  $\mu$ M) for 24 h and HexCer levels were measured by HPLC/MS as described. The HexCer levels were normalized to Pi concentrations, all the HexCer species were summed and final levels are represented on the Y axis as pmol/nmol Pi. The error bars represent the SD from 3 different experiments. ns  $P > 0.05$ , \* $P < 0.05$ , \*\* $P < 0.01$ .

Additionally, total hexosylceramide levels were decreased by 85% with eliglustat treatment and stayed at the similar levels with imatinib in presence of eliglustat, suggesting that ceramide production through *de novo* synthesis in response to imatinib can no longer be shunted through hexosylceramide in presence of eliglustat (Figure 3.27). On the other hand, sphingomyelin levels are not significantly changed by imatinib and eliglustat treatment separately whereas it increases by ~90% with eliglustat and imatinib cotreatment (Figure 3.28). This data suggests that, ceramide produced by imatinib is further shunted towards sphingomyelin in case of a blockage in flux through hexosylceramides.

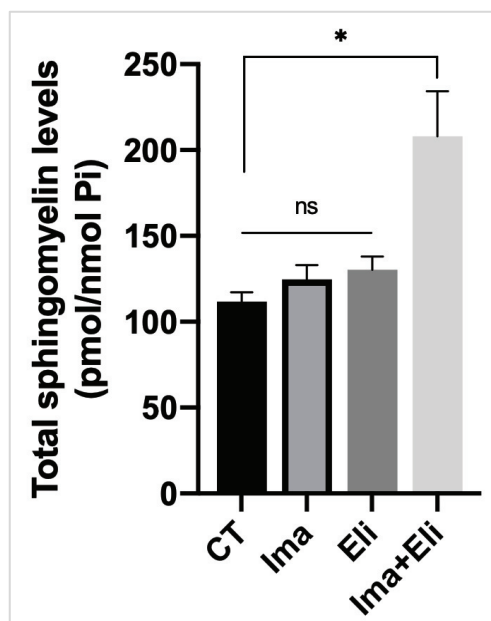


Figure 3.28. The changes in the total sphingomyelin levels of SD-1 cells treated with imatinib and eliglustat and their combination. SD-1 cells, grown in T25 flasks (seeded at  $0.3 \times 10^6$  cells/ml) were treated with vehicle (DMSO), imatinib ( $5 \mu\text{M}$ ), eliglustat ( $100 \text{nM}$ ) and eliglustat ( $100 \text{nM}$ )+imatinib( $5 \mu\text{M}$ ) for 24 h and SM levels were measured by HPLC/MS as described. The SM levels were normalized to Pi concentrations, all the SM species were summed and final levels are represented on the Y axis as pmol/nmol Pi. The error bars represent the SD from 3 different experiments. ns  $P > 0.05$ ,  $*P < 0.05$ .

Additionally, another member of sphingolipids; sphingosine too, similar to the changes in ceramide, is increased by more than 2-fold in imatinib treated cells and further increased by  $\sim 5$  fold with imatinib and eliglustat cotreatment (Figure 3.29). While control cells have sphingosine levels at around  $0.1 \text{ pmol/nmol Pi}$ , imatinib treatment elevated sphingosine levels to the levels of  $2.5 \text{ pmol/nmol Pi}$ . In presence of eliglustat, imatinib is able to further increase sphingosine levels to over  $0.4 \text{ pmol/nmol Pi}$ . This data is suggesting that in addition to ceramide, sphingosine is also accumulated by imatinib treatment in presence of eliglustat.

Overall these results show that we were able to further increase ceramide and sphingosine levels with imatinib treatment at sub-growth inhibitory concentrations by blocking the flux through hexosylceramide with eliglustat. Overall these results show that blocking the flux through glucosylceramide with eliglustat effectively enhances the effects of imatinib on accumulation of the cytotoxic sphingolipids, ceramide and sphingosine.



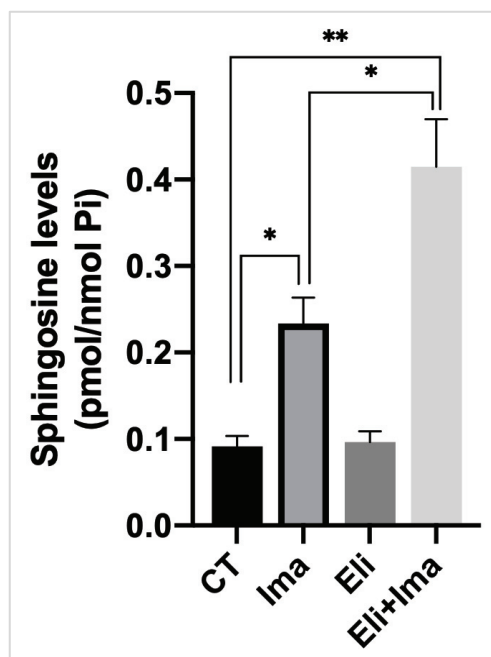


Figure 3.29. The changes in the sphingosine levels of SD-1 cells treated with imatinib and eliglustat and their combination. SD-1 cells, grown in T25 flasks (seeded at  $0.3 \times 10^6$  cells/ml) were treated with vehicle (DMSO), imatinib ( $5 \mu\text{M}$ ), eliglustat ( $100 \text{nM}$ ) and eliglustat ( $100 \text{nM}$ )+imatinib ( $5 \mu\text{M}$ ) for 24 h and sphingosine levels were measured by HPLC/MS as described. The sphingosine levels were normalized to Pi concentrations and final levels are represented on the Y axis as pmol/nmol Pi. The error bars represent the SD from 3 different experiments. ns  $P > 0.05$ , \* $P < 0.05$ , \*\* $P < 0.01$ .

We further investigated the effect of modulation of these sphingolipids on the antiproliferative effect of imatinib on SD-1 cells. Therefore, using the same experimental settings as above, SD-1 cells were pretreated with  $100 \text{nM}$  of eliglustat and then exposed to  $5 \mu\text{M}$  imatinib for 24 and 48h and cell number was assessed by trypan blue exclusion assay. Whereas treatment with imatinib alone inhibited SD-1 proliferation by  $\sim 30\%$  at 24h, cotreatment of imatinib and eliglustat significantly enhanced this effect ( $\sim 50\%$ ).

Interestingly, eliglustat by itself did not exhibit any effect on cell proliferation, suggesting a synergistic cytostatic effect on these cells with eliglustat and imatinib treatment (Figure 3.30). The synergistic effect of eliglustat and imatinib could also be seen at 48h where imatinib treatment inhibited SD-1 cell number by  $\sim 50\%$  at 48h and the combination further inhibited it by  $\sim 75\%$  (Figure 3.30). These data demonstrate that, enhancing accumulation of cytotoxic sphingolipids like ceramide and sphingosine by inhibiting GCS activity, result in sensitization of SD-1 cells to the anticarcinogenic effects of imatinib.

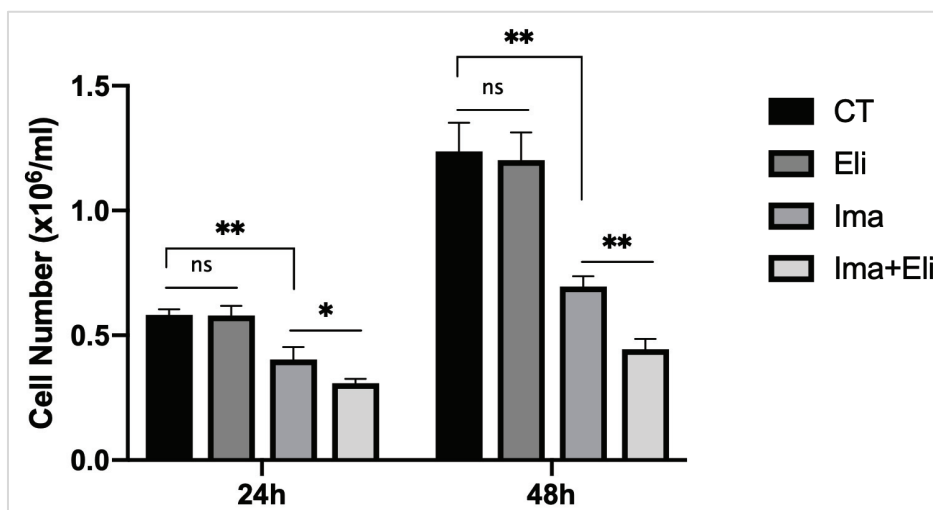


Figure 3.30. The effect of treatment with imatinib, eliglustat and their combination on cell viability of SD-1 cells. Cell viability is assessed by trypan blue assay for SD-1 cells seeded at  $0.3 \times 10^6$  cells/ml and treated with vehicle (DMSO), imatinib ( $5 \mu\text{M}$ ), eliglustat ( $100 \text{ nM}$ ) and eliglustat+imatinib for 24 and 48 h. The error bars represent the SD from 3 different experiments. ns  $P > 0.05$ , \* $P < 0.05$ , \*\* $P < 0.01$ .

### 3.8. The Effect of siRNA Mediated Knock-Down of GCS on Imatinib Induced Changes in Endogenous Sphingolipid Levels and Cell Number of SD-1 Cells

To confirm that the observed effects with eliglustat treatment were actually due to GCS inhibition and not to off-target effects, we tested the effects of downregulation of GCS on lipids and cell number alone and in combination with imatinib. GCS expression was silenced with different amounts of siRNA while non-targeting siRNA was used as control.

Several concentrations of siRNA and modalities of transfection were tested and analysis of mRNA expression by Real Time PCR revealed that the maximal down-regulation of GCS was obtained with  $100 \text{ nM}$  siRNA (Figure 3.31 A); on the other hand, this resulted in a little over 50% decrease of in situ glucosylceramide synthase (GCS) activity as measured by the conversion of NBD-C6-ceramide into NBD-C6-hexosylceramide (Figure 3.31 B).

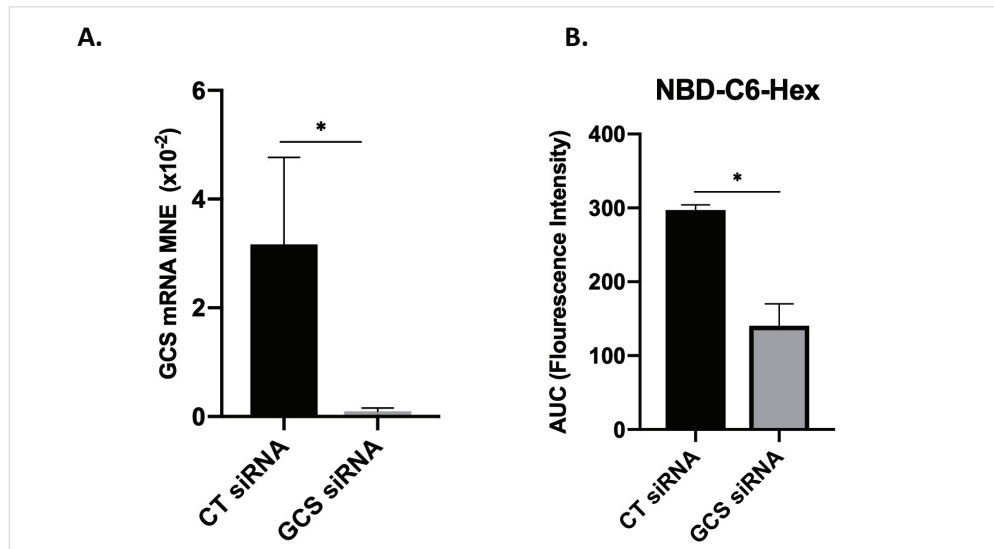


Figure 3.31. The effects of GCS siRNA transfection on GCS activity measured by A.GCS mRNA levels and B.NBD-C6-hexosylceramide levels. SD-1 cells, grown in T25 flask (total  $2 \times 10^6$  cells) transfected with 100nM of siRNA for 24 h and the effects of GCS siRNA and control siRNA (non-targeting scrambled) was measured as A. GCS mRNA expression level is measured by Real-Time PCR as described in the methods. Expression of mRNA is normalized to GAPDH and represented as mean normalized expression (MNE). B. GCS activity is detected by measuring NBD-C6-hexosylceramide levels by HPLC as described in the methods. The error bars represent the SD from 3 different experiments. ns  $P > 0.05$ , \* $P < 0.05$ .

Then, 24 h after the transfection with control and GCS siRNAs, the cells were exposed to 5 $\mu$ M imatinib for additional 24 h and endogenous sphingolipid levels were measured by HPLC/MS. As shown in Figure 3.32, although imatinib treatment in control siRNA transfected cells increased the hexosylceramide levels in SD-1 cells; total hexosylceramide production was inhibited by ~50% with GCS siRNA treatment and stayed at the same level when imatinib is applied (Figure 3.32).

On the other hand, ceramide levels were elevated significantly with only GCS siRNA treatment compared to control cells. As anticipated, imatinib treatment increased the ceramide levels by ~40% in control siRNA transfected cells and by ~80% in the cells which GCS is silenced by siRNA.

Overall these data suggest that, reflecting the sphingolipid levels changes observed in eliglustat and imatinib cotreatment; imatinib treated cells are able to further accumulate ceramide levels when GCS is silenced, and ceramide is no longer able to be converted to hexosylceramide in the cells (Figure 3.33).

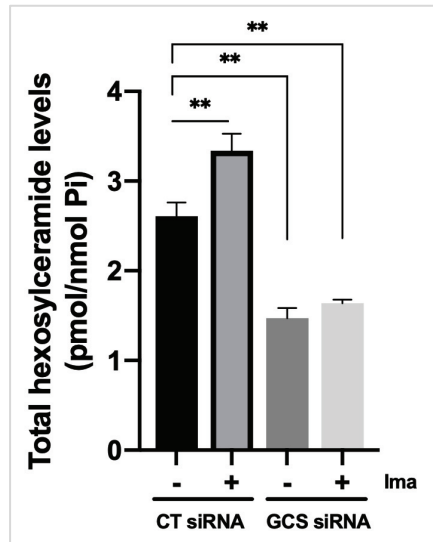


Figure 3.32. Effect of GCS knockdown and imatinib treatment on the levels of hexosylceramides in SD-1 cells. 24 hours after the transfection with control and GCS siRNAs, SD-1 cells were treated with vehicle (DMSO) or imatinib (5  $\mu$ M) for 24 h and HexCer levels were measured by HPLC/MS as described. HexCer levels were normalized to Pi concentrations, and final levels are represented on the Y axis as pmol/nmol Pi. The error bars represent the SD from 3 different experiments. ns  $P > 0.05$ , \* $P < 0.05$ , \*\* $P < 0.01$ .

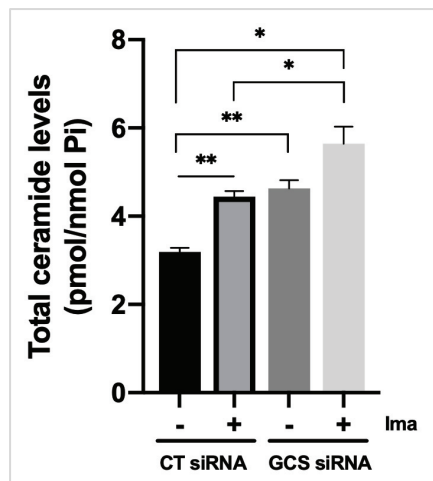


Figure 3.33. Effect of GCS knockdown and imatinib treatment on the levels of ceramide in SD-1 cells. 24 hours after the transfection with control and GCS siRNAs, SD-1 cells were treated with vehicle (DMSO) or imatinib (5  $\mu$ M) for 24 h and ceramide levels were measured by HPLC/MS as described. Ceramide levels were normalized to Pi concentrations, and final levels are represented on the Y axis as pmol/nmol Pi. The error bars represent the SD from 3 different experiments. ns  $P > 0.05$ , \* $P < 0.05$  \*\* $P < 0.01$ .

Furthermore, sphingomyelin levels are increased with imatinib treatment as anticipated from previous data whereas GCS inhibition by siRNA also showed an increase in the sphingomyelin levels suggesting that in case of a blockage on the pathway through hexosylceramides, ceramide is converted to sphingomyelin in a greater rate. Additionally, when imatinib is applied to GCS siRNA transfected cells, sphingomyelin levels are increased even more, showing an additional effect on the increase in sphingomyelin levels (Figure 3.34).

Sphingosine levels are changed in a similar manner to the other sphingolipids. imatinib treatment increased sphingosine levels by ~4-fold in control cells whereas it increased sphingosine accumulation by ~7-fold in GCS siRNA transfected cells (Figure 3.35). This data suggests that as well as ceramide levels, sphingosine level is also additively increasing with imatinib treatment on GCS siRNA transfected cells.

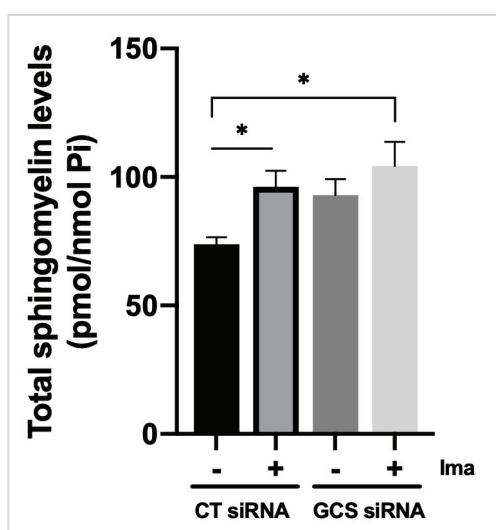


Figure 3.34. Effect of GCS knockdown and imatinib treatment on the levels of sphingomyelin in SD-1 cells. 24 hours after the transfection with control and GCS siRNAs, SD-1 cells were treated with vehicle (DMSO) or imatinib (5 $\mu$ M) for 24 h and SM levels were measured by HPLC/MS as described. The SM levels were normalized to Pi concentrations, all the SM species were summed, and final levels are represented on the Y axis as pmol/nmol Pi. The error bars represent the standard deviation (SD) from 3 different experiments. Asterisks indicate statistical significance: ns P>0.05, \*P<0.05.

Finally, we wanted to see whether these changes in sphingolipids are implicated in the proliferation phenotype, we examined the changes in cell viability with trypan blue exclusion assay on GCS siRNA transfected cells with and without imatinib treatment.

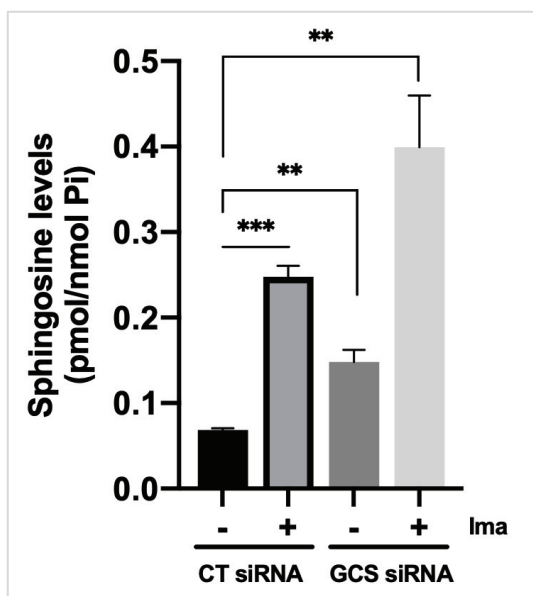


Figure 3.35. Effect of GCS knockdown and imatinib treatment on the levels of sphingosine in SD-1 cells. 24 hours after the transfection with control and GCS siRNAs, cells were treated with vehicle (DMSO) or imatinib (5 $\mu$ M) for 24 h and sphingosine levels were measured by HPLC/MS as described. Sphingosine levels were normalized to Pi concentrations and represented on the Y axis as pmol/nmol Pi. The error bars represent the SD from 3 different experiments.: ns  $P > 0.05$ , \* $P < 0.05$ , \*\* $P < 0.01$ , \*\*\* $P < 0.001$ .

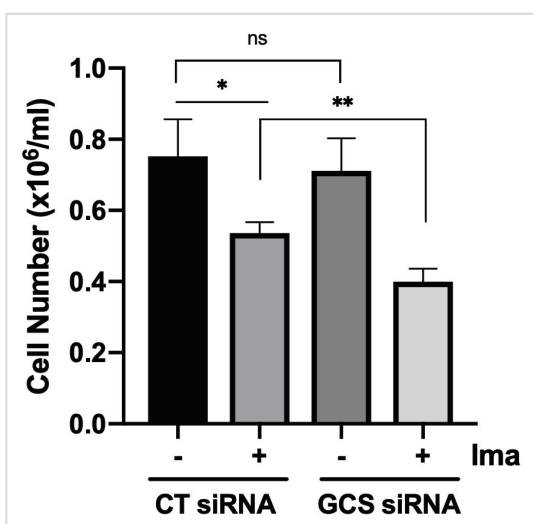


Figure 3.36. Effect of GCS knockdown together with imatinib treatment on cell viability in SD-1 cells. Cell viability is assessed by trypan blue exclusion assay for SD-1 cells transfected with control and GCS siRNAs and then treated with imatinib (5 $\mu$ M) for 24 hours. The error bars represent the SD from 3 different experiments. ns  $P > 0.05$ , \* $P < 0.05$ , \*\* $P < 0.01$ .

Correlatively to the previous data, imatinib treatment on control cells inhibited cell proliferation by 30% and by 50% where GCS is silenced by siRNA in SD-1 cells (Figure 3.36). Together these data confirm that synergistic cytostatic effect of imatinib and eliglustat cotreatment is actually due to GCS inhibition since similar changes both at sphingolipid and cell proliferation level were seen by inhibiting GCS expression with siRNA transfection. Again, these data strengthen the idea of blocking the sphingolipid flux through by inhibiting GCS can be used as a treatment approach to sensitize SD-1 cells to imatinib treatment by increasing the endogenous ceramide and/or sphingosine levels.

### **3.9. Generation of Imatinib Resistant SD-1 Cells (SD-1R)**

Considering the clinical relevance of imatinib resistance in the treatment of Ph+ ALL, we sought to test the efficacy of targeting sphingolipid metabolism in imatinib-resistant Ph+ ALL cells. To this aim, we generated an imatinib resistant SD-1 cell line to mimic development of secondary resistance in Ph+ ALL patients who are receiving TKI treatment. Secondary resistance is likely acquired by cells that are intrinsically more resistant, survive treatment and continue to be exposed to the drug. Since SD-1 cells are intrinsically more resistant to imatinib than other Ph+ ALL cell lines (Figure 3.1), they were selected for this purpose and they were exposed to gradually increasing concentrations of imatinib starting from 0.05 $\mu$ M. During the process, imatinib concentration is doubled when the cells reach the same confluency and growth rate as parental cell line. The escalation of the dose was stopped when the newly generated resistant cell line was able to be maintained in the presence of 10  $\mu$ M of imatinib in the medium and they are referred to as SD-1R cells. The detailed protocol for generation of resistant cell line can be found in methods section (Figure 2.1).

In these conditions, parental SD-1 cells showed more than a 70% inhibition of viable cells whereas SD-1R showed no significant change at 48 h (Figure 3.37 A). Cell viability was also measured by MTT assay at 48h of treatment with increasing concentrations of imatinib (Figure 3.37 B). As shown in the figure, IC<sub>50</sub> value are calculated at ~5  $\mu$ M and ~15  $\mu$ M for parental SD-1 and SD-1R cells, respectively, with

a 3-fold increase of resistance in newly generated imatinib resistant SD-1R cells compared to parental cell line.

Resistance of SD-1R to imatinib was also confirmed by absence of caspase-3 cleavage in response to imatinib (Figure 3.38 A). In fact, while imatinib treatment was found to increase caspase-3 cleavage in SD-1 cells, caspase 3 activation was not detected in SD-1R cells. Since we saw a change in an apoptotic protein we wanted to check if any other apoptotic proteins are involved into imatinib resistance in SD-1R cells. To this end, we checked the protein levels of BCL2 and BCL-XL but there was no change at the levels of these proteins between sensitive and resistant cells (Figure 3.38 B).

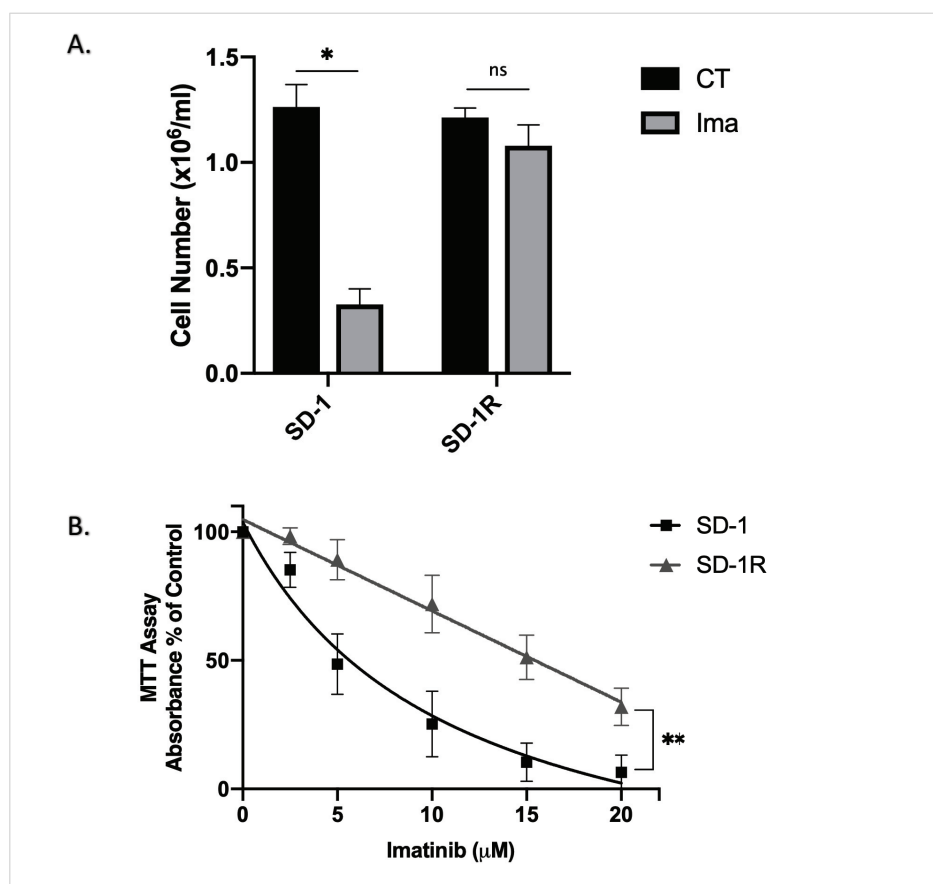


Figure 3.37. Comparative response to imatinib treatment by SD-1 and SD-1R cells measured by A. trypan blue assay B. MTT assay. A. Cell viability is assessed by trypan blue exclusion assay for SD-1 and SD-1R cells seeded at  $0.3 \times 10^6$  cells/ml in a 6-well plate and treated with  $10 \mu\text{M}$  imatinib for 48 h. B. The effect of imatinib on cell viability is evaluated by an MTT assay procedure on SD-1 and SD-1R cells incubated with increased concentrations of imatinib ( $2.5$ -,  $5$ -,  $10$ -,  $15$ -,  $20 \mu\text{M}$ ) for 48 h. Results are represented in the graph as the percentage of the absorbance and normalized by untreated control cells. The error bars represent the SD from 3 different experiments. ns  $P > 0.05$ , \* $P < 0.05$ , \*\* $P < 0.01$ .



Lastly, we wanted to check one of the commonly seen type of resistance mechanism in BCR/ABL positive cells which is elevating the levels of BCR/ABL as previously indicated by various studies both in CML and Ph+ ALL cases.

As seen in Figure 3.38 C, SD-1R cells revealed increased levels of BCR/ABL protein suggesting that newly generated SD-1R cells showed an increase in BCR/ABL protein levels suggesting this upregulation as a contributor to the resistance mechanism in these cells. Since upregulation of BCR/ABL levels is a common resistance mechanism for BCR/ABL positive cells, this data indicates similar to other BCR/ABL positive cell lines, SD-1R cells might reveal a BCR/ABL dependent mechanism for imatinib resistance.

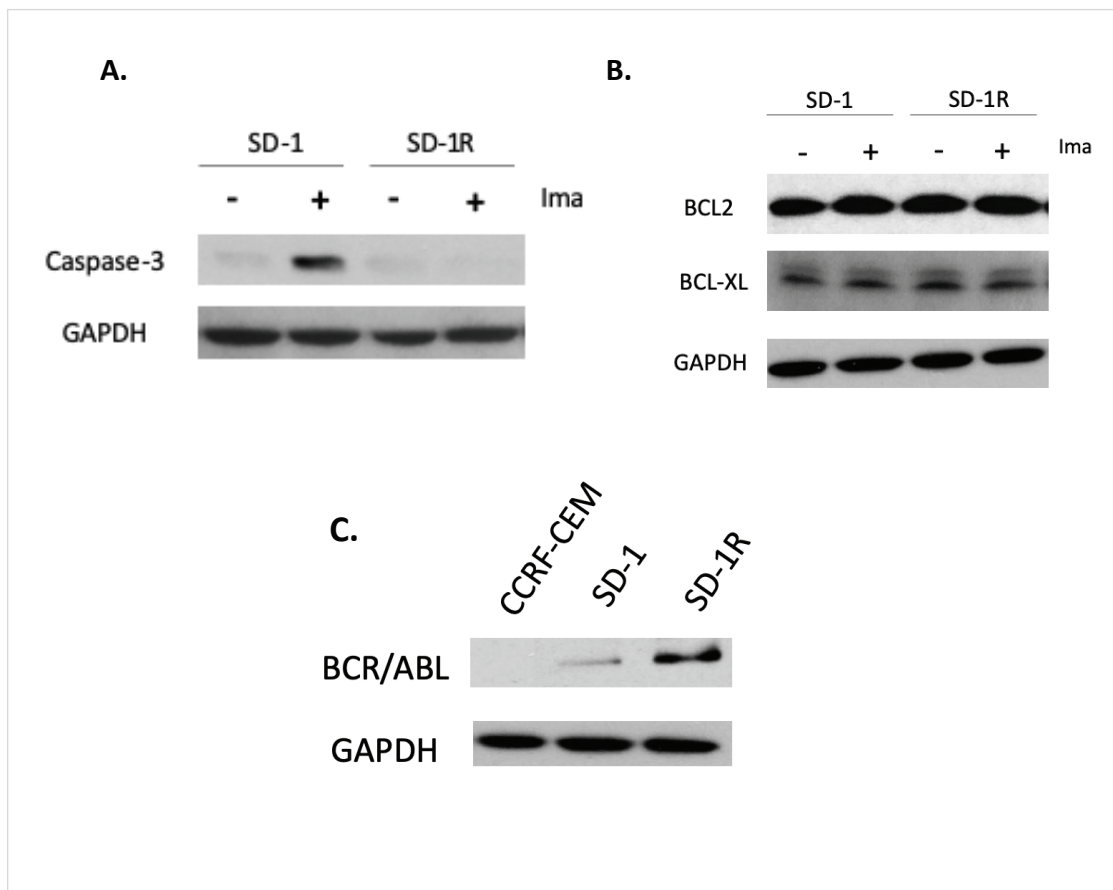


Figure 3.38. Mechanism of resistance to apoptosis induced by imatinib in SD-1R cells.

A. Cleaved caspase-3 B. BCL2 and BCL-XL C. BCR/ABL levels. A. Cleaved caspase-3 (17-19kDa) levels B. Levels of apoptotic proteins BCL2 (26kDa) and BCL-XL (30kDa) C. BCR/ABL (190 kDa) protein levels were determined by western blotting on SD-1 and SD-1R cells treated with 10 $\mu$ M imatinib for 48 h. GAPDH (37kDa) is used as internal control representing a housekeeping protein.

### 3.10. Blunted Imatinib Induced Changes in Endogenous Sphingolipid Levels of SD-1R cells

To test whether targeting sphingolipid metabolism could also sensitize imatinib-resistant Ph+ ALL cells in addition to parental SD-1 cells, we first assessed the changes in sphingolipid profile between SD-1 and SD-1R cells by HPLC/MS/MS following imatinib treatment with 10  $\mu$ M for 24 h (Figure 3.39, 3.40, 3.41, 3.42). While imatinib treatment resulted in a significant increase in total ceramide levels in SD-1 cells no changes were observed in SD-1R cells (Figure 3.39), suggesting that failure to accumulate ceramide might be involved in resistance to imatinib in SD-1R cells.

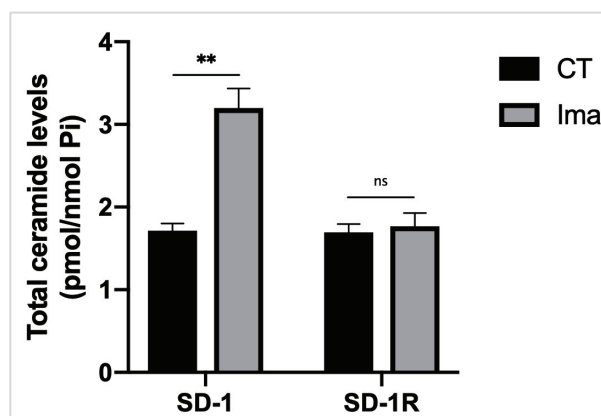


Figure 3.39. Changes in endogenous ceramide levels of SD-1 and SD-1R cells in response to imatinib. SD-1 and SD-1R cells are seeded at  $0.3 \times 10^6$  cells/ml in a 6-well plate and treated with vehicle (DMSO) or 10  $\mu$ M imatinib for 24 h and ceramide levels were measured by HPLC/MS as described. The ceramide levels were normalized to Pi concentrations and final levels are represented on the Y axis as pmol/nmol Pi. The error bars represent the SD from 3 different experiments. ns  $P > 0.05$ , \* $P < 0.05$ , \*\* $P < 0.01$ .

Interestingly, total HexCer levels were similarly elevated in both SD-1 and SD-1R cells (Figure 3.40) indicating that this metabolic pathway is still operational in SD-1R cells. Therefore, the data suggest that imatinib resistance in SD-1R cells is associated to a deficiency in production but not in further metabolization of ceramide. Additionally, while sphingosine levels were increased by  $\sim 3$ -fold following imatinib treatment in SD-1 cells, they seemed to trend towards an increase in SD-1R cells, although the change is

not statistically significant (Figure 3.41). Furthermore, while SM levels increased significantly in SD-1 cells, they remained unchanged in SD-1R cells (Figure 3.42).

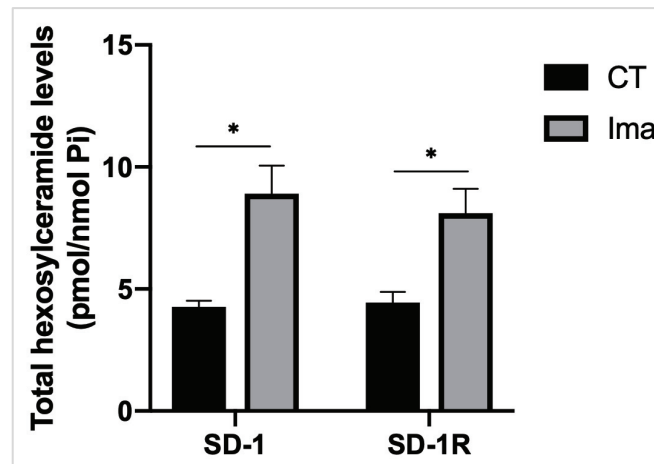


Figure 3.40. Changes in endogenous hexosylceramide levels of SD-1 and SD-1R cells in response to imatinib. SD-1 and SD-1R cells are seeded at  $0.3 \times 10^6$  cells/ml in a 6-well plate and treated with vehicle (DMSO) or  $10 \mu\text{M}$  imatinib for 24 h and HexCer levels were measured by HPLC/MS as described. HexCer levels were normalized to Pi concentrations, final levels are represented on the Y axis as pmol/nmol Pi. The error bars represent the SD from 3 different experiments. ns  $P > 0.05$ , \* $P < 0.05$ .

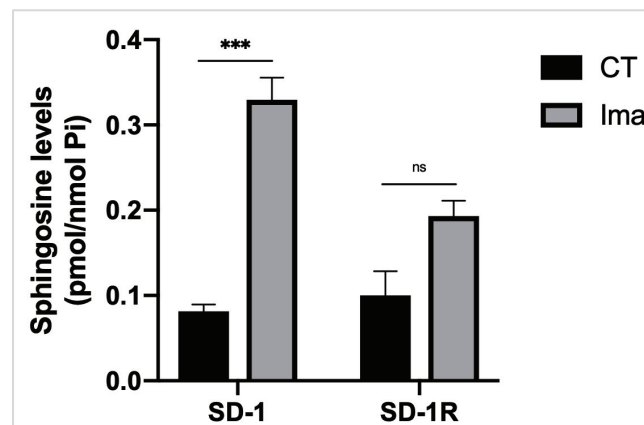


Figure 3.41. Changes in endogenous sphingosine levels of SD-1 and SD-1R cells in response to imatinib. SD-1 and SD-1R cells are seeded at  $0.3 \times 10^6$  cells/ml in a 6-well plate and treated with vehicle (DMSO) or  $10 \mu\text{M}$  imatinib for 24 h and sphingosine levels were measured by HPLC/MS as described. The sphingosine levels were normalized to Pi concentrations and represented on the Y axis as pmol/nmol Pi. The error bars represent the SD from 3 different experiments. ns  $P > 0.05$ , \*\*\* $P < 0.001$ .

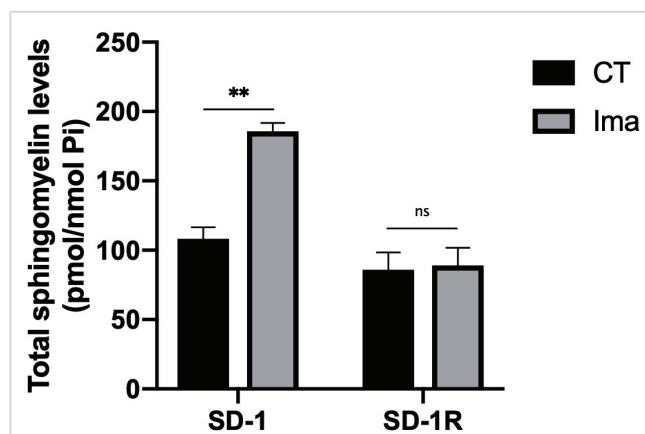


Figure 3.42. Changes in endogenous sphingomyelin levels of SD-1 and SD-1R cells in response to imatinib. SD-1 and SD-1R cells are seeded at  $0.3 \times 10^6$  cells/ml in a 6-well plate and treated with vehicle (DMSO) or  $10 \mu\text{M}$  imatinib for 24 hours and sphingomyelin levels were measured by HPLC/MS as described. The SM levels were normalized to Pi concentrations and represented on the Y axis as pmol/nmol Pi. The error bars represent the SD from 3 different experiments. ns  $P > 0.05$ , \* $P < 0.05$ , \*\* $P < 0.01$ .

Overall, these results showed a blunted sphingolipids response of SD-1R cells to imatinib compared to sensitive SD-1 cells (the overall sphingolipids changes were significantly reduced compared to sensitive SD-1 cells) and growth inhibitory sphingolipids were not accumulated; however, they also demonstrated a preserved ability of these cells to channel sphingolipids towards HexCers in response to imatinib.

### 3.11. Inhibition of GCS in Combination with Imatinib Treatment Promotes Accumulation of Growth Inhibitory Sphingolipids and Resensitizes SD-1R Cells to the Drug

Next, we applied the same treatment strategy as used in SD-1 cells to modulate sphingolipid metabolism in order to accumulate ceramide and/or sphingosine levels to see whether this intracellular changes in sphingolipid levels could overcome imatinib resistance in SD-1R cells. For this purpose, cells were treated with  $10 \mu\text{M}$  imatinib, the concentration that they grow with in media with or without  $100 \text{ nM}$  eliglustat pre-treatment and sphingolipid levels were detected as described above. Begin with, the data

showed that eliglustat treatment decreased hexosylceramide levels to 1.07 pmol/nmol Pi and kept them at 1.55 pmol/nmol Pi when imatinib added onto eliglustat; although they are increased to 6.04 pmol/nmol with imatinib alone treatment compared to 3.8 pmol/nmol hexosylceramides in control cells (Figure 3.43). This data is suggesting that eliglustat is inhibiting GCS activity and blocking the conversion of ceramide to hexosylceramides in SD-1R cells similar to SD-1 cells.

Additionally, total ceramide levels are elevated by 2-fold with eliglustat and imatinib cotreatment although imatinib and eliglustat alone treatments also showed an increase but not as much in total ceramide levels suggesting a synergistic effect on the accumulation of ceramides with eliglustat and imatinib cotreatment (Figure 3.44).

Furthermore, treatment with imatinib alone increased the levels of sphingosine by 2-fold while it resulted in a further increase by more than 3-fold in presence of eliglustat (Figure 3.45). Again, this data suggests that, similar to the effect on ceramides, imatinib and eliglustat cotreatment shows a synergistic increase in the levels of sphingosine in SD-1R cells.

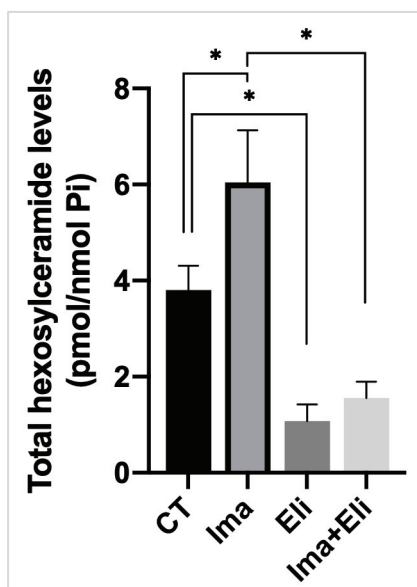


Figure 3.43. The changes in the hexosylceramide levels of SD-1R cells treated with imatinib and eliglustat and their combination. SD-1 cells, grown in T25 flasks (seeded at  $0.3 \times 10^6$  cells/ml) were treated with vehicle (DMSO), imatinib (10  $\mu$ M), eliglustat (100nM) and eliglustat+imatinib for 24 h and HexCer levels were measured by HPLC/MS as described. HexCer levels were normalized to Pi concentrations final levels are represented on the Y axis as pmol/nmol Pi. The error bars represent the SD from 3 different experiments. ns  $P > 0.05$ , \* $P < 0.05$ .

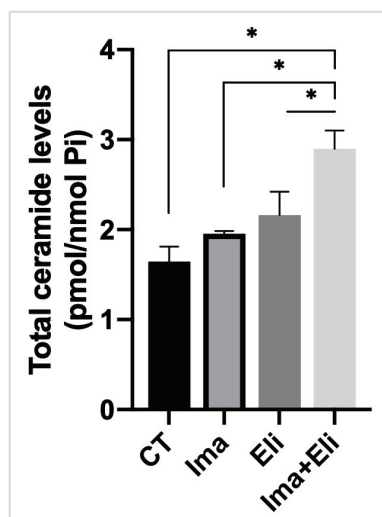


Figure 3.44. The changes in the ceramide levels of SD-1R cells treated with imatinib and eliglustat and their combination. SD-1 cells, grown in T25 flasks (seeded at  $0.3 \times 10^6$  cells/ml) were treated with vehicle (DMSO), imatinib ( $10 \mu\text{M}$ ), eliglustat ( $100 \text{nM}$ ) and eliglustat +imatinib for 24 h and ceramide levels were measured by HPLC/MS as described. The ceramide levels were normalized to Pi concentrations, all the sphingolipid species were summed, and final levels are represented on the Y axis as pmol/nmol Pi. The error bars represent the SD from 3 different experiments. ns  $P > 0.05$ , \* $P < 0.05$ .

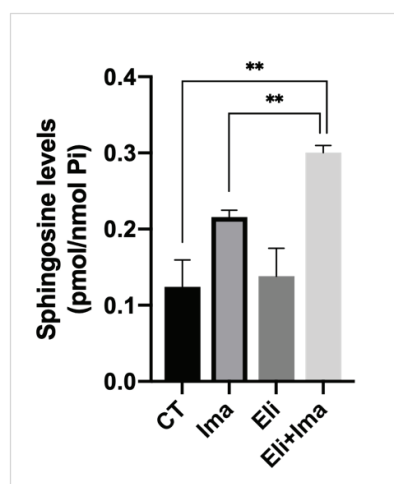


Figure 3.45. The changes in the sphingosine levels of SD-1R cells treated with imatinib and eliglustat and their combination. SD-1 cells, grown in T25 flasks (seeded at  $0.3 \times 10^6$  cells/ml) were treated with vehicle (DMSO), imatinib ( $10 \mu\text{M}$ ), eliglustat ( $100 \text{nM}$ ) and eliglustat ( $100 \text{nM}$ )+imatinib( $10 \mu\text{M}$ ) for 24 h and sphingosine levels were measured by HPLC/MS as described. The sphingosine levels were normalized to Pi concentrations, all the sphingolipid species were summed, and final levels are represented on the Y axis as pmol/nmol Pi. The error bars represent the SD from 3 different experiments. ns  $P > 0.05$ , \* $P < 0.05$ , \*\* $P < 0.01$ .

Lastly, to see the effect of these changes in sphingolipid levels on the sensitivity to imatinib, we assessed a cell viability test with trypan blue exclusion assay to the cells treated with imatinib with or without eliglustat. As shown in Figure 3.46, imatinib and eliglustat alone treatments did not show any effect on cell viability at neither at 24 not at 48 h. Impressively, cotreatment of imatinib and eliglustat resulted in sensitization of SD-1R cells to imatinib treatment by showing a decrease in cell number by ~40% and ~70% at 24 and 48 h respectively. This data is suggesting that, a reversal in resistance to imatinib can be achieved by treating cells with eliglustat to inhibit GCS activity together with imatinib resulted by an accumulation in ceramide and sphingosine levels synergistically.

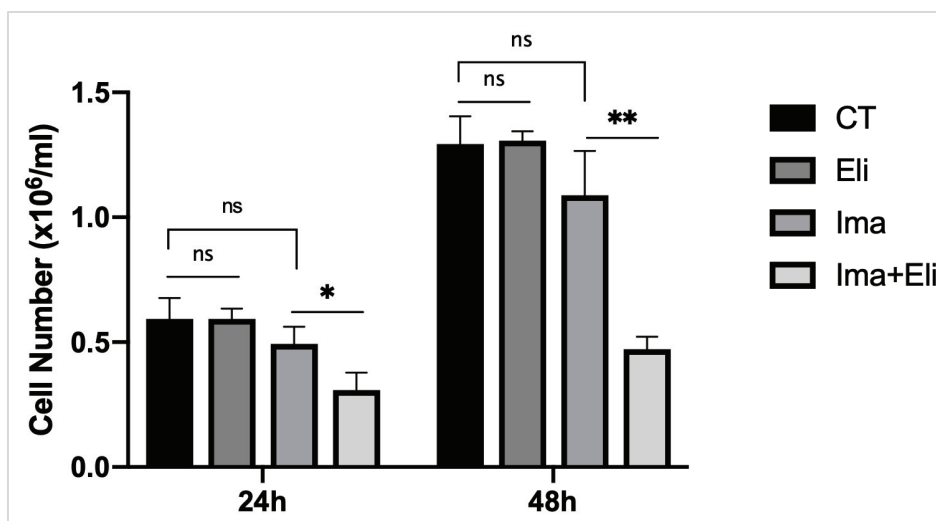


Figure 3.46. The effect of treatment with imatinib, eliglustat and their combination on cell viability of SD-1R cells. Cell viability is assessed by trypan blue exclusion assay for SD-1R cells seeded at  $0.3 \times 10^6$  cells/ml and treated with vehicle (DMSO), imatinib ( $10 \mu\text{M}$ ), eliglustat ( $100 \text{nM}$ ) and eliglustat ( $100 \text{nM}$ )+imatinib ( $10 \mu\text{M}$ ) for 24 and 48 h. The error bars represent the SD from 3 different experiments. ns  $P > 0.05$ , \* $P < 0.05$ , \*\* $P < 0.01$ .

Finally, similar to the data obtained in SD-1 cells, to further prove that overcoming imatinib resistance is actually through GCS inhibition but not by any possible off-target effects of eliglustat, we repeated the viability assay by applying the same concentration of imatinib onto cells that are transfected by control and GCS siRNAs. The data showed that, indeed as eliglustat does, silencing GCS by siRNA is able to sensitize SD-1R cells to imatinib treatment whereas the cells transfected with control siRNA were unresponsive to imatinib treatment at the cell viability level (Figure 3.47).

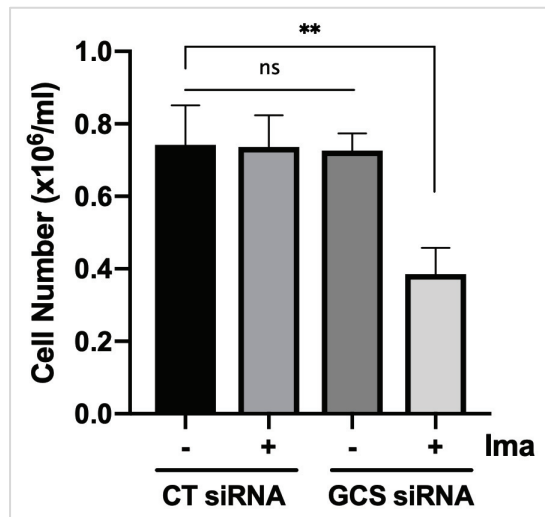


Figure 3.47. Effect of GCS knockdown together with imatinib treatment on cell viability in SD-1R cells. Cell viability is assessed by trypan blue exclusion assay for SD-1 cells transfected with control and GCS siRNAs and then treated with imatinib (10  $\mu$ M) for 24 hours. The error bars represent the standard deviation (SD) from 3 different experiments. Asterisks indicate statistical significance: ns  $P > 0.05$ , \* $P < 0.05$ , \*\* $P < 0.01$ .

Taken together, these data reveal the involvement of sphingolipids by a defect in production of majorly ceramide and/or sphingosine into secondary resistance to imatinib as well as intrinsic imatinib resistance. Moreover, the data showed the reversal of imatinib resistance following modulation of sphingolipids with inhibiting GCS activity by eliglustat in order to accumulate ceramide and/or sphingosine to achieve cytotoxic levels of these sphingolipids in secondary resistant Ph+ ALL cells. All together these results suggest that lack of ceramide and/or sphingosine accumulation following imatinib treatment is associated with secondary resistance to imatinib in SD-1R cells and that blocking GCS activity was sufficient to cause the accumulation of these growth inhibitory sphingolipids and to re-sensitize SD-1R cells to imatinib.



## CHAPTER 4

### DISCUSSION

Ph+ ALL is the most commonly seen subtype of adult B-ALL with the incidence of 20-30% in adults<sup>30</sup>. The prognosis has significantly improved after the approval of a first-generation TKI, imatinib mesylate as a first-line therapy in Ph+ ALL<sup>247</sup>. Even monotherapy with TKIs have been shown to be effective enough for the patients to reach complete remission in older patients; it also has been shown that using TKIs in combination with multi-agent chemotherapy led to disease free survival and better outcomes in long-term<sup>30,248</sup>. Although the advancements in the prognosis of Ph+ ALL with the developments of new treatment options; the disease is still considered as high-risk with high risk of relapse and the overall survival rate is still around 30-45%<sup>6,249</sup>. So far, development of imatinib resistance has been considered as the one of the major mechanisms that cause the failure of treatment. In this regard, studies with second generation TKIs such as dasatinib, nilotinib and bosutinib showed that they might only partially overcome imatinib resistance in the patients with T315I mutation<sup>33,250</sup>. Therefore, recent studies have been focused on discovering the signaling pathways that potentially contribute the development of resistance to eventually find targetable molecules in order to prevent the development of resistance from the beginning of the treatment or overcome the existent resistance.

Imatinib resistant Ph+ ALL cell lines have been shown to depend on alternative survival pathways other than BCR/ABL itself, including RAS/RAF/MEK pathway<sup>251</sup> and PI3K/AKT pathway<sup>94,252</sup>. Nevertheless, the roles of these pathways in imatinib resistant Ph+ ALL patients are not fully understood and the number of studies focusing on this issue remains limited. Therefore, our study carries importance in two major points: i) revealing the involvement of bioactive sphingolipids in imatinib induced growth inhibition in Ph+ ALL cells ii) introducing a new treatment strategy to reverse imatinib resistance by manipulating sphingolipid pathway.

To begin with, Ph+ ALL cell lines are known to be intrinsically more resistant to imatinib compared to CML cell lines due to their molecular complexity<sup>94</sup>. Considering

this fact, between two different Ph+ ALL having different sensitivity to imatinib, we picked an intrinsically more resistant cell line SD-1 to start with in order to mimic the condition of intrinsically imatinib resistant patients (Figure 3.1). Another reason is that thinking the clinical relevance, intrinsically more resistant patients are more likely to develop secondary and stronger resistance to imatinib as they go through treatment, which is modeled in our newly generated SD-1R cells by using SD-1 cells as parental cell line (Figure 3.37).

On the other hand, bioactive sphingolipids and their regulation on the progression of cancer have been studied in various type of cancers previously<sup>166,228,253–255</sup>. Sphingosine kinase, in particular has been shown to regulate imatinib induced apoptosis and resistant to imatinib through regulation of BCR/ABL in CML cell lines<sup>207,228</sup> and in the most recent studies targeting sphingosine kinase-1 and -2 has been demonstrated as a new treatment strategy in Ph+ ALL<sup>236,256</sup>. Interestingly, we could not detect any effect of SK-1 inhibition in addition to the effects of imatinib when applied together, suggesting the regulation of ceramide for the development of imatinib resistance can vary among different cell lines (Figure 3.7). Interestingly, SK-1 levels were significantly decreasing with imatinib treatment both at the activity level and the protein expression level (Figure 3.5 and 3.6) suggesting a highly possible relation between BCR/ABL and SK-1 in Ph+ ALL. On the other hand, SK-1 activity level did not change by doubling the concentration of PF543 from 400 nM to 800 nM, suggesting that PF543 was at maximal inhibitory concentration at 400 nM and the leftover SK activity is coming from SK-2 because PF543 is known to be specific for SK-1 (Figure 3.4). Another interesting point is that, imatinib and PF543 were adding onto SK-1 activity levels as shown in Figure 3.6 but the additive effect on SK-1 activity level did not reflect on cell number data in Figure 3.7. When we screened the previous studies revealing the roles of SK-1 into Ph+ ALL or CML, we realized that instead of PF543, SKI-II were used as a pharmacological inhibitor of SK. As Cingolani et al. reported, SKI-II were detected to inhibit dihydroceramide desaturase (DES) activity and as some of the effects seen by SKI-II attributed to decreased SIP could actually be caused by augmented dhCers and/or their metabolite instead of a direct result of only SK inhibition<sup>257</sup>. Therefore, the same possibility should be taken into account in the case for Ph+ ALL after evaluating our results with previous reports.

On the other hand, other studies showed the involvement of ceramide into TKI induced cell death in CML cell lines<sup>231,258</sup>. Our study is in agreement with the previous studies showing that the action of imatinib requires regulation of sphingolipid

metabolism. As shown in Figure 3.8-3.16, imatinib treatment resulted an increase in the levels of dihydrosphingosine, dihydroceramide, most of the ceramide species, and sphingosine as well as complex sphingolipids including hexosylceramides and sphingomyelin; suggesting that not only generation of ceramide but further metabolization of it to HexCer and SM is initiated by imatinib treatment in these cells. On the other hand, the level of ceramide and other sphingolipids including the members of *de novo* synthesis pathway was not changed with imatinib treatment in SD-1R cells suggesting that there is a defect in induction of *de novo* synthesis pathway in SD-1R cells which might be one of the resistance mechanisms in these cells. As previously reported, imatinib treatment induces ceramide accumulation by activation of *de novo* synthesis pathway through regulating serine palmitoyltransferase long chain-1 SPTLC1 (SPT), the enzyme catalyzes the first and rate-limiting step reaction of *de novo* synthesis in CML cells <sup>259</sup>. Thus, it is pointing the idea that the defect in *de novo* synthesis pathway in SD-1R cells might be due to dysregulation of serine palmitoyltransferase (SPT). Another possibility for the defect in *de novo* synthesis is the involvement of ceramide synthases (CerS1-6), the enzymes that catalyze the formation of ceramides from sphingoid base and their suppression in SD-1R cells as a resistance mechanism. Previously, reported by <sup>231,232</sup>, CerS genes are upregulated by TKI treatment in CML cell lines which supports the question as to whether there is a correlation between these genes and response to imatinib in Ph+ ALL. So, we are currently focused on addressing these possibilities to fully understand the mechanism of imatinib resistance in Ph+ ALL cells from sphingolipids perspective. Interestingly, imatinib treatment was able to increase HexCer levels in SD-1R cells in a similar manner with SD-1 cells; suggesting the possibility of GCS activity being at maximum rate in both cells. Apparently, these cells are using HexCer as a sink for ceramide to prevent accumulation of ceramide by a similar mechanism which previously reported in different leukemias <sup>200</sup>.

The increase in the members of *de novo* synthesis pathway that is seen in SD-1 cells but not in SD-1R cells led us to test the involvement of this pathway in imatinib induced cytostaticity in SD-1 cells. With our findings; although the cytostatic effect of imatinib is not fully rely on sphingolipids (ceramide and/or sphingosine), we are able to show that sphingolipids are involved in part in imatinib induced cytotoxicity. Apart from to the previous studies, we showed that the action of imatinib on sphingolipids are through induction of *de novo* synthesis pathway proved by our data shown in Figure 3.17-3.22. Myriocin is a serine palmitoyltransferase inhibitor which inhibits the first and rate-

limiting step reaction of *de novo* synthesis pathway used in various studies <sup>260</sup>. To prove the induction of *de novo* synthesis pathway by imatinib, we measured sphingolipid levels with imatinib treatment in presence of myriocin which blocks the first reaction of *de novo* synthesis pathway. Indeed, imatinib was not able to modulate same sphingolipids when myriocin is present in the media, proving that the changes in sphingolipids by imatinib treatment are due to induction of *de novo* synthesis pathway. We also showed that blocking the first step reaction of *de novo* synthesis by using myriocin protects the cells from imatinib induced cytotoxicity and suggesting that production of sphingolipids by induction of *de novo* synthesis pathway is in part involved in the cytostatic effects of imatinib. It should be noted that imatinib has multiple targets other than BCR/ABL in the cells <sup>261</sup> and given the detected and used relatively high IC<sub>50</sub> value of imatinib (5 μM and 15 μM for SD-1 and SD-1R cells, respectively) in this study suggesting that by inhibiting *de novo* synthesis of sphingolipids it is only possible to rescue cells from the effects of one of the downstream signaling targets of imatinib.

Previous studies have revealed the mechanism of ceramide shunting through glucosylceramide by the enzyme GCS and the role of GCS activation in regulation of chemotherapy resistance in various type of cancers. So, blocking the generation of glucosylceramide by different agents has been proposed as an approach to restore sensitivity to these chemotherapeutics mainly by inducing the accumulation of ceramide to reach the cytotoxic levels <sup>262-267</sup>. With the same sense of purpose, we manipulated sphingolipid metabolism in our cells to further accumulate ceramide to sensitize them to imatinib. Since imatinib treatment also increased the levels of hexosylceramides in both SD-1 and SD-1R cells, we aimed to block the conversion of ceramide to hexosylceramides by inhibiting GCS activity by using an FDA approved GCS inhibitor eliglustat which is used in the patients with Gaucher's disease. Eliglustat has been shown to be highly tolerated in humans <sup>246,268</sup> and proposed to use in combinational treatments of GCS inhibition with chemotherapeutic agents <sup>245,269</sup>. Indeed, we were able to see a further accumulation in certain type of sphingolipids including ceramide as well as sphingosine and sphingomyelin with eliglustat treatment in combination with imatinib although eliglustat by itself was not sufficient to increase ceramide levels. A class of previously developed glucosylceramide synthase inhibitors (PDMP and P4) has been shown to accumulate ceramide through other mechanisms independently from only inhibition of glucosylceramide levels <sup>270</sup>. Our result with eliglustat here is contradictory to these data in the sense of inhibiting glucosylceramide accumulation without increasing ceramide

levels or inhibiting cell growth which makes eliglustat more selective and tolerated in healthy tissues. As confirmed with the data shown in Figure 3.26 and 3.29 for SD-1 and 3.44 and 3.45 for SD-1R the levels of ceramide and/or sphingosine accumulated in the cells with eliglustat and imatinib cotreatment was enough to sensitize the cells to imatinib treatment in SD-1 cells and to overcome secondary resistance to imatinib in SD-1R cells. In passing, it should be noted that as well as ceramide, sphingosine is known as its cytotoxic effects in the cells<sup>271,272</sup>. So, the sensitization to imatinib might be due to further accumulation of either ceramide and/or sphingosine. The growth inhibitory effect of ceramide has been shown to be through a number of pathways including suppression of Akt, c-Myc and BCR/ABL signaling<sup>230,273,274</sup>. Therefore, the growth inhibitory effect of eliglustat and imatinib due to ceramide accumulation could be due to suppression of one of the listed signaling pathways. Specific to Ph+ ALL, there are multiple molecular pathways playing critical roles for the orchestration of the progression of Ph+ ALL<sup>275,276</sup>. PI3K/AKT signaling, as being one of them is reported as BCR/ABL independent resistance mechanism in Ph+ ALL cell lines<sup>94</sup> and proposed as the responsible mechanism for unresponsiveness to imatinib. This confrontation suggesting that the mechanism of sensitization to imatinib might be actually due to the effects of ceramide on AKT signaling rather than on BCR/ABL given the previously reported inhibitory effect of ceramide on AKT signaling<sup>189</sup>.

Since there is still an appreciable amount of ceramide being converted to SM in response to imatinib and eliglustat cotreatment (Figure 3.28); considering this amount of ceramide as getting lost; a more effective approach to sensitize the cells to imatinib treatment would be to inhibit both GCS and SMS activities with imatinib treatment at the same time. The only obstacle for this approach is that currently even the most commonly used inhibitor D609 has been shown to have other targets besides SMS in the sphingolipid pathway which makes the readout of the effect of this inhibitor difficult and unreliable<sup>277</sup>.

In this study, we reported the biological changes by using only one cell line (SD-1) and its resistant derivative (SD-1R) and we still do not know if these findings can be translatable to a subset or all imatinib resistant patients. Therefore, our follow-up projects include using primary cultures obtained from imatinib sensitive and resistant patients and testing the efficiency of imatinib and eliglustat treatment on these cell cultures as well as xenografting a panel of Ph+ ALL samples into mice and testing the antileukemic effects of eliglustat and imatinib cotreatment in animal models. On the other hand, we can extend

this approach on both CML and Ph+ ALL cases by establishing this approach as a tool against imatinib resistance.

In conclusion, here for the first time in the literature we showed that *de novo* synthesis pathway of sphingolipids is involved in response to imatinib induced growth inhibition in Ph+ ALL cells. Moreover, it is revealed that manipulation of sphingolipid metabolism by inhibiting GCS together with conventional chemotherapy is promising for imatinib resistant patients in Ph+ ALL.

## REFERENCES

1. Jabbour E, O'Brien S, Konopleva M, Kantarjian H. New insights into the pathophysiology and therapy of adult acute lymphoblastic leukemia. *Cancer*. 2015. doi:10.1002/cncr.29383
2. German J. Bloom's syndrome. XX. The first 100 cancers. *Cancer Genet Cytogenet*. 1997. doi:10.1016/S0165-4608(96)00336-6
3. Bielora B, Fisher T, Waldman D, et al. Acute lymphoblastic leukemia in early childhood as the presenting sign of ataxia-telangiectasia variant. *Pediatr Hematol Oncol*. 2013. doi:10.3109/08880018.2013.777949
4. American Cancer Society. *Cancer Facts & Figures 2019*.; 2019.
5. Terwilliger T, Abdul-Hay M. Acute lymphoblastic leukemia: a comprehensive review and 2017 update. *Blood Cancer J*. 2017;7(6):e577. doi:10.1038/bcj.2017.53
6. Daver N, Thomas D, Ravandi F, et al. Final report of a phase II study of imatinib mesylate with hyper-CVAD for the front-line treatment of adult patients with Philadelphia chromosome-positive acute lymphoblastic Leukemia. *Haematologica*. 2015. doi:10.3324/haematol.2014.118588
7. Jabbour EJ, Faderl S, Kantarjian HM. Adult acute lymphoblastic leukemia. In: *Mayo Clinic Proceedings*. ; 2005. doi:10.4065/80.11.1517
8. Alvarnas JC, Brown PA, Aoun P, et al. Acute lymphoblastic leukemia, version 2.2015: Clinical practice guidelines in oncology. *JNCCN J Natl Compr Cancer Netw*. 2015;13(10):1240-1279. doi:10.6004/jnccn.2015.0153
9. Bennett JM, Catovsky D, Daniel M-T, et al. Proposals for the Classification of the Acute Leukaemias French-American-British (FAB) Co-operative Group. *Br J Haematol*. 1976;33(4):451-458. doi:10.1111/j.1365-2141.1976.tb03563.x
10. Harris NL, Jaffe ES, Diebold J, et al. World Health Organization Classification of Neoplastic Diseases of the Hematopoietic and Lymphoid Tissues: Report of the Clinical Advisory Committee Meeting—Airlie House, Virginia, November 1997. *J Clin Oncol*. 1999;17(12):3835-3849. doi:10.1200/JCO.1999.17.12.3835
11. Vardiman JW, Thiele J, Arber DA, et al. The 2008 revision of the World Health Organization (WHO) classification of myeloid neoplasms and acute leukemia: rationale and important changes. *Blood*. 2009;114(5):937-951. doi:10.1182/blood-

2009-03-209262

12. Wang S, He G. 2016 Revision to the WHO classification of acute lymphoblastic leukemia. *J Transl Intern Med.* 2016. doi:10.1515/jtim-2016-0040
13. Rowe JM. Prognostic factors in adult acute lymphoblastic leukaemia. *Br J Haematol.* June 2010;no-no. doi:10.1111/j.1365-2141.2010.08246.x
14. Rowe JM, Buck G, Burnett AK, et al. Induction therapy for adults with acute lymphoblastic leukemia: results of more than 1500 patients from the international ALL trial: MRC UKALL XII/ECOG E2993. *Blood.* 2005;106(12):3760-3767. doi:10.1182/blood-2005-04-1623
15. Mullighan CG, Collins-Underwood JR, Phillips LAA, et al. Rearrangement of CRLF2 in B-progenitor-and Down syndrome-associated acute lymphoblastic leukemia. *Nat Genet.* 2009. doi:10.1038/ng.469
16. Roberts KG, Morin RD, Zhang J, et al. Genetic Alterations Activating Kinase and Cytokine Receptor Signaling in High-Risk Acute Lymphoblastic Leukemia. *Cancer Cell.* 2012. doi:10.1016/j.ccr.2012.06.005
17. Mullighan CG, Goorha S, Radtke I, et al. Genome-wide analysis of genetic alterations in acute lymphoblastic leukaemia. *Nature.* 2007. doi:10.1038/nature05690
18. Terwilliger T, Abdul-Hay M. Acute lymphoblastic leukemia: a comprehensive review and 2017 update. *Blood Cancer J.* 2017;7:577. doi:10.1038/bcj.2017.53
19. Burmeister T, Schwartz S, Bartram CR, Gökbuget N, Hoelzer D, Thiel E. Patients' age and BCR-ABL frequency in adult B-precursor ALL: A retrospective analysis from the GMALL study group. *Blood.* 2008. doi:10.1182/blood-2008-04-149286
20. Thomas X, Heiblig M. Diagnostic and treatment of adult Philadelphia chromosome-positive acute lymphoblastic leukemia. *Int J Hematol Oncol.* 2016;5(2):77-90. doi:10.2217/ijh-2016-0009
21. Chan LC, Karhi KK, Rayter SI, et al. A novel abl protein expressed in Philadelphia chromosome positive acute lymphoblastic leukaemia positive acute lymphoblastic leukaemia. *Nature.* 1987. doi:10.1038/325635a0
22. Forghieri F, Luppi M, Potenza L. Philadelphia chromosome-positive Acute Lymphoblastic Leukemia Philadelphia chromosome-positive Acute Lymphoblastic Leukemia. 2015;8454. doi:10.1179/1024533215Z.000000000402
23. Dombret H, Gabert J, Boiron JM, et al. Outcome of treatment in adults with Philadelphia chromosome-positive acute lymphoblastic leukemia - Results of the



- prospective multicenter LALA-94 trial. *Blood*. 2002. doi:10.1182/blood-2002-03-0704
24. Iqbal N, Iqbal N. Imatinib: A Breakthrough of Targeted Therapy in Cancer. *Chemother Res Pract*. 2014. doi:10.1155/2014/357027
  25. Kantarjian HM, O'Brien S, Smith TL, et al. Results of treatment with hyper-CVAD, a dose-intensive regimen, in adult acute lymphocytic leukemia. *J Clin Oncol*. 2000.
  26. Dalle IA, Jabbour EJ, Short NJ, Ravandi F. Treatment of Philadelphia Chromosome-Positive Acute Lymphoblastic Leukemia. *Curr Treat Options Oncol*. 2019;20(4):1-13. doi:10.1007/s11864-019-0603-z
  27. Deininger MWN, Druker BJ. Specific targeted therapy of chronic myelogenous leukemia with imatinib. *Pharmacol Rev*. 2003. doi:10.1124/pr.55.3.4
  28. Vigneri P, Wang JYJ. Induction of apoptosis in chronic myelogenous leukemia cells through nuclear entrapment of BCR-ABL tyrosine kinase. *Nat Med*. 2001. doi:10.1038/84683
  29. Wassmann B, Pfeifer H, Goekbuget N, et al. Alternating versus concurrent schedules of imatinib and chemotherapy as front-line therapy for Philadelphia-positive acute lymphoblastic leukemia (Ph+ALL). *Blood*. 2006. doi:10.1182/blood-2005-11-4386
  30. Fielding AK, Rowe JM, Buck G, et al. UKALLXII/ECOG2993: Addition of imatinib to a standard treatment regimen enhances long-term outcomes in Philadelphia positive acute lymphoblastic leukemia. *Blood*. 2014. doi:10.1182/blood-2013-09-529008
  31. Chalandon Y, Thomas X, Hayette S, et al. Randomized study of reduced-intensity chemotherapy combined with imatinib in adults with Ph-positive acute lymphoblastic leukemia. *Blood*. 2015. doi:10.1182/blood-2015-02-627935
  32. Ottmann OG, Larson RA, Kantarjian HM, et al. Phase II study of nilotinib in patients with relapsed or refractory Philadelphia chromosome - Positive acute lymphoblastic leukemia. *Leukemia*. 2013. doi:10.1038/leu.2012.324
  33. Kim DY, Joo YD, Lim SN, et al. Nilotinib combined with multiagent chemotherapy for newly diagnosed Philadelphia-positive acute lymphoblastic leukemia. *Blood*. 2015. doi:10.1182/blood-2015-03-636548
  34. Ottmann OG, Pfeifer H, Cayuela J-M, et al. Nilotinib (Tasigna) and Low Intensity Chemotherapy for First-Line Treatment of Elderly Patients with BCR-ABL1-

- Positive Acute Lymphoblastic Leukemia: Final Results of a Prospective Multicenter Trial (EWALL-PH02). *Blood*. 2018. doi:10.1182/blood-2018-99-114552
35. Chalandon Y, Rousselot P, Cayuela J-M, Thomas X, Clappier E, Havelange V. Nilotinib combined with lower-intensity chemotherapy for front-line treatment of younger adults with Ph-positive acute lymphoblastic leukemia (ALL): interim analysis of the GRAAPH-2014 trial. In: European Hematology Association (EHA); 2018.
  36. Shah NP, Tran C, Lee FY, Chen P, Norris D, Sawyers CL. Overriding imatinib resistance with a novel ABL kinase inhibitor. *Science* (80- ). 2004. doi:10.1126/science.1099480
  37. Tokarski JS, Newitt JA, Chang CYJ, et al. The structure of dasatinib (BMS-354825) bound to activated ABL kinase domain elucidates its inhibitory activity against imatinib-resistant ABL mutants. *Cancer Res*. 2006. doi:10.1158/0008-5472.CAN-05-4187
  38. Ottmann O, Dombret H, Martinelli G, et al. Dasatinib induces rapid hematologic and cytogenetic responses in adult patients with Philadelphia chromosome-positive acute lymphoblastic leukemia with resistance or intolerance to imatinib: Interim results of a phase 2 study. *Blood*. 2007. doi:10.1182/blood-2007-02-073528
  39. Ravandi F, O'Brien SM, Cortes JE, et al. Long-term follow-up of a phase 2 study of chemotherapy plus dasatinib for the initial treatment of patients with Philadelphia chromosome-positive acute lymphoblastic leukemia. *Cancer*. 2015. doi:10.1002/cncr.29646
  40. Foà R, Vitale A, Vignetti M, et al. Dasatinib as first-line treatment for adult patients with Philadelphia chromosome-positive acute lymphoblastic leukemia. *Blood*. 2011. doi:10.1182/blood-2011-05-351403
  41. Chiaretti S, Vitale A, Elia L, et al. Multicenter Total Therapy Gimema LAL 1509 Protocol for De Novo Adult Ph+ Acute Lymphoblastic Leukemia (ALL) Patients. Updated Results and Refined Genetic-Based Prognostic Stratification. *Blood*. 2015.
  42. Rousselot P, Coudé MM, Gokbuget N, et al. Dasatinib and low-intensity chemotherapy in elderly patients with Philadelphia chromosome-positive ALL. *Blood*. 2016. doi:10.1182/blood-2016-02-700153
  43. Soverini S, De Benedittis C, Papayannidis C, et al. Drug resistance and BCR-ABL kinase domain mutations in Philadelphia chromosome-positive acute lymphoblastic

- leukemia from the imatinib to the second-generation tyrosine kinase inhibitor era: The main changes are in the type of mutations, but not in the fr. *Cancer*. 2014. doi:10.1002/cncr.28522
44. Pfeifer H, Wassmann B, Pavlova A, et al. Kinase domain mutations of BCR-ABL frequently precede imatinib-based therapy and give rise to relapse in patients with de novo Philadelphia-positive acute lymphoblastic leukemia (Ph+ ALL). *Blood*. 2007. doi:10.1182/blood-2006-11-052373
  45. Jabbour E, Kantarjian H, Ravandi F, et al. Combination of hyper-CVAD with ponatinib as first-line therapy for patients with Philadelphia chromosome-positive acute lymphoblastic leukaemia: A single-centre, phase 2 study. *Lancet Oncol*. 2015. doi:10.1016/S1470-2045(15)00207-7
  46. Short NJ, Kantarjian HM, Ravandi F, et al. Frontline hyper-CVAD plus ponatinib for patients with Philadelphia chromosome-positive acute lymphoblastic leukemia: Updated results of a phase II study. *J Clin Oncol*. 2017. doi:10.1200/jco.2017.35.15\_suppl.7013
  47. Dorer DJ, Knickerbocker RK, Baccarani M, et al. Impact of dose intensity of ponatinib on selected adverse events: Multivariate analyses from a pooled population of clinical trial patients. *Leuk Res*. 2016. doi:10.1016/j.leukres.2016.07.007
  48. Le Jeune C, Thomas X. Antibody-based therapies in B-cell lineage acute lymphoblastic leukaemia. *Eur J Haematol*. 2015. doi:10.1111/ejh.12408
  49. Kantarjian HM, DeAngelo DJ, Stelljes M, et al. Inotuzumab ozogamicin versus standard therapy for acute lymphoblastic leukemia. *N Engl J Med*. 2016. doi:10.1056/NEJMoa1509277
  50. Topp MS, Kufer P, Gökbuget N, et al. Targeted therapy with the T-cell - Engaging antibody blinatumomab of chemotherapy-refractory minimal residual disease in B-lineage acute lymphoblastic leukemia patients results in high response rate and prolonged leukemia-free survival. *J Clin Oncol*. 2011. doi:10.1200/JCO.2010.32.7270
  51. Martinelli G, Boissel N, Chevallier P, et al. Complete hematologic and molecular response in adult patients with relapsed/refractory philadelphia chromosome-positive B-precursor acute lymphoblastic leukemia following treatment with blinatumomab: Results from a phase II, single-arm, multicenter study. *J Clin Oncol*. 2017. doi:10.1200/JCO.2016.69.3531

52. Miliotou AN, Papadopoulou LC. CAR T-cell Therapy: A New Era in Cancer Immunotherapy. *Curr Pharm Biotechnol*. 2018. doi:10.2174/1389201019666180418095526
53. Geyer MB, Manjunath SH, Evans AG, et al. Concurrent therapy of chronic lymphocytic leukemia and Philadelphia chromosome-positive acute lymphoblastic leukemia utilizing CD19-targeted CAR T-cells. *Leuk Lymphoma*. 2018. doi:10.1080/10428194.2017.1390237
54. Copelan EA. Hematopoietic Stem-Cell Transplantation. *New Engl J Medicine*. 2006;354:1813-1826.
55. Thomas X, Boiron JM, Huguet F, et al. Outcome of treatment in adults with acute lymphoblastic leukemia: Analysis of the LALA-94 Trial. *J Clin Oncol*. 2004. doi:10.1200/JCO.2004.10.050
56. Short NJ, Jabbour E, Sasaki K, et al. Impact of complete molecular response on survival in patients with Philadelphia chromosome-positive acute lymphoblastic leukemia. *Blood*. 2016. doi:10.1182/blood-2016-03-707562
57. Shami PJ, Deininger M. Evolving treatment strategies for patients newly diagnosed with chronic myeloid leukemia: The role of second-generation BCR-ABL inhibitors as first-line therapy. *Leukemia*. 2012. doi:10.1038/leu.2011.217
58. O'hare T, Zabriskie MS, Eiring AM, Deininger MW. Pushing the limits of targeted therapy in chronic myeloid leukaemia. *Nat Rev Cancer*. 2012. doi:10.1038/nrc3317
59. Sierra JR, Cepero V, Giordano S. Molecular mechanisms of acquired resistance to tyrosine kinase targeted therapy. *Mol Cancer*. 2010. doi:10.1186/1476-4598-9-75
60. Khorashad JS, Kelley TW, Szankasi P, et al. BCR-ABL1 compound mutations in tyrosine kinase inhibitor-resistant CML: Frequency and clonal relationships. *Blood*. 2013. doi:10.1182/blood-2012-05-431379
61. O'Hare T, Walters DK, Stoffregen EP, et al. In vitro activity of Bcr-Abl inhibitors AMN107 and BMS-354825 against clinically relevant imatinib-resistant Abl kinase domain mutants. *Cancer Res*. 2005. doi:10.1158/0008-5472.CAN-05-0259
62. Talpaz M, Shah NP, Kantarjian H, et al. Dasatinib in imatinib-resistant Philadelphia chromosome-positive leukemias. *N Engl J Med*. 2006. doi:10.1056/NEJMoa055229
63. Lockwood WW, Coe BP, Williams AC, MacAulay C, Lam WL. Whole genome tiling path array CGH analysis of segmental copy number alterations in cervical cancer cell lines. *Int J Cancer*. 2007. doi:10.1002/ijc.22335
64. Smolen GA, Sordella R, Muir B, et al. Amplification of MET may identify a subset

- of cancers with extreme sensitivity to the selective tyrosine kinase inhibitor PHA-665752. *Proc Natl Acad Sci U S A*. 2006. doi:10.1073/pnas.0508776103
65. Hellman A, Zlotorynski E, Scherer SW, et al. A role for common fragile site induction in amplification of human oncogenes. *Cancer Cell*. 2002. doi:10.1016/S1535-6108(02)00017-X
  66. Gorre ME, Mohammed M, Ellwood K, et al. Clinical resistance to STI-571 cancer therapy caused by BCR-ABL gene mutation or amplification. *Science (80- )*. 2001. doi:10.1126/science.1062538
  67. Nielsen DL, Andersson M, Kamby C. HER2-targeted therapy in breast cancer. Monoclonal antibodies and tyrosine kinase inhibitors. *Cancer Treat Rev*. 2009. doi:10.1016/j.ctrv.2008.09.003
  68. Mahon FX, Deininger MWN, Schultheis B, et al. Selection and characterization of BCR-ABL positive cell lines with differential sensitivity to the tyrosine kinase inhibitor STI571: Diverse mechanisms of resistance. *Blood*. 2000.
  69. Ercan D, Zejnullahu K, Yonesaka K, et al. Amplification of EGFR T790M causes resistance to an irreversible EGFR inhibitor. *Oncogene*. 2010. doi:10.1038/onc.2009.526
  70. Stölzel F, Steudel C, Oelschlägel U, et al. Mechanisms of resistance against PKC412 in resistant FLT3-ITD positive human acute myeloid leukemia cells. *Ann Hematol*. 2010. doi:10.1007/s00277-009-0889-1
  71. Pillay V, Allaf L, Wilding AL, et al. The plasticity of oncogene addiction: Implications for targeted therapies directed to receptor tyrosine kinases. *Neoplasia*. 2009. doi:10.1593/neo.09230
  72. Turke AB, Zejnullahu K, Wu YL, et al. Preexistence and Clonal Selection of MET Amplification in EGFR Mutant NSCLC. *Cancer Cell*. 2010. doi:10.1016/j.ccr.2009.11.022
  73. Bachleitner-Hofmann T, Sun MY, Chen CT, et al. HER kinase activation confers resistance to MET tyrosine kinase inhibition in MET oncogene-addicted gastric cancer cells. *Mol Cancer Ther*. 2008. doi:10.1158/1535-7163.MCT-08-0374
  74. Engelman JA, Zejnullahu K, Mitsudomi T, et al. MET amplification leads to gefitinib resistance in lung cancer by activating ERBB3 signaling. *Science (80- )*. 2007. doi:10.1126/science.1141478
  75. Khorashad JS, De Melo VA, Fiegler H, et al. Multiple sub-microscopic genomic lesions are a universal feature of chronic myeloid leukaemia at diagnosis.

- Leukemia*. 2008. doi:10.1038/leu.2008.210
76. Gregory RI, Shiekhattar R, Gregory RI, Shiekhattar R. MicroRNA Biogenesis and Cancer MicroRNA Biogenesis and Cancer. *Cancer Res*. 2005.
  77. Weiss GJ, Bemis LT, Nakajima E, et al. EGFR regulation by microRNA in lung cancer: Correlation with clinical response and survival to gefitinib and EGFR expression in cell lines. *Ann Oncol*. 2008. doi:10.1093/annonc/mdn006
  78. Seike M, Goto A, Okano T, et al. MiR-21 is an EGFR-regulated anti-apoptotic factor in lung cancer in never-smokers. *Proc Natl Acad Sci U S A*. 2009. doi:10.1073/pnas.0905234106
  79. Pogribny IP, Filkowski JN, Tryndyak VP, Golubov A, Shpyleva SI, Kovalchuk O. Alterations of microRNAs and their targets are associated with acquired resistance of MCF-7 breast cancer cells to cisplatin. *Int J Cancer*. 2010. doi:10.1002/ijc.25191
  80. Sorrentino A, Liu CG, Addario A, Peschle C, Scambia G, Ferlini C. Role of microRNAs in drug-resistant ovarian cancer cells. *Gynecol Oncol*. 2008. doi:10.1016/j.ygyno.2008.08.017
  81. Nishioka C, Ikezoe T, Yang J, Nobumoto A, Tsuda M, Yokoyama A. Downregulation of miR-217 correlates with resistance of ph+ leukemia cells to ABL tyrosine kinase inhibitors. *Cancer Sci*. 2014. doi:10.1111/cas.12339
  82. Ying HQ, Chen J, He BS, et al. The effect of BIM deletion polymorphism on intrinsic resistance and clinical outcome of cancer patient with kinase inhibitor therapy. *Sci Rep*. 2015. doi:10.1038/srep11348
  83. Mikhailov I. BCR-ABL exon 7 deletion and novel point mutation in patient with chronic myelogenous leukemia and TKI resistance. *Clin Case Reports*. 2018. doi:10.1002/ccr3.1794
  84. Pfeifer H, Raum K, Markovic S, et al. Genomic CDKN2A/2B deletions in adult Ph+ ALL are adverse despite allogeneic stem cell transplantation. *Blood*. 2018;131:1464-1475. doi:https://doi.org/10.1182/blood-2017-07-796862
  85. Mahon FX, Hayette S, Lagarde V, et al. Evidence that resistance to nilotinib may be due to BCR-ABL, Pgp, or Src kinase overexpression. *Cancer Res*. 2008. doi:10.1158/0008-5472.CAN-08-1008
  86. Pennacchietti S, Michieli P, Galluzzo M, Mazzone M, Giordano S, Comoglio PM. Hypoxia promotes invasive growth by transcriptional activation of the met protooncogene. *Cancer Cell*. 2003. doi:10.1016/S1535-6108(03)00085-0
  87. Noro R, Gemma A, Miyanaga A, et al. PTEN inactivation in lung cancer cells and

- the effect of its recovery on treatment with epidermal growth factor receptor tyrosine kinase inhibitors. *Int J Oncol*. 2007.
88. Lee TF, Tseng YC, Nguyen PA, Li YC, Ho CC, Wu CW. Enhanced YAP expression leads to EGFR TKI resistance in lung adenocarcinomas. *Sci Rep*. 2018. doi:10.1038/s41598-017-18527-z
  89. Kwak EL, Jankowski J, Thayer SP, et al. Epidermal growth factor receptor kinase domain mutations in esophageal and pancreatic adenocarcinomas. *Clin Cancer Res*. 2006. doi:10.1158/1078-0432.CCR-06-0189
  90. Yang L, Li J, Ran L, et al. Phosphorylated Insulin-Like Growth Factor 1 Receptor is Implicated in Resistance to the Cytostatic Effect of Gefitinib in Colorectal Cancer Cells. *J Gastrointest Surg*. 2011. doi:10.1007/s11605-011-1504-z
  91. Kim SM, Kim JS, Kim JH, et al. Acquired resistance to cetuximab is mediated by increased PTEN instability and leads cross-resistance to gefitinib in HCC827 NSCLC cells. *Cancer Lett*. 2010. doi:10.1016/j.canlet.2010.04.006
  92. Nishioka C, Ikezoe T, Yang J, Yokoyama A. Long-term exposure of leukemia cells to multi-targeted tyrosine kinase inhibitor induces activations of AKT, ERK and STAT5 signaling via epigenetic silencing of the PTEN gene. *Leukemia*. 2010. doi:10.1038/leu.2010.145
  93. Vivanco I, Rohle D, Versele M, et al. The phosphatase and tensin homolog regulates epidermal growth factor receptor (EGFR) inhibitor response by targeting EGFR for degradation. *Proc Natl Acad Sci U S A*. 2010. doi:10.1073/pnas.0911188107
  94. Quentmeier H, Eberth S, Romani J, Zaborski M, Drexler HG. BCR-ABL1-independent PI3Kinase activation causing imatinib-resistance. *J Hematol Oncol*. 2011;4(1):6. doi:10.1186/1756-8722-4-6
  95. Xia W, Bacus S, Hegde P, et al. A model of acquired autoresistance to a potent ErbB2 tyrosine kinase inhibitor and a therapeutic strategy to prevent its onset in breast cancer. *Proc Natl Acad Sci U S A*. 2006. doi:10.1073/pnas.0602468103
  96. Mori A, Wada H, Nishimura Y, Okamoto T, Takemoto Y, Kakishita E. Expression of the antiapoptosis gene survivin in human leukemia. *Int J Hematol*. 2002. doi:10.1007/BF02982021
  97. Hernández-Boluda JC, Bellosillo B, Vela MC, Colomer D, Alvarez-Larrán A, Cervantes F. Survivin expression in the progression of chronic myeloid leukemia: A sequential study in 16 patients. *Leuk Lymphoma*. 2005.

doi:10.1080/10428190500052131

98. Carter BZ, Mak DH, Schober WD, et al. Regulation of survivin expression through Bcr-Abl/MAPK cascade: targeting survivin overcomes imatinib resistance and increases imatinib sensitivity in imatinib-responsive CML cells. *Blood*. 2006;107(4):1555-1563.
99. Nestal de Moraes G, Souza PS, Costas FC de F, Vasconcelos FC, Reis FRS, Maia RC. The Interface between BCR-ABL-Dependent and -Independent Resistance Signaling Pathways in Chronic Myeloid Leukemia. *Leuk Res Treatment*. 2012. doi:10.1155/2012/671702
100. Tao LY, Liang YJ, Wang F, et al. Cediranib (recentin, AZD2171) reverses ABCB1- and ABCC1-mediated multidrug resistance by inhibition of their transport function. *Cancer Chemother Pharmacol*. 2009. doi:10.1007/s00280-009-0949-1
101. Dai C ling, Liang Y ju, Wang Y sheng, et al. Sensitization of ABCG2-overexpressing cells to conventional chemotherapeutic agent by sunitinib was associated with inhibiting the function of ABCG2. *Cancer Lett*. 2009. doi:10.1016/j.canlet.2009.01.027
102. Mahon FX, Belloc F, Lagarde V, et al. MDR1 gene overexpression confers resistance to imatinib mesylate in leukemia cell line models. *Blood*. 2003. doi:10.1182/blood.V101.6.2368
103. Che XF, Nakajima Y, Sumizawa T, et al. Reversal of P-glycoprotein mediated multidrug resistance by a newly synthesized 1,4-benzothiazipine derivative, JTV-519. *Cancer Lett*. 2002. doi:10.1016/S0304-3835(02)00359-2
104. Rumpold H, Wolf AM, Gruenewald K, Gastl G, Gunsilius E, Wolf D. RNAi-mediated knockdown of P-glycoprotein using a transposon-based vector system durably restores imatinib sensitivity in imatinib-resistant CML cell lines. *Exp Hematol*. 2005. doi:10.1016/j.exphem.2005.03.014
105. Hiwase DK, Saunders V, Hewett D, et al. Dasatinib cellular uptake and efflux in chronic myeloid leukemia cells: therapeutic implications. *Clin Cancer Res*. 2008. doi:10.1158/1078-0432.CCR-07-5095
106. Shukla S, Robey RW, Bates SE, Ambudkar S V. Sunitinib (Sutent, SU11248), a small-molecule receptor tyrosine kinase inhibitor, blocks function of the ATP-binding cassette (ABC) transporters P-glycoprotein (ABCB1) and ABCG2. *Drug Metab Dispos*. 2009. doi:10.1124/dmd.108.024612
107. Elkind NB, Szentpétery Z, Apáti Á, et al. Multidrug transporter ABCG2 prevents



- tumor cell death induced by the epidermal growth factor receptor inhibitor Iressa (ZD1839, Gefitinib). *Cancer Res.* 2005. doi:10.1158/0008-5472.CAN-04-3303
108. Kuwazuru Y, Yoshimura A, Hanada S, et al. Expression of the multidrug transporter, P-glycoprotein, in chronic myelogenous leukaemia cells in blast crisis. *Br J Haematol.* 1990. doi:10.1111/j.1365-2141.1990.tb02533.x
  109. Vasconcelos FC, Silva KL, Souza PS De, et al. Variation of MDR proteins expression and activity levels according to clinical status and evolution of CML patients. *Cytom Part B - Clin Cytom.* 2011. doi:10.1002/cyto.b.20580
  110. Nakanishi T, Shiozawa K, Hassel BA, Ross DD. Complex interaction of BCRP/ABCG2 and imatinib in BCR-ABL-expressing cells: BCRP-mediated resistance to imatinib is attenuated by imatinib-induced reduction of BCRP expression. *Blood.* 2006. doi:10.1182/blood-2005-10-4020
  111. Imai Y, Nakane M, Kage K, et al. C421A polymorphism in the human breast cancer resistance protein gene is associated with low expression of Q141K protein and low-level drug resistance. *Mol Cancer Ther.* 2002.
  112. Mizuarai S, Aozasa N, Kotani H. Single nucleotide polymorphisms result in impaired membrane localization and reduced atpase activity in multidrug transporter ABCG2. *Int J Cancer.* 2004. doi:10.1002/ijc.11669
  113. Daley GQ, Van Etten RA, Baltimore D. Induction of chronic myelogenous leukemia in mice by the P210 bcr/abl gene of the Philadelphia chromosome. *Science (80- ).* 1990. doi:10.1126/science.2406902
  114. Sattler M, Mohi MG, Pride YB, et al. Critical role for Gab2 in transformation by BCR/ABL. *Cancer Cell.* 2002. doi:10.1016/S1535-6108(02)00074-0
  115. Wöhrle FU, Halbach S, Aumann K, et al. Gab2 signaling in chronic myeloid leukemia cells confers resistance to multiple Bcr-Abl inhibitors. *Leukemia.* 2013. doi:10.1038/leu.2012.222
  116. Ghaffari S, Jagani Z, Kitidis C, Lodish HF, Khosravi-Far R. Cytokines and BCR-ABL mediate suppression of TRAIL-induced apoptosis through inhibition of forkhead FOXO3a transcription factor. *Proc Natl Acad Sci U S A.* 2003. doi:10.1073/pnas.0731871100
  117. Naka K, Hoshii T, Muraguchi T, et al. TGF-B-FOXO signalling maintains leukaemia-initiating cells in chronic myeloid leukaemia. *Nature.* 2010. doi:10.1038/nature08734

118. Mayerhofer M, Aichberger KJ, Florian S, et al. Identification of mTOR as a novel bifunctional target in chronic myeloid leukemia: Dissection of growth-inhibitory and VEGF-suppressive effects of rapamycin in leukemic cells. *FASEB J*. 2005. doi:10.1096/fj.04-1973fje
119. Mohi MG, Boulton C, Gu TL, et al. Combination of rapamycin and protein tyrosine kinase (PTK) inhibitors for the treatment of leukemias caused by oncogenic PTKs. *Proc Natl Acad Sci U S A*. 2004. doi:10.1073/pnas.0400063101
120. Janes MR, Limon JJ, So L, et al. Effective and selective targeting of leukemia cells using a TORC1/2 kinase inhibitor. *Nat Med*. 2010. doi:10.1038/nm.2091
121. Carayol N, Vakana E, Sassano A, et al. Critical roles for mTORC2- and rapamycin-insensitive mTORC1-complexes in growth and survival of BCR-ABL-expressing leukemic cells. *Proc Natl Acad Sci U S A*. 2010. doi:10.1073/pnas.1005114107
122. Inoki K, Li Y, Xu T, Guan KL. Rheb GTPase is a direct target of TSC2 GAP activity and regulates mTOR signaling. *Genes Dev*. 2003. doi:10.1101/gad.1110003
123. Puissant A, Robert G, Fenouille N, et al. Resveratrol promotes autophagic cell death in chronic myelogenous leukemia cells via JNK-mediated p62/SQSTM1 expression and AMPK activation. *Cancer Res*. 2010. doi:10.1158/0008-5472.CAN-09-3537
124. Vakana E, Plataniias LC. AMPK in BCR-ABL expressing leukemias. Regulatory effects and therapeutic implications. *Oncotarget*. 2011.
125. Puil L, Liu J, Gish G, et al. Bcr-Abl oncoproteins bind directly to activators of the Ras signalling pathway. *EMBO J*. 1994. doi:10.1002/j.1460-2075.1994.tb06319.x
126. Quintás-Cardama A, Cortes J. Molecular biology of bcr-abl1-positive chronic myeloid leukemia. *Blood*. 2009. doi:10.1182/blood-2008-03-144790
127. Mancini M, Veljkovic N, Corradi V, et al. 14-3-3 ligand prevents nuclear import of c-ABL protein in chronic myeloid leukemia. *Traffic*. 2009. doi:10.1111/j.1600-0854.2009.00897.x
128. Sillaber C, Gesbert F, Frank DA, Sattler M, Griffin JD. STAT5 activation contributes to growth and viability in Bcr/Abl- transformed cells. *Blood*. 2000.
129. Scherr M, Chaturvedi A, Battmer K, et al. Enhanced sensitivity to inhibition of SHP2, STAT5, and Gab2 expression in chronic myeloid leukemia (CML). *Blood*. 2006. doi:10.1182/blood-2005-08-3087
130. Xie S, Wang Y, Liu J, et al. Involvement of Jak2 tyrosine phosphorylation in Bcr-Abl transformation. *Oncogene*. 2001. doi:10.1038/sj.onc.1204834

131. Wertheim JA, Perera SA, Hammer DA, Ren R, Boettiger D, Pear WS. Localization of BCR-ABL to F-actin regulates cell adhesion but does not attenuate CML development. *Blood*. 2003. doi:10.1182/blood-2003-01-0062
132. Hantschel O, Warsch W, Eckelhart E, et al. BCR-ABL uncouples canonical JAK2-STAT5 signaling in chronic myeloid leukemia. *Nat Chem Biol*. 2012. doi:10.1038/nchembio.775
133. Traer E, MacKenzie R, Snead J, et al. Blockade of JAK2-mediated extrinsic survival signals restores sensitivity of CML cells to ABL inhibitors. *Leukemia*. 2012. doi:10.1038/leu.2011.325
134. Regl G, Kasper M, Schnidar H, et al. Activation of the BCL2 promoter in response to Hedgehog/GLI signal transduction is predominantly mediated by GLI2. *Cancer Res*. 2004. doi:10.1158/0008-5472.CAN-04-1085
135. Dierks C, Beigi R, Guo GR, et al. Expansion of Bcr-Abl-Positive Leukemic Stem Cells Is Dependent on Hedgehog Pathway Activation. *Cancer Cell*. 2008. doi:10.1016/j.ccr.2008.08.003
136. Goff D, Jamieson C. Cycling toward Elimination of Leukemic Stem Cells. *Cell Stem Cell*. 2010. doi:10.1016/j.stem.2010.03.008
137. Jamieson CHM, Ailles LE, Dylla SJ, et al. Granulocyte-macrophage progenitors as candidate leukemic stem cells in blast-crisis CML. *N Engl J Med*. 2004. doi:10.1056/NEJMoa040258
138. Radich JP, Dai H, Mao M, et al. Gene expression changes associated with progression and response in chronic myeloid leukemia. *Proc Natl Acad Sci U S A*. 2006. doi:10.1073/pnas.0510423103
139. Heidel FH, Bullinger L, Feng Z, et al. Genetic and pharmacologic inhibition of  $\beta$ -catenin targets imatinib-resistant leukemia stem cells in CML. *Cell Stem Cell*. 2012. doi:10.1016/j.stem.2012.02.017
140. Bartke N, Hannun YA. Bioactive sphingolipids: Metabolism and function. *J Lipid Res*. 2009. doi:10.1194/jlr.R800080-JLR200
141. Pewzner-Jung Y, Ben-Dor S, Futerman AH. When do Lasses (longevity assurance genes) become CerS (ceramide synthases)? Insights into the regulation of ceramide synthesis. *J Biol Chem*. 2006. doi:10.1074/jbc.R600010200
142. Causeret C, Geeraert L, Van der Hoeven G, Mannaerts GP, Van Veldhoven PP. Further characterization of rat dihydroceramide desaturase: Tissue distribution, subcellular localization, and substrate specificity. *Lipids*. 2000.

doi:10.1007/s11745-000-0627-6

143. Wijesinghe DS, Massiello A, Subramanian P, Szulc Z, Bielawska A, Chalfant CE. Substrate specificity of human ceramide kinase. *J Lipid Res.* 2005.  
doi:10.1194/jlr.M500313-JLR200
144. Raas-Rothschild A, Pankova-Kholmyansky I, Kacher Y, Futerman AH. Glycosphingolipidoses: Beyond the enzymatic defect. *Glycoconj J.* 2004.  
doi:10.1023/B:GLYC.0000046272.38480.ef
145. Tafesse FG, Ternes P, Holthuis JCM. The multigenic sphingomyelin synthase family. *J Biol Chem.* 2006. doi:10.1074/jbc.R600021200
146. Hakomori S itiroh. Traveling for the glycosphingolipid path. *Glycoconj J.* 2000.  
doi:10.1023/A:1011086929064
147. Ichikawa S, Hirabayashi Y. Glucosylceramide synthase and glycosphingolipid synthesis. *Trends Cell Biol.* 1998. doi:10.1016/S0962-8924(98)01249-5
148. Marchesini N, Hannun YA. Acid and neutral sphingomyelinases: Roles and mechanisms of regulation. *Biochem Cell Biol.* 2004. doi:10.1139/o03-091
149. Bandhuvula P, Saba JD. Sphingosine-1-phosphate lyase in immunity and cancer: silencing the siren. *Trends Mol Med.* 2007. doi:10.1016/j.molmed.2007.03.005
150. Xu R, Jin J, Hu W, et al. Golgi alkaline ceramidase regulates cell proliferation and survival by controlling levels of sphingosine and S1P. *FASEB J.* 2006.  
doi:10.1096/fj.05-5689com
151. Galadari S, Wu BX, Mao C, Roddy P, El Bawab S, Hannun YA. Identification of a novel amidase motif in neutral ceramidase. *Biochem J.* 2006.  
doi:10.1042/BJ20050682
152. Hait NC, Oskeritzian CA, Paugh SW, Milstien S, Spiegel S. Sphingosine kinases, sphingosine 1-phosphate, apoptosis and diseases. *Biochim Biophys Acta - Biomembr.* 2006. doi:10.1016/j.bbamem.2006.08.007
153. Romiti E, Vasta V, Meacci E, et al. Characterization of sphingomyelinase activity released by thrombin- stimulated platelets. *Mol Cell Biochem.* 2000.
154. Delon C, Manifava M, Wood E, et al. Sphingosine kinase 1 is an intracellular effector of phosphatidic acid. *J Biol Chem.* 2004. doi:10.1074/jbc.M405771200
155. López-Montero I, Rodriguez N, Cribier S, Pohl A, Vélez M, Devaux PF. Rapid transbilayer movement of ceramides in phospholipid vesicles and in human erythrocytes. *J Biol Chem.* 2005. doi:10.1074/jbc.M412052200
156. Khan WA, Mascarella SW, Lewin AH, Wyrick CD, Carroll FI, Hannun YA. Use of

- D-erythro-sphingosine as a pharmacological inhibitor of protein kinase C in human platelets. *Biochem J*. 1991. doi:10.1042/bj2780387
157. Jazwinski SM, Conzelmann A. LAG1 puts the focus on ceramide signaling. *Int J Biochem Cell Biol*. 2002. doi:10.1016/S1357-2725(02)00044-4
158. Venkataraman K, Riebeling C, Bodennec J, et al. Upstream of growth and differentiation factor 1 (uog1), a mammalian homolog of the yeast longevity assurance gene 1 (LAG1), regulates N-stearoyl-sphinganine (C18-(dihydro)ceramide) synthesis in a fumonisin B1-independent manner in mammalian cells. *J Biol Chem*. 2002. doi:10.1074/jbc.M205211200
159. Spassieva S, Seo JG, Jiang JC, et al. Necessary role for the Lag1p motif in (Dihydro)ceramide synthase activity. *J Biol Chem*. 2006. doi:10.1074/jbc.M608092200
160. Mesika A, Ben-Dor S, Laviad EL, Futerman AH. A new functional motif in hox domain-containing ceramide synthases: Identification of a novel region flanking the hox and TLC domains essential for activity. *J Biol Chem*. 2007. doi:10.1074/jbc.M703487200
161. Saddoughi SA, Song P, Ogretmen B. Roles of bioactive sphingolipids in cancer biology and therapeutics. *Subcell Biochem*. 2008.
162. Mullen TD, Hannun YA, Obeid LM. Ceramide synthases at the centre of sphingolipid metabolism and biology. *Biochem J*. 2012. doi:10.1042/BJ20111626
163. Merrill AH. De novo sphingolipid biosynthesis: A necessary, but dangerous, pathway. *J Biol Chem*. 2002. doi:10.1074/jbc.R200009200
164. Karahatay S, Thomas K, Koybasi S, et al. Clinical relevance of ceramide metabolism in the pathogenesis of human head and neck squamous cell carcinoma (HNSCC): Attenuation of C18-ceramide in HNSCC tumors correlates with lymphovascular invasion and nodal metastasis. *Cancer Lett*. 2007. doi:10.1016/j.canlet.2007.06.003
165. Moro K, Kawaguchi T, Tsuchida J, et al. Ceramide species are elevated in human breast cancer and are associated with less aggressiveness. *Oncotarget*. 2018. doi:10.18632/oncotarget.24903
166. Ogretmen B, Hannun YA. Biologically active sphingolipids in cancer pathogenesis and treatment. *Nat Rev Cancer*. 2004. doi:10.1038/nrc1411
167. Snook CF, Jones JA, Hannun YA. Sphingolipid-binding proteins. *Biochim Biophys Acta - Mol Cell Biol Lipids*. 2006. doi:10.1016/j.bbalip.2006.06.004

168. Dobrowsky RT, Hannun YA. Ceramide stimulates a cytosolic protein phosphatase. *J Biol Chem.* 1992.
169. Heinrich M, Neumeyer J, Jakob M, et al. Cathepsin D links TNF-induced acid sphingomyelinase to Bid-mediated caspase-9 and -3 activation. *Cell Death Differ.* 2004. doi:10.1038/sj.cdd.4401382
170. Wang G, Silva J, Krishnamurthy K, Tran E, Condie BG, Bieberich E. Direct binding to ceramide activates protein kinase C $\zeta$  before the formation of a pro-apoptotic complex with PAR-4 in differentiating stem cells. *J Biol Chem.* 2005. doi:10.1074/jbc.M501492200
171. Swanton C, Marani M, Pardo O, et al. Regulators of Mitotic Arrest and Ceramide Metabolism Are Determinants of Sensitivity to Paclitaxel and Other Chemotherapeutic Drugs. *Cancer Cell.* 2007. doi:10.1016/j.ccr.2007.04.011
172. Fox TE, Houck KL, O'Neill SM, et al. Ceramide recruits and activates protein kinase C  $\zeta$  (PKC $\zeta$ ) within structured membrane microdomains. *J Biol Chem.* 2007. doi:10.1074/jbc.M700082200
173. Koybasi S, Senkal CE, Sundararaj K, et al. Defects in cell growth regulation by C18:0-ceramide and longevity assurance gene 1 in human head and neck squamous cell carcinomas. *J Biol Chem.* 2004. doi:10.1074/jbc.M406920200
174. Novgorodov SA, Chudakova DA, Wheeler BW, et al. Developmentally regulated ceramide synthase 6 increases mitochondrial Ca<sup>2+</sup> loading capacity and promotes apoptosis. *J Biol Chem.* 2011. doi:10.1074/jbc.M110.164392
175. Fekry B, Esmailniakooshkghazi A, Krupenko SA, Krupenko NI. Ceramide synthase 6 is a novel target of methotrexate mediating its antiproliferative effect in a p53-dependent manner. *PLoS One.* 2016. doi:10.1371/journal.pone.0146618
176. Obeid LM, Linardic CM, Karolak LA, Hannun YA. Programmed cell death induced by ceramide. *Science (80- ).* 1993. doi:10.1126/science.8456305
177. Zhang SH, Zhou J, Zhang CL, et al. Arsenic trioxide inhibits HCCLM3 cells invasion through de novo ceramide synthesis and sphingomyelinase-induced ceramide production. *Med Oncol.* 2012. doi:10.1007/s12032-011-0023-9
178. Modrak DE, Leon E, Goldenberg DM, Gold D V. Ceramide regulates gemcitabine-induced senescence and apoptosis in human pancreatic cancer cell lines. *Mol Cancer Res.* 2009. doi:10.1158/1541-7786.MCR-08-0457
179. Smyth MJ, Perry DK, Zhang J, Poirier GG, Hannun YA, Obeid LM. pICE: A downstream target for ceramide-induced apoptosis and for the inhibitory action of

- Bcl-2. *Biochem J*. 1996. doi:10.1042/bj3160025
180. Nica AF, Chun CT, Watt JC, et al. Ceramide promotes apoptosis in chronic myelogenous leukemia-derived K562 cells by a mechanism involving caspase-8 and JNK. *Cell Cycle*. 2008. doi:10.4161/cc.7.21.6894
181. Maguer-Satta V, Burl S, Liu L, et al. BCR-ABL accelerates C2-ceramide-induced apoptosis. *Exp Hematol*. 1997.
182. Liu X, Ryland L, Yang J, et al. Targeting of survivin by nanoliposomal ceramide induces complete remission in a rat model of NK-LGL leukemia. *Blood*. 2010. doi:10.1182/blood-2010-02-271080
183. Ogretmen B, Pettus BJ, Rossi MJ, et al. Biochemical mechanisms of the generation of endogenous long chain ceramide in response to exogenous short chain ceramide in the A549 human lung adenocarcinoma cell line. Role for endogenous ceramide in mediating the action of exogenous ceramide. *J Biol Chem*. 2002. doi:10.1074/jbc.M110699200
184. Senkal CE, Ponnusamy S, Rossi MJ, et al. Role of human longevity assurance gene 1 and C18-ceramide in chemotherapy-induced cell death in human head and neck squamous cell carcinomas. *Mol Cancer Ther*. 2007. doi:10.1158/1535-7163.MCT-06-0558
185. Senkal CE, Ponnusamy S, Bielawski J, Hannun YA, Ogretmen B. Antiapoptotic roles of ceramide-synthase-6-generated C16- ceramide via selective regulation of the ATF6/ CHOP arm of ER-stress-response pathways. *FASEB J*. 2010. doi:10.1096/fj.09-135087
186. Dbaiibo GS, Pushkareva MY, Jayadev S, et al. Retinoblastoma gene product as a downstream target for a ceramide-dependent pathway of growth arrest. *Proc Natl Acad Sci U S A*. 1995. doi:10.1073/pnas.92.5.1347
187. Lee JY, Bielawska AE, Obeid LM. Regulation of cyclin-dependent kinase 2 activity by ceramide. *Exp Cell Res*. 2000. doi:10.1006/excr.2000.5028
188. Charles R, Sandirasegarane L, Yun J, et al. Ceramide-coated balloon catheters limit neointimal hyperplasia after stretch injury in carotid arteries. *Circ Res*. 2000. doi:10.1161/01.RES.87.4.282
189. Bourbon NA, Sandirasegarane L, Kester M. Ceramide-induced inhibition of Akt is mediated through protein kinase Czeta: implications for growth arrest. *J Biol Chem*. 2002;277(5):3286-3292. doi:10.1074/jbc.M110541200
190. Venable ME, Lee JY, Smyth MJ, Bielawska A, Obeid LM. Role of ceramide in

- cellular senescence. *J Biol Chem*. 1995. doi:10.1074/jbc.270.51.30701
191. Wooten LG, Ogretmen B. Sp1/Sp3-dependent regulation of human telomerase reverse transcriptase promoter activity by the bioactive sphingolipid ceramide. *J Biol Chem*. 2005. doi:10.1074/jbc.M413444200
192. Ogretmen B, Kraveka JM, Schady D, Usta J, Hannun YA, Obeid LM. Molecular Mechanisms of Ceramide-mediated Telomerase Inhibition in the A549 Human Lung Adenocarcinoma Cell Line. *J Biol Chem*. 2001. doi:10.1074/jbc.M101350200
193. Sundararaj KP, Wood RE, Ponnusamy S, et al. Rapid Shortening of Telomere Length in Response to Ceramide Involves the Inhibition of Telomere Binding Activity of Nuclear Glyceraldehyde-3-phosphate Dehydrogenase. *J Biol Chem*. 2004. doi:10.1074/jbc.M310549200
194. Ogretmen B, Hannun YA. Updates on functions of ceramide in chemotherapy-induced cell death and in multidrug resistance. *Drug Resist Updat*. 2001. doi:10.1054/drup.2001.0225
195. Senchenkov A, Litvak DA, Cabot MC. Targeting ceramide metabolism - A strategy for overcoming drug resistance. *J Natl Cancer Inst*. 2001. doi:10.1093/jnci/93.5.347
196. Radin NS. The development of aggressive cancer: A possible role for sphingolipids. *Cancer Invest*. 2002. doi:10.1081/CNV-120002495
197. Gouaze-Andersson V, Cabot MC. Glycosphingolipids and drug resistance. *Biochim Biophys Acta - Biomembr*. 2006. doi:10.1016/j.bbamem.2006.08.012
198. Gouazé V, Yu JY, Bleicher RJ, et al. Overexpression of glucosylceramide synthase and P-glycoprotein in cancer cells selected for resistance to natural product chemotherapy. *Mol Cancer Ther*. 2004.
199. Gouazé V, Liu YY, Prickett CS, Yu JY, Giuliano AE, Cabot MC. Glucosylceramide synthase blockade down-regulates P-glycoprotein and resensitizes multidrug-resistant breast cancer cells to anticancer drugs. *Cancer Res*. 2005. doi:10.1158/0008-5472.CAN-04-2329
200. Itoh M, Kitano T, Watanabe M, et al. Possible role of ceramide as an indicator of chemoresistance: decrease of the ceramide content via activation of glucosylceramide synthase and sphingomyelin synthase in chemoresistant leukemia. *Clin Cancer Res*. 2003;9(1):415-423. <http://www.ncbi.nlm.nih.gov/pubmed/12538495>. Accessed March 3, 2019.
201. Xie P, Shen YF, Shi YP, et al. Overexpression of glucosylceramide synthase in



- associated with multidrug resistance of leukemia cells. *Leuk Res.* 2008.  
doi:10.1016/j.leukres.2007.07.006
202. Mao C, Obeid LM. Ceramidases: regulators of cellular responses mediated by ceramide, sphingosine, and sphingosine-1-phosphate. *Biochim Biophys Acta - Mol Cell Biol Lipids.* 2008. doi:10.1016/j.bbalip.2008.06.002
  203. Morales A, París R, Villanueva A, Llacuna L, García-Ruiz C, Fernández-Checa JC. Pharmacological inhibition or small interfering RNA targeting acid ceramidase sensitizes hepatoma cells to chemotherapy and reduces tumor growth in vivo. *Oncogene.* 2007. doi:10.1038/sj.onc.1209834
  204. Strelow A, Bernardo K, Adam-Klages S, et al. Overexpression of acid ceramidase protects from tumor necrosis factor-induced cell death. *J Exp Med.* 2000.  
doi:10.1084/jem.192.5.601
  205. Taha TA, Hannun YA, Obeid LM. Sphingosine kinase: Biochemical and cellular regulation and role in disease. *J Biochem Mol Biol.* 2006.
  206. Heffernan-Stroud LA, Obeid LM. Sphingosine Kinase 1 in Cancer. In: *Advances in Cancer Research.* ; 2013. doi:10.1016/B978-0-12-394274-6.00007-8
  207. Bonhoure E, Lauret A, Barnes DJ, et al. Sphingosine kinase-1 is a downstream regulator of imatinib-induced apoptosis in chronic myeloid leukemia cells. *Leukemia.* 2008;22(5):971-979. doi:10.1038/leu.2008.95
  208. Sobue S, Iwasaki T, Sugisaki C, et al. Quantitative RT-PCR analysis of sphingolipid metabolic enzymes in acute leukemia and myelodysplastic syndromes [4]. *Leukemia.* 2006. doi:10.1038/sj.leu.2404386
  209. Sobue S, Nemoto S, Murakami M, et al. Implications of sphingosine kinase 1 expression level for the cellular sphingolipid rheostat: Relevance as a marker for daunorubicin sensitivity of leukemia cells. *Int J Hematol.* 2008.  
doi:10.1007/s12185-008-0052-0
  210. Illuzzi G, Bernacchioni C, Aureli M, et al. Sphingosine kinase mediates resistance to the synthetic retinoid N-(4-hydroxyphenyl)retinamide in human ovarian cancer cells. *J Biol Chem.* 2010. doi:10.1074/jbc.M109.072801
  211. Akao Y, Banno Y, Nakagawa Y, et al. High expression of sphingosine kinase 1 and SIP receptors in chemotherapy-resistant prostate cancer PC3 cells and their camptothecin-induced up-regulation. *Biochem Biophys Res Commun.* 2006.  
doi:10.1016/j.bbrc.2006.02.070
  212. Nemoto S, Nakamura M, Osawa Y, et al. Sphingosine kinase isoforms regulate

- oxaliplatin sensitivity of human colon cancer cells through ceramide accumulation and Akt activation. *J Biol Chem*. 2009. doi:10.1074/jbc.M900735200
213. Fox TE, Finnegan CM, Blumenthal R, Kester M. The clinical potential of sphingolipid-based therapeutics. *Cell Mol Life Sci*. 2006. doi:10.1007/s00018-005-5543-z
214. Ogretmen B. Sphingolipids in cancer: Regulation of pathogenesis and therapy. *FEBS Lett*. 2006. doi:10.1016/j.febslet.2006.08.052
215. Modrak DE, Cardillo TM, Newsome GA, Goldenberg DM, Gold D V. Synergistic interaction between sphingomyelin and gemcitabine potentiates ceramide-mediated apoptosis in pancreatic cancer. *Cancer Res*. 2004. doi:10.1158/0008-5472.CAN-04-2988
216. Veldman RJ, Zerp S, Van Blitterswijk WJ, Verheij M. N-hexanoyl-sphingomyelin potentiates in vitro doxorubicin cytotoxicity by enhancing its cellular influx. *Br J Cancer*. 2004. doi:10.1038/sj.bjc.6601581
217. Selzner M, Bielawska A, Morse MA, et al. Induction of apoptotic cell death and prevention of tumor growth by ceramide analogues in metastatic human colon cancer. *Cancer Res*. 2001.
218. Samsel L, Zaidel G, Drumgoole HM, et al. The Ceramide Analog, B13, Induces Apoptosis in Prostate Cancer Cell Lines and Inhibits Tumor Growth in Prostate Cancer Xenografts. *Prostate*. 2004. doi:10.1002/pros.10350
219. Meng A, Luberto C, Meier P, et al. Sphingomyelin synthase as a potential target for D609-induced apoptosis in U937 human monocytic leukemia cells. *Exp Cell Res*. 2004. doi:10.1016/j.yexcr.2003.10.001
220. Saad AF, Meacham WD, Bai A, et al. The functional effects of acid ceramidase overexpression in prostate cancer progression and resistance to chemotherapy. *Cancer Biol Ther*. 2007.
221. Jiang Q, Wong J, Fyrst H, Saba JD, Ames BN.  $\gamma$ -Tocopherol or combinations of vitamin E forms induce cell in human cells by interrupting sphingolipid synthesis. *Proc Natl Acad Sci U S A*. 2004. doi:10.1073/pnas.0408340102
222. Schulz A, Mousallem T, Venkataramani M, et al. The CLN9 protein, a regulator of dihydroceramide synthase. *J Biol Chem*. 2006. doi:10.1074/jbc.M509483200
223. Zheng W, Kollmeyer J, Symolon H, et al. Ceramides and other bioactive sphingolipid backbones in health and disease: Lipidomic analysis, metabolism and roles in membrane structure, dynamics, signaling and autophagy. *Biochim Biophys*

*Acta - Biomembr.* 2006. doi:10.1016/j.bbamem.2006.08.009

224. Maurer BJ. Synergistic Cytotoxicity in Solid Tumor Cell Lines Between N-(4-Hydroxyphenyl)retinamide and Modulators of Ceramide Metabolism. *J Natl Cancer Inst.* 2000. doi:10.1093/jnci/92.23.1897
225. Jendiroba DB, Klostergaard J, Keyhani A, Pagliaro L, Freireich EJ. Effective cytotoxicity against human leukemias and chemotherapy-resistant leukemia cell lines by N,N-dimethylsphingosine. *Leuk Res.* 2002. doi:10.1016/S0145-2126(01)00129-1
226. Shirahama T, Sweeney EA, Sakakura C, et al. In vitro and in vivo induction of apoptosis by sphingosine and N,N-dimethylsphingosine in human epidermoid carcinoma KB-3-1 and its multidrug-resistant cells. *Clin Cancer Res.* 1997.
227. Huang WC, Tsai CC, Chen CL, et al. Glucosylceramide synthase inhibitor PDMP sensitizes chronic myeloid leukemia T315I mutant to Bcr-Abl inhibitor and cooperatively induces glycogen synthase kinase-3-regulated apoptosis. *FASEB J.* 2011. doi:10.1096/fj.10-180190
228. Baran Y, Salas A, Senkal CE, et al. Alterations of ceramide/sphingosine 1-phosphate rheostat involved in the regulation of resistance to imatinib-induced apoptosis in K562 human chronic myeloid leukemia cells. *J Biol Chem.* 2007;282(15):10922-10934. doi:10.1074/jbc.M610157200
229. Li QF, Huang WR, Duan HF, Wang H, Wu CT, Wang LS. Sphingosine kinase-1 mediates BCR/ABL-induced upregulation of Mcl-1 in chronic myeloid leukemia cells. *Oncogene.* 2007. doi:10.1038/sj.onc.1210587
230. Salas A, Ponnusamy S, Senkal CE, et al. Sphingosine kinase-1 and sphingosine 1-phosphate receptor 2 mediate Bcr-Abl1 stability and drug resistance by modulation of protein phosphatase 2A. *Blood.* 2011;117(22):5941-5952. doi:10.1182/blood-2010-08-300772
231. Gencer EB, Ural AU, Avcu F, Baran Y. A novel mechanism of dasatinib-induced apoptosis in chronic myeloid leukemia; ceramide synthase and ceramide clearance genes. *Ann Hematol.* 2011;90(11):1265-1275. doi:10.1007/s00277-011-1212-5
232. Camgoz A, Gencer EB, Ural AU, Avcu F, Baran Y. Roles of ceramide synthase and ceramide clearance genes in nilotinib-induced cell death in chronic myeloid leukemia cells. *Leuk Lymphoma.* 2011;52(8):1574-1584. doi:10.3109/10428194.2011.568653
233. Evangelisti C, Evangelisti C, Teti G, et al. Assessment of the effect of sphingosine

- kinase inhibitors on apoptosis, unfolded protein response and autophagy of T-cell acute lymphoblastic leukemia cells; indications for novel therapeutics. *Oncotarget*. 2014;5(17):7886-7901. doi:10.18632/oncotarget.2318
234. Wallington-Beddoe CT, Powell JA, Tong D, Pitson SM, Bradstock KF, Bendall LJ. Sphingosine kinase 2 promotes acute lymphoblastic leukemia by enhancing myc expression. *Cancer Res*. 2014. doi:10.1158/0008-5472.CAN-13-2732
235. Wallington-Beddoe CT, Xie V, Tong D, et al. *Identification of Sphingosine Kinase 1 as a Therapeutic Target in B-Lineage Acute Lymphoblastic Leukaemia*. Vol 184.; 2019:443-447. doi:10.1111/bjh.15097
236. Wallington-Beddoe CT, Xie V, Tong D, et al. Identification of sphingosine kinase 1 as a therapeutic target in B-lineage acute lymphoblastic leukaemia. *Br J Haematol*. 2018;1:10-13. doi:10.1111/bjh.15097
237. Adan A, Kiraz Y, Baran Y. Cell Proliferation and Cytotoxicity Assays. *Curr Pharm Biotechnol*. 2016;17(14):1213-1221. <http://www.ncbi.nlm.nih.gov/pubmed/27604355>. Accessed January 2, 2019.
238. Kiraz Y, Neergheen-Bhujun VS, Rummun N, Baran Y. Apoptotic effects of non-edible parts of Punica granatum on human multiple myeloma cells. *Tumor Biol*. 2016;37(2):1803-1815. doi:10.1007/s13277-015-3962-5
239. Moorthi S, Burns TA, Yu G-Q, Luberto C. Bcr-Abl regulation of sphingomyelin synthase 1 reveals a novel oncogenic-driven mechanism of protein up-regulation. *FASEB J*. 2018;32(8):4270-4283. doi:10.1096/fj.201701016R
240. Carroll BL, Bonica J, Shamseddine AA, Hannun YA, Obeid LM. A role for caspase-2 in sphingosine kinase 1 proteolysis in response to doxorubicin in breast cancer cells - implications for the CHK1-suppressed pathway. *FEBS Open Bio*. 2018;8(1):27-40. doi:10.1002/2211-5463.12344
241. Kim JA, Cho K, Shin MS, et al. A novel electroporation method using a capillary and wire-type electrode. *Biosens Bioelectron*. 2008;23(9):1353-1360. doi:10.1016/J.BIOS.2007.12.009
242. Snider JM, Snider AJ, Obeid LM, Luberto C, Hannun YA. Probing de novo sphingolipid metabolism in mammalian cells utilizing mass spectrometry. *J Lipid Res*. 2018;59(6):1046-1057. doi:10.1194/jlr.D081646
243. Snider JM, Trayssac M, Clarke CJ, et al. Flux analysis reveals regulation of the sphingolipid network by doxorubicin in breast cancer cells. *J Lipid Res*. December 2018;jlr.M089714. doi:10.1194/jlr.M089714

244. Schnute ME, McReynolds MD, Kasten T, et al. Modulation of cellular S1P levels with a novel, potent and specific inhibitor of sphingosine kinase-1. *Biochem J*. 2012. doi:10.1042/BJ20111929
245. Shayman JA. Eliglustat tartrate, a prototypic glucosylceramide synthase inhibitor. *Expert Rev Endocrinol Metab*. 2013;8(6):491-504. doi:10.1586/17446651.2013.846213
246. Mistry PK, Lukina E, Turkia H Ben, et al. Effect of oral eliglustat on splenomegaly in patients with Gaucher disease type 1: The ENGAGE randomized clinical trial. *JAMA - J Am Med Assoc*. 2015. doi:10.1001/jama.2015.459
247. De Labarthe A, Rousselot P, Huguet-Rigal F, et al. Imatinib combined with induction or consolidation chemotherapy in patients with de novo Philadelphia chromosome-positive acute lymphoblastic leukemia: Results of the GRAAPH-2003 study. *Blood*. 2007. doi:10.1182/blood-2006-03-011908
248. Ravandi F, O'Brien S, Thomas D, et al. First report of phase 2 study of dasatinib with hyper-CVAD for the frontline treatment of patients with Philadelphia chromosome-positive (Ph +) acute lymphoblastic leukemia. *Blood*. 2010. doi:10.1182/blood-2009-12-261586
249. Lalit JS, Brandwein. New Treatment Strategies for Philadelphia Chromosome-Positive Acute Lymphoblastic Leukemia. *Curr Hematol Malig Rep*. 2017. doi:10.1007/s11899-017-0372-3
250. Rousselot P, Coudé MM, Huguet F, et al. Dasatinib (Sprycel®) and Low Intensity Chemotherapy for First-Line Treatment in Patients with De Novo Philadelphia Positive ALL Aged 55 and Over: Final Results of the EWALL-Ph-01 Study. *Blood*. 2012.
251. Redig AJ, Vakana E, Plataniias LC. Regulation of mammalian target of rapamycin and mitogen activated protein kinase pathways by BCR-ABL. *Leuk Lymphoma*. 2011;52(sup1):45-53. doi:10.3109/10428194.2010.546919
252. Ultimo S, Simioni C, Martelli AM, et al. PI3K isoform inhibition associated with anti Bcr-Abl drugs shows in vitro increased anti-leukemic activity in Philadelphia chromosome-positive B-acute lymphoblastic leukemia cell lines. *Oncotarget*. 2017;8(14):23213-23227. doi:10.18632/oncotarget.15542
253. Taha TA, Mullen TD, Obeid LM. A house divided: ceramide, sphingosine, and sphingosine-1-phosphate in programmed cell death. *Biochim Biophys Acta*. 2006;1758(12):2027-2036. doi:10.1016/j.bbame.2006.10.018

254. Daido S, Kanzawa T, Yamamoto A, Takeuchi H, Kondo Y, Kondo S. Pivotal role of the cell death factor BNIP3 in ceramide-induced autophagic cell death in malignant glioma cells. *Cancer Res.* 2004. doi:10.1158/0008-5472.CAN-03-3084
255. Sarkar S, Maceyka M, Hait NC, et al. Sphingosine kinase 1 is required for migration, proliferation and survival of MCF-7 human breast cancer cells. *FEBS Lett.* 2005. doi:10.1016/j.febslet.2005.08.055
256. Xie V, Tong D, Wallington-Beddoe CT, Bradstock KF, Bendall LJ. Sphingosine kinase 2 supports the development of BCR/ABL-independent acute lymphoblastic leukemia in mice. *Biomark Res.* 2018;6(1):6. doi:10.1186/s40364-018-0120-4
257. Cingolani F, Casasampere M, Sanllehi P, Casas J, Bujons J, Fabrias G. Inhibition of dihydroceramide desaturase activity by the sphingosine kinase inhibitor SKI II. *J Lipid Res.* 2014. doi:10.1194/jlr.M049759
258. Nica AF, Tsao CC, Jiffar T, Kurinna S, Ruvolo P. Role for JNK in ceramide-induced apoptosis in chronic myelogenous leukemia derived K562 cells. *Cancer Res.* 2005;65(9 Supplement).
259. Taouji S, Higa A, Delom F, et al. Phosphorylation of serine palmitoyltransferase long chain-1 (SPTLC1) on tyrosine 164 inhibits its activity and promotes cell survival. *J Biol Chem.* 2013. doi:10.1074/jbc.M112.409185
260. Wadsworth JM, Clarke DJ, McMahon SA, et al. The Chemical Basis of Serine Palmitoyltransferase Inhibition by Myriocin. *J Am Chem Soc.* 2013;135(38):14276-14285. doi:10.1021/ja4059876
261. Pardanani A, Tefferi A. Imatinib targets other than bcr/abl and their clinical relevance in myeloid disorders. *Blood.* 2004;104(7):1931-1939. doi:10.1182/blood-2004-01-0246
262. Huang C, Tu Y, Freter CE. Fludarabine-resistance associates with ceramide metabolism and leukemia stem cell development in chronic lymphocytic leukemia. *Oncotarget.* 2018;9(69):33124-33137. doi:10.18632/oncotarget.26043
263. Kartal Yandim M, Apohan E, Baran Y. Therapeutic potential of targeting ceramide/glucosylceramide pathway in cancer. *Cancer Chemother Pharmacol.* 2013;71(1):13-20. doi:10.1007/s00280-012-1984-x
264. Huang W-C, Tsai C-C, Chen C-L, et al. Glucosylceramide synthase inhibitor PDMP sensitizes chronic myeloid leukemia T315I mutant to Bcr-Abl inhibitor and cooperatively induces glycogen synthase kinase-3-regulated apoptosis. *FASEB J.* 2011;25(10):3661-3673. doi:10.1096/fj.10-180190

265. Zhang X, Wu X, Su P, et al. Doxorubicin Influences the Expression of Glucosylceramide Synthase in Invasive Ductal Breast Cancer. *PLoS One*. 2012. doi:10.1371/journal.pone.0048492
266. Liu YY, Patwardhan GA, Xie P, Gu X, Giuliano AE, Cabot MC. Glucosylceramide synthase, a factor in modulating drug resistance, is overexpressed in metastatic breast carcinoma. *Int J Oncol*. 2011. doi:10.3892/ijo.2011.1052
267. Baran Y, Bielawski J, Gunduz U, Ogretmen B. Targeting glucosylceramide synthase sensitizes imatinib-resistant chronic myeloid leukemia cells via endogenous ceramide accumulation. *J Cancer Res Clin Oncol*. 2011. doi:10.1007/s00432-011-1016-y
268. Cox TM, Drelichman G, Cravo R, et al. Eliglustat maintains long-term clinical stability in patients with Gaucher disease type 1 stabilized on enzyme therapy. *Blood*. 2017. doi:10.1182/blood-2016-12-758409
269. Lewis AC, Wallington-Beddoe CT, Powell JA, Pitson SM. Targeting sphingolipid metabolism as an approach for combination therapies in haematological malignancies. *Cell death Discov*. 2018;4:4. doi:10.1038/s41420-018-0075-0
270. Shayman JA, Lee L, Abe A, Shu L. Inhibitors of Glucosylceramide Synthase. *Methods Enzymol*. 1999;31(1993):373-387.
271. Chang S-E, Kim K-J, Ro K-H, et al. Sphingosine may have cytotoxic effects via apoptosis on the growth of keloid fibroblasts. *J Dermatol*. 2004;31(1):1-5. <http://www.ncbi.nlm.nih.gov/pubmed/14739495>. Accessed February 24, 2019.
272. Yang J, Duerksen-Hughes PJ. Activation of a p53-independent, Sphingolipid-mediated Cytolytic Pathway in p53-negative Mouse Fibroblast Cells Treated with *N*-Methyl-*N*-nitro-*N*-nitrosoguanidine. *J Biol Chem*. 2001;276(29):27129-27135. doi:10.1074/jbc.M100729200
273. Lin C-F, Chiang C-W, Lin Y-S, Chen C-L, Huang W-C, Jan M-S. GSK-3beta acts downstream of PP2A and the PI 3-kinase-Akt pathway, and upstream of caspase-2 in ceramide-induced mitochondrial apoptosis. *J Cell Sci*. 2007. doi:10.1242/jcs.03473
274. Sultan I, Song P, Arnold HK, et al. Direct interaction between the inhibitor 2 and ceramide via sphingolipid-protein binding is involved in the regulation of protein phosphatase 2A activity and signaling. *FASEB J*. 2008. doi:10.1096/fj.08-120550
275. Brown VI, Seif AE, Reid GSD, Teachey DT, Grupp SA. Novel molecular and cellular therapeutic targets in acute lymphoblastic leukemia and

lymphoproliferative disease. *Immunol Res.* 2008;42(1-3):84-105.

doi:10.1007/s12026-008-8038-9

276. Layton Tovar CF, Mendieta Zerón H. Intracellular Signaling Pathways Involved in Childhood Acute Lymphoblastic Leukemia; Molecular Targets. *Indian J Hematol Blood Transfus.* 2016;32(2):141-153. doi:10.1007/s12288-015-0609-z
277. Adibhatla RM, Hatcher JF, Gusain A. Tricyclodecan-9-yl-xanthogenate (D609) mechanism of actions: a mini-review of literature. *Neurochem Res.* 2012;37(4):671-679. doi:10.1007/s11064-011-0659-z



# VITA

**DATE OF BIRTH /PLACE:** 04.08.1991 / Malatya, TURKEY

## EDUCATION

**PhD** İzmir Institute of Technology – Molecular Biology and Genetics (2015-2019)

**Visiting Research Scholar** Stony Brook University – Health Science Center (2017-2019)

**MSc** İzmir Institute of Technology – Molecular Biology and Genetics (2015-2019)

**Bachelor's Degree** İstanbul University – Molecular Biology and Genetics (2009-2013)

## PUBLICATIONS

1. Unlu M, Kiraz Y, Kacı FN, Baran Y\*. Multidrug Resistance in Chronic Myeloid Leukemia. Turkish Journal of Biology, 2014;38(6):806-816.
2. Kiraz Y, Unlu M, Kartal Yandım M, Baran Y\*. Molecular Biology of Stem Cells. Hematolog, 2014;4(2):255-265 (Invited Book Chapter).
3. Mutlu P, Kiraz Y, Gündüz U, Baran Y\*. An Update on Molecular Biology And Drug Resistance Mechanisms of Multiple Myeloma. Critical Reviews in Biotechnology, 2015;96(3):413-24.
4. Kartal Yandım M, Adan A, Kiraz Y, Baran Y\*. Regenerative Medicine. J Med Oncol-Special Topics 2015;8(2):10-4.
5. Kiraz Y, Neergheen-Bhujun VS, Rummun N, Baran Y\*. Apoptotic effects of non-edible parts of Punica granatum on human multiple myeloma cells. Tumor Biology, 2016;37(2):1803-15.
6. Kiraz Y, Baran Y\*, Nalbant A\*. T cells in tumor microenvironment. Tumor Biology, 2016;37(1):39-45
7. Adan A, Kiraz Y, Baran Y\*. Cell Proliferation and Cytotoxicity Assays. Special issue for Current Pharmaceutical Biotechnology, 2016. (Invited Review Article).
8. Kiraz Y, Gokbulut AA, Yandım MK, Baran Y\*. Major apoptotic mechanisms and genes involved in apoptosis. Tumor Biology, 2016;37(7):8471-86.
9. Amuk NG, Kurt G, Baran Y, Seyrantepe V, Yandım MK, Adan A, Demir SA, Kiraz Y, Sonmez MF. Effects of cell-mediated osteoprotegerin gene transfer and mesenchymal stem cell applications on orthodontically induced root resorption of rat teeth. Eur J Orthod, 2016.
10. Adan A, Alizada G, Kiraz Y, Nalbant A\*, Baran Y\*. Flow cytometry: Basic Principles and Applications. Critical Reviews in Biotechnology 2017;37(2):163-176.
11. Kiraz Y, Baran Y. Introduction to Cancer. Cancer Molecular Biology. Kisayol Publishing. ISBN: 978-605-2329-28-3; 2018.Ulu GT,
12. Kiraz Y, Baran Y\*. The Role of Polyunsaturated Fatty Acids in Cancer and Their Use in Cancer Treatment. Reviews in Clinical Medicine. 2019;6(3):84-90.

## SELECTED AWARDS

1. "The Best Project Award" AMGEN 1<sup>st</sup> Biotechnology Fair, 2019
2. "Young Researcher Award" 45<sup>th</sup> Congress of Turkish Hematology Association, 2019
3. "Experimental Hematology Award" 45<sup>th</sup> Congress of Turkish Hematology Association, 2019
4. "EHA Travel Grant" 24<sup>th</sup> Congress of European Hematology Association, 2019
5. "Selected for International Research Fellowship Programme for Doctoral Students" TUBITAK, 2019
6. "Health Security Partners Futures Fellowship" Health Security Partners, 2016
7. "Nejat F. Eczacıbaşı Scientific Project Support Award" 2015
8. "Qualified in a global competition among young scientists worldwide to participate in the 65<sup>th</sup> Lindau Nobel Laureate Meeting", 2015.
9. "Experimental Hematology Award" Experimental Hematology Congress, 2014
10. "The Best Hypothesis Award" International Symposium on Cancer Nanomedicine, 2013